What lies beneath?

Using the National Forest Inventory tree core archive to assess environmental changes in Swedish boreal forests

Kelley R. Bassett
Faculty of Forest Sciences
Department of Forest Ecology and Management
Umeå

SLU
SWEDISH UNIVERSITY OF AGRICULTURAL SCIENCES

DOCTORAL THESIS
Umeå 2026

Acta Universitatis Agriculturae Sueciae
2026:30

Cover: Swedish forest. Photo: Martin Fryklund

ISSN 1652-6880
ISBN (print version) 978-91-8124-247-8
ISBN (electronic version) 978-91-8124-277-5
https://doi.org/10.54612/a.7i9rgdiapn

Swedish University of Agricultural Sciences, Department of Forest Ecology and Management, Umeå, Sweden

Print: SLU Grafisk service, Uppsala 2026

What lies beneath? Using the National Forest Inventory tree core archive to assess environmental changes in Swedish boreal forests

Abstract

Boreal forests represent a major global carbon (C) sink, yet the persistence of their enhanced growth in response to environmental change, e.g., rising atmospheric carbon dioxide (CO_2), remains uncertain. In this thesis, I investigate long-term changes in boreal forest functioning using stemwood traits, stable-isotope chronologies, and structural properties derived from the unique tree-core archive of the Swedish National Forest Inventory, spanning the mid-20th century to the present.

A central result is the widespread and consistent decline in wood stable nitrogen isotopes ($\delta^{15}N$), indicating decreased nitrogen (N) availability in boreal forests. This trend is observed across large gradients in atmospheric N deposition and is best explained by rising CO_2 rather than N deposition or temperature variability. Comparisons between N_2-fixing and non-fixing tree genera further demonstrate that these declines are driven by changes in soil N cycling processes, providing strong evidence for Progressive Nitrogen Limitation (PNL) as the driving mechanism. In parallel, stemwood chemistry and structure show significant variability over time and space. Wood N concentrations were stable, while C concentrations and C:N ratios declined. Wood density and C concentration also varied with species, latitude, elevation, and tree size, challenging the assumption of constant traits used in forest C accounting. Methodologically, this work highlights the limitations of conventional dendrochronological approaches for mobile elements such as N, which I have shown require improved sampling strategies. Overall, my findings indicate that boreal forests are undergoing increasing N limitation under elevated CO_2, which may constrain their future capacity to sequester C.

Keywords: boreal forests, progressive nitrogen limitation (PNL), wood $\delta^{15}N$, carbon dioxide (CO_2), dendroecology; isotope natural abundance, wood density, carbon and nitrogen concentration

Vad döljer sig undan ytan? Användning av Riksskogstaxeringens borrspånsarkiv för att bedöma miljöförändring i Sveriges boreala skogar

Sammanfattning

De boreala skogarna utgör en viktig global kolsänka (C), men det är osäkert om deras ökade tillväxt som svar på miljöförändringar, till exempel stigande koldioxidhalter (CO_2) i atmosfären, kommer att bestå. I denna avhandling undersöker jag långsiktiga förändringar i boreala skogars funktion med hjälp av stamvedsegenskaper. Kronologier, som sträcker sig från mitten av 1900-talet till idag, baserade på stabila isotoper och strukturella egenskaper har skapats med hjälp av det unika arkivet med borrkärnor från den svenska Riksskogstaxeringen.

Ett centralt resultat är den utbredda och konsekventa minskningen av stabila kväveisotoper ($\delta^{15}N$) i stamveden, vilket indikerar minskad tillgång på kväve (N) i boreala skogar. Denna trend observeras över stora gradienter i atmosfärisk kvävedeposition och förklaras bäst av stigande koldioxidhalter snarare än kvävedeposition eller temperaturvariationer. Jämförelser mellan kvävefixerande och icke-fixerande trädarter visar också att dessa minskningar drivs av förändringar i kvävecykeln i marken, vilket ger starka belägg för progressiv kvävebegränsning (PNL) som den drivande mekanismen. Parallellt med detta uppvisar stamvedens kemiska sammansättning och struktur betydande variationer över tid och rum. Kvävehalterna i träet var stabila, medan kolhalterna och C:N-förhållandena minskade. Trädets densitet och kolhalt varierade också beroende på trädart, latitud, höjd över havet och trädstorlek, vilket ifrågasätter antagandet om konstanta vedegenskaper som används i beräkningar av skogens kollager. Ur metodologisk synvinkel belyser denna studiebegränsningarna hos konventionella dendrokronologiska metoder när det gäller rörliga ämnen som kväve, vilket jag har visat kräver förbättrade provtagningsstrategier. Sammantaget tyder mina resultat på att de boreala skogarna utsätts för en allt större kvävebegränsning vid förhöjda koldioxidhalter, vilket kan hämma deras framtida förmåga att binda kol.

Nyckelord: boreala skog, progressiv kvävebegränsning, $\delta^{15}N$ i trä, koldioxid (CO_2), dendroekologi; naturlig isotopförekomst, trädensitet, kol- och kvävekoncentration

Photo: Kelley R. Bassett

Photo: Kelley R. Bassett

Contents

List of publications

This thesis is based on the work contained in the following papers, referred to by Roman numerals in the text:

I. **Bassett, K.R.***, Östlund, L., Gundale, M.J., Fridman, J., & Jämtgård, S. (2023). Forest inventory tree core archive reveals changes in boreal wood traits over seven decades. *Science of the Total Environment*, 900 (165795). https://doi.org/10.1016/j.scitotenv.2023.165795

II. **Bassett, K.R.***, Hupperts, S.F., Jämtgård, S., Östlund, L., Fridman, J., Perakis, S.S., & Gundale, M.J. (2026). Rising atmospheric CO_2 reduces nitrogen availability in boreal forests. *Nature,* 650, 629–635. https://doi.org/10.1038/s41586-025-10039-5

III. **Bassett, K.R.**, Fridman, J., Östlund, L., & Jämtgård, S. Multi-decadal changes in wood density and carbon concentration across Swedish boreal forests (manuscript)

IV. **Bassett, K.R.**, Hupperts, S.F., Jämtgård, S., Östlund, L., Fridman, J., Perakis, S.S., & Gundale, M.J. Divergent wood $\delta^{15}N$ chronologies of N-fixing and non-N-fixing trees highlight progressive nitrogen limitation with rising CO_2 (manuscript)

*** Corresponding author**
All published papers are open access.

The contribution of Kelley R. Bassett to the papers included in this thesis was as follows:

I. Collaborated in the development of sampling methodology; conducted sample collection, preparation, and curation; performed non-analytical methods; conducted statistical analyses; led manuscript writing and editing; and secured external funding to support analysis costs.

II. Collaborated in the development of sampling methodology; conducted sample collection, preparation, and curation; performed non-analytical methods; conducted statistical analyses; led manuscript writing and editing.

III. Collaborated in the development of sampling methodology; coordinated and conducted data collection and sample preparation; conducted statistical analyses; led the manuscript writing and editing.

IV. Collaborated in project conceptualization and sampling methodology; coordinated project management, including sample collection and preparation; conducted statistical analyses; led manuscript writing and editing.

List of figures

Abbreviations

‰	Per mille (parts per thousand)
^{12}C	Light carbon (C) stable isotope
^{13}C	Heavy carbon (C) stable isotope
^{14}N	Light nitrogen (N) stable isotope
^{15}N	Heavy nitrogen (N) stable isotope
BNF	Biological Nitrogen Fixation
CRU TS	Climatic Research Unit gridded Time Series (v.4.0774)
δ	Delta notation
$\delta^{13}C$	Ratio of ^{13}C:^{12}C of the sample relative to its standard, VPDB
$\delta^{15}N$	Ratio of ^{15}N:^{14}N of the sample relative to its standard, N_2
Δ	Isotopic discrimination
EcM	Ectomycorrhizae
eCO_2	Elevated carbon dioxide
IPCC	Intergovernmental Panel on Climate Change
ISIMIP	Inter-Sectoral Impact Model Intercomparison Project (v.3a)
*i*WUE	Intrinsic water use efficiency
LDON	low-molecular-weight dissolved organic nitrogen (N)
MTM	Multiple-tree method
N_2	Dinitrogen; International reference standard for $\delta^{15}N$
N_2O	Nitrous oxide
NFI	National Forest Inventory
NH_3	Ammonia
NH_4^+	Ammonium
NH_y	Reduced nitrogen
NH_y:NO_x	Ratio of reduced to oxidized nitrogen

NO_3^-	Nitrate
NO_x	Oxidized nitrogen
Nr	Reactive nitrogen
Pg	Petagram (10^{15} grams)
PNL	Progressive Nitrogen Limitation
PNUE	Photosynthetic Nitrogen Use Efficiency
SOM	Soil organic matter
STM	Single-tree method (90–115-year age class)
Tg	Teragram (10^{12} grams)
VPD	Vapor pressure deficit
VPDB	Vienna PeeDee Belemnite; International reference standard for $\delta^{13}C$

1. Introduction

1.1 Boreal Forests

The circumpolar boreal forest is the world's largest terrestrial biome, covering approximately 14 million square kilometers, nearly one-third of Earth's forested area (Brandt, 2009; Gauthier et al., 2015; Thiffault, 2019) , and extending across the high northern latitudes of North America and Eurasia (Figure 1). It exhibits ecological diversity with regional differences in species composition, successional pathways, and landscape features (Boonstra et al., 2016; Nikolov & Helmisaari, 1992). Generally, boreal forests exhibit a cold climate with high seasonal variability characterized by relatively low mean annual temperatures and short growing seasons (Bonan & Shugart, 1989). Vegetation exhibits low species richness and relatively simple forest structure (Esseen et al., 1997). Fennoscandian boreal forests are dominated mainly by evergreen conifers, namely Scots pine (*Pinus sylvestris* L.) and Norway spruce (*Picea abies* (L.) H. Karst.). A deciduous broadleaf component including silver birch (*Betula pendula* Roth.), downy birch (*Betula pubescens* Ehrh.), and European aspen (*Populus tremula* L.) often appear in the early stages of ecological succession but rarely dominates in later successional stages of forest development (McLaren & Turkington, 2013; Thiffault, 2019).

Cool, humid climatic conditions and the dominance of evergreen conifers promote processes that give rise to distinctive soils, mainly Podzols (Lundström et al., 2000). These soils are characterized by high acidity, low fertility, and slow decomposition of soil organic matter (McLaren & Turkington, 2013), leading to reduced nutrient availability in boreal ecosystems (Bonan & Shugart, 1989; Näsholm et al., 1998; Vallotton & Unc, 2024).

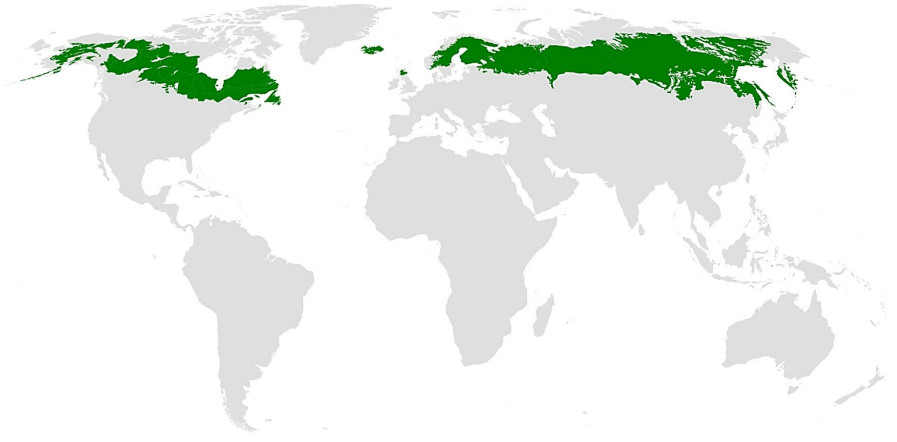

Figure 1. The circumpolar boreal biome, highlighted in green, covers the high-latitude regions of North America, Europe, and Russia. Source: Sémhur, 2010.

1.1.1 Carbon and nitrogen cycling in the boreal forest

Boreal forests are critical to the global carbon (C) cycle due to their capacity to take up and store substantial amounts of C in living and dead biomass and soils (DeLuca & Boisvenue, 2012; Lucas et al., 2016; Pan et al., 2011). The biome stores approximately 272 ± 23 petagrams (Pg) of C, or roughly 32% of total terrestrial C stocks (Pan et al., 2011). Given the magnitude of this reservoir, it is vital to understand what controls boreal C storage and sequestration—especially the factors that regulate primary productivity in a changing climate. An important factor is nutrient availability, particularly nitrogen (N). In boreal ecosystems, N is widely regarded as the primary limiting nutrient, constraining photosynthesis and thereby regulating net primary productivity (NPP), biomass accumulation, and long-term C sequestration (LeBauer & Treseder, 2008; Tamm, 1991; Vitousek & Howarth, 1991). Thus, C and N cycles are tightly coupled, and factors that alter N availability have direct implications for the boreal C balance.

Dinitrogen (N_2) gas constitutes 78% of Earth's atmosphere; however, its strong N≡N triple bond renders it inaccessible to most organisms for direct uptake, necessitating its conversion to bioavailable forms to support metabolism and growth (Stein & Klotz, 2016). In boreal ecosystems, N originates from three primary pathways: 1) biological N_2 fixation (BNF); 2) atmospheric reactive N (Nr) deposition; and 3) internal recycling of accumulated soil organic matter (SOM; IPCC, 2013).

Biological N_2 fixation (BNF) converts atmospheric N_2 into bioavailable ammonium (NH_4^+) by specialized organisms possessing the nitrogenase enzyme (Threatt & Rees, 2022). In boreal forests, BNF rates are relatively low, approximately 2–7 kg N ha^{-1} yr^{-1} (Hupperts et al., 2025; Lindo et al., 2013). The main mediators of BNF are free-living cyanobacteria, moss-associated diazotrophs, and symbiotic associations (Binkley et al., 1994; DeLuca et al., 2002). Atmospheric deposition supplies both reduced (NH_4^+) and oxidized (NO_3^-) forms of Nr to the terrestrial land surface. Since the 1960s, anthropogenic activities—the industrial Haber-Bosch process, the increased cultivation of N_2-fixing crops, and fossil fuel pollution—have increased global Nr inputs approximately tenfold (Erisman et al., 2011; Galloway et al., 2004). In Swedish boreal forests, Nr deposition varies along a north-to-south gradient, ranging from 1–3 kg N ha^{-1} yr^{-1} in the north to 10–15 kg N ha^{-1} yr^{-1} in the south (Gundale et al., 2011; Pihl Karlsson et al., 2011). Despite global Nr increases, rates in Sweden have been stable since the late 20th century, with slight increases in the north and declines in the south (Lövblad, 2000; Lucas et al., 2016).

Among the primary pathways, internal cycling dominates N supply in boreal forests, with annual internal fluxes (~15–50 kg N ha^{-1}) nearly an order of magnitude greater than external inputs (Binkley & Högberg, 1997; Korhonen et al., 2013), highlighting the boreal biome's reliance on recycled nutrients to sustain primary productivity. Internal N cycling is driven by the breakdown (depolymerization) of complex SOM into low-molecular-weight dissolved organic N (LDON, e.g., amino acids), an enzymatic process widely considered a primary bottleneck in the N cycle (Schimel & Bennett, 2004). Following depolymerization, LDON and the ammonification-derived NH_4^+ become available for plant uptake (assimilation) or microbial immobilization (Bobbink et al., 2010; Näsholm et al., 1998; Sponseller et al., 2016). Net mineralization rates remain relatively low (-5–15 kg N ha^{-1} yr^{-1}; Sponseller et al., 2016), due to low temperatures, high soil acidity, and the recalcitrant nature of conifer litter (Prescott, 2010). Although NH_4^+ can be oxidized to NO_3^- via nitrification, rates in upland boreal soils are generally low (Högberg et al., 2006). Consequently, LDON and NH_4^+ dominate the available N pool, forcing vegetation to compete intensely with microbes for these limited resources.

As a result, boreal forests are characterized by efficient internal retention of N, as biological demand generally exceeds supply. Most of the available

N is rapidly immobilized by plants and soil microorganisms, thereby limiting losses from the system (Sponseller et al., 2016; Tamm, 1991). Nitrate leaching may occur when nitrification exceeds biological uptake, particularly following disturbance, although such losses are typically minimal in upland boreal systems (Tamm, 1991). Similarly, gaseous losses via denitrification (reduction of NO_3^- to nitrous oxide, N_2O and N_2) are restricted to anaerobic sites or saturated soils and are typically low in well-drained boreal forests (Firestone & Davidson, 1989; Maljanen et al., 2010).

Due to the imbalance between soil N supply and plant demand, most boreal species establish symbiotic relationships with ectomycorrhizal (EcM) fungi (Smith & Read, 2008). These fungal partners enhance the host plant's access to both organic and inorganic N sources in exchange for plant-derived C (Bunn et al., 2024; Näsholm et al., 1998). This association creates a direct functional link between belowground C allocation and N acquisition.

1.1.2 Climate change impacts on the boreal forest

Since the start of the industrial revolution, human activities, including fossil fuel combustion, cement production, and land-use changes, have driven substantial increases in atmospheric carbon dioxide (CO_2; Canadell et al., 2007). Annually, global emissions are approximately 11 Pg C of CO_2 (Friedlingstein et al., 2022), and the Intergovernmental Panel on Climate Change (IPCC, 2013) projects that atmospheric CO_2 levels could more than double by the end of the century. These changes may have implications for boreal forests, which now face atmospheric CO_2 concentrations more than 50% higher than pre-industrial levels (NOAA, 2022).

Rising atmospheric CO_2 serves as the dominant driver of climate change. High-latitude ecosystems, including the boreal forest, are particularly sensitive to climate change, experiencing more rapid and severe changes than other regions, such as temperate and tropical biomes (Gauthier et al., 2014; Giorgi, 2006). Changes such as rising temperatures, altered precipitation regimes, and projected increases in drought frequency (IPCC, 2013; Kellomäki et al., 2008) exert direct and indirect effects on forest function. Annual temperature increases exceeding 1.5 °C have already been observed across much of the boreal biome, with even more severe consequences expected as temperatures continue to rise (IPCC, 2018; 2023). Simultaneous increases in CO_2 concentrations and temperature directly influence plant metabolic processes (Ainsworth & Rogers, 2007). While elevated CO_2

(eCO_2) and warming can enhance C gain through photosynthesis, rising temperatures also increase the land-atmosphere vapor pressure deficit (VPD), the principal driver of water loss via evaporation and transpiration, which can intensify drought stress and offset the advantages of longer growing seasons (Rawson et al., 1977; Yuan et al., 2019).

1.1.3 Progressive Nitrogen Limitation

Rising atmospheric CO_2 is fundamentally altering the coupling between C and N cycles, with important consequences for ecosystem productivity and nutrient availability. Elevated CO_2 generally stimulates NPP, as demonstrated in Free-Air CO_2 Enrichment (FACE) experiments (e.g., Norby et al., 2010). However, this stimulation is often constrained by N availability (Reich et al., 2006). Increased plant growth under eCO_2 elevates ecosystem N demand, which can reduce soil mineral N availability and intensify N limitation, a process described as Progressive Nitrogen Limitation (PNL; Luo et al., 2004). Over time, ecosystems may shift towards more oligotrophic conditions, characterized by declining nutrient availability relative to C inputs (Craine et al., 2018; Hungate et al., 2003). This progression largely results from the long-term sequestration of N into woody biomass and recalcitrant SOM pools (Luo et al., 2004), which limits the recycling of plant-available N through depolymerization and mineralization pathways (Finzi et al., 2006; Norby et al., 2010). Meta-analyses further indicate that N availability is a primary constraint on ecosystem productivity, with N additions enhancing C uptake and storage (Yue et al., 2016).

Additional mechanisms further reinforce the decline in N availability under eCO_2. Elevated CO_2 can increase plant C:N ratios, which may promote microbial N immobilization during decomposition and further reduce soil N availability (Luo et al., 2004). Moreover, plant litter with a high C:N ratio decomposes more slowly and immobilizes N more effectively than litter with a low C:N ratio (Manzoni et al., 2008; Taylor et al., 1989). In N-limited boreal forests, these mechanisms may constrain long-term C sequestration and alter N cycling despite improved photosynthetic capacity. Consequently, PNL may act as a key constraint on sustained ecosystem productivity under rising CO_2. However, uncertainty remains about the future of terrestrial N limitation, with significant implications for the accuracy of Earth-system model predictions of the terrestrial C sink (Canadell et al., 2021).

As N limitation intensifies under eCO_2, the N cycle may become increasingly tight or closed, characterized by reduced losses via leaching and gaseous pathways (Luo et al., 2004). This enhanced retention of N reflects a shift toward more conservative nutrient cycling as ecosystem demand for N increases. In addition, plants may increasingly rely on mycorrhizal fungi for N acquisition under eCO_2 conditions (Terrer et al., 2016). These symbiotic associations facilitate access to N pools and can alter the partitioning and retention of N within the ecosystem (Franklin et al., 2014; Hasselquist et al., 2016; Hobbie & Högberg, 2012; Näsholm et al., 2013). Together, these processes reinforce N limitation by reducing N losses and increasing biological control, further constraining ecosystem responses to eCO_2.

1.2 National Forest Inventory

Since 1923, systematic national forest inventories (NFI) have been conducted across Sweden (Thorell & Östlin, 1931; Figure 2). Initial inventories were conducted using line-and-belt surveys to assess available forest resources and measure annual forest growth, ensuring that timber harvest did not exceed the annual growth increment (Thorell & Östlin, 1931). Survey methods evolved in 1938 with the introduction of sample plots, which reduced the high correlation between plots (Eriksson, 1985). In 1953, line surveys were fully replaced by sample-plot inventories clustered within designated tracts, a practice that continues to this day. In the 1980s, a new approach combined temporary plots, surveyed only once, with permanent plots revisited every five years (Eriksson, 1985; Figure 3). Temporary plot tracts are square or rectangular, with side lengths ranging from 300 to 1500 meters, and include eight to twelve volume sample plots along the perimeter of each tract, each with a radius of approximately seven meters. The exact side lengths and number of volume sample plots vary by region (Fridman et al., 2014). Sample trees within the volume plots are selected to estimate volume, age, and growth increment (Fridman et al., 2014). Additional variables related to site, area, volume, growth, mortality, regeneration, and felling are also collected and serve as metadata for each sample tree (Fridman et al., 2014). The inclusion of both temporary and permanent plots was intended to facilitate monitoring of change and to support future research (Fridman et al., 2014). The goals of the initial forest inventory also expanded beyond measurements of forest area, volume, and composition to encompass

detailed assessments of various ecosystem goods and services (Eriksson, 1985; Fridman et al., 2014). The value of NFIs thus extends beyond their traditional role, providing information for forest, climate, and environmental policy decisions at regional, national, and international levels (Fridman et al., 2014).

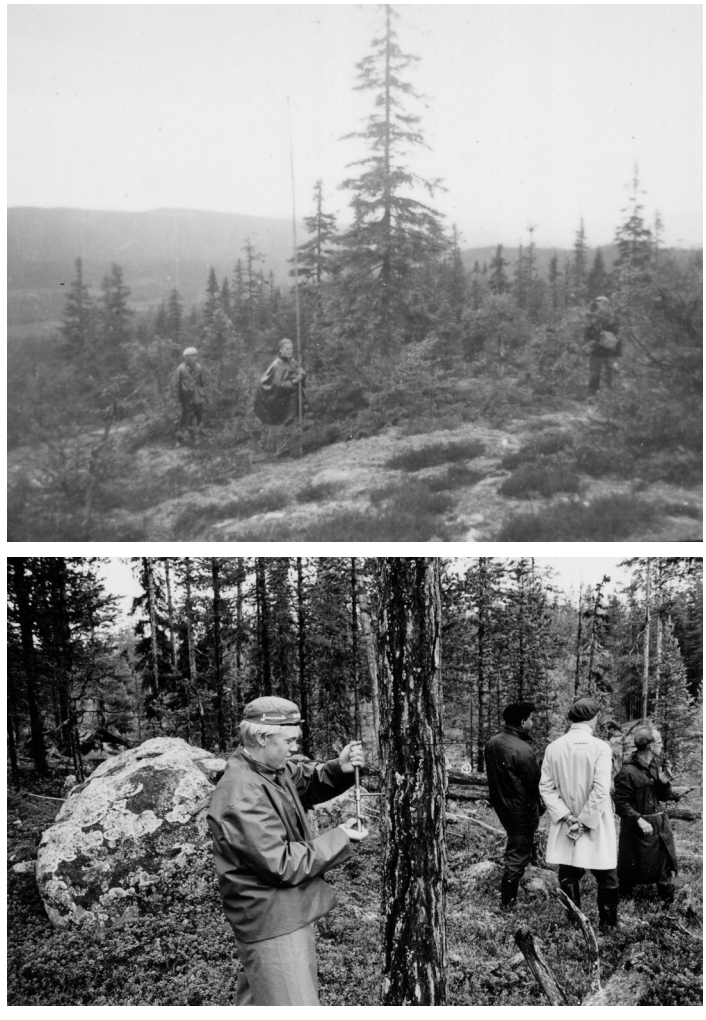

Figure 2. Top: Swedish National Forest Inventory (NFI) fieldwork in Jämtland, c. 1939; Bottom: Collecting tree cores in Norrbotten, c. 1966. Source: SLU Media Bank.

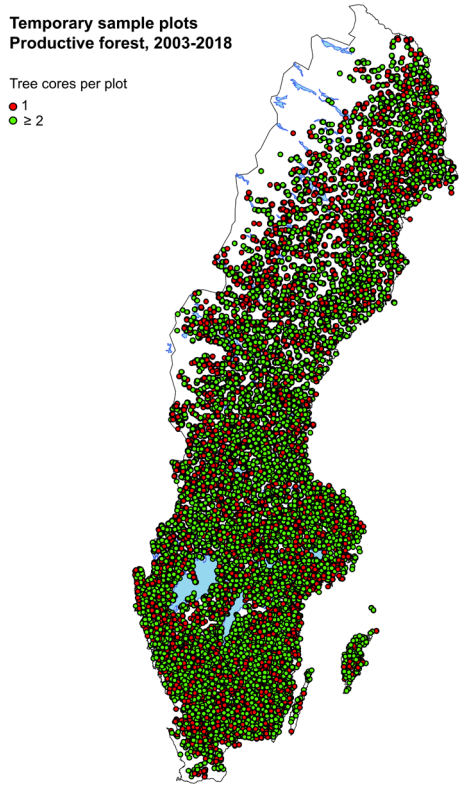

Figure 3. Swedish National Forest Inventory (NFI) temporary plot locations, 2003-2018. Tree cores collected per plot are indicated by red (one core) or green (two or more cores). Source: SLU NFI/Riksskogstaxeringen.

1.2.1 Tree core archive

As part of the annual forest inventory, the NFI (Riksskogstaxeringen) systematically collects tree cores from approximately 10,000 temporary plots (Figure 3). Sample trees are cored at breast height (1.3 m; diameter at breast height, DBH) and used to measure age and radial increment (Fridman et al., 2014); numerous other site-related variables, such as crown class, moisture classification, ground cover, elevation, and geographic coordinates, are also collected on the plots and serve as valuable metadata for each tree core (Riksskogstaxeringen, 2025). The NFI archives tree cores at the Swedish University of Agricultural Sciences (SLU, Umeå; Figure 4). The archive currently holds approximately one million samples dating from 1961 to the present.

Figure 4. National Forest Inventory (NFI) tree core archive at SLU, Umeå (left and center); example of tree core samples from temporary plots (right). Photos: K.R. Bassett.

1.3 Dendrochronological Methods

While the NFI provides an invaluable archive of forest structure and composition, extracting detailed insights into environmental change over time requires specialized analytical approaches—most notably, dendrochronological methods.

1.3.1 Classic and alternative methodologies

Chronologies (time series) derived from single-tree cores within forest stands are valuable for reconstructing past environmental and climatic events (Fritts, 1976) but have inherent limitations when scaled to landscape-level responses to environmental change. A primary constraint of a single-tree method (STM; Figure 5) is the simultaneous change in both the individual tree's age and the forest's successional age over the time series. This co-variation can potentially be problematic because a tree's competitive ability for resources changes with age (Forrester, 2019), and nutrient limitations, specifically N, often increase as forests reach later successional stages (Bond-Lamberty et al., 2006; DeLuca et al., 2008; Hart & Classen, 2003; Lagerström et al., 2007). Some elements, such as N, are highly mobile, and therefore constructing chronologies using the STM may be insensitive to reveal changes through time, due to remobilization and translocation via ray parenchyma cells that may contaminate historical rings with contemporary N transported in the xylem water (Mead & Preston, 1994; Nömmik, 1966; Peuke, 2010). Consequently, interpretations based on the STM may falsely suggest that landscape-scale N availability has or has not changed over time, when the observed patterns may reflect other processes.

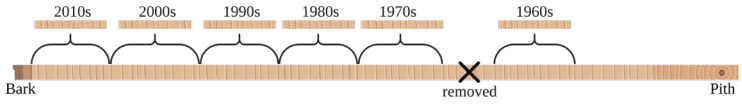

Figure 5. Classic dendrochronological approach where 10-year segments are collected along the length of a single tree core (single-tree method, STM). Within each grid (location), a single core (age class: 90-115 years from 2016-2018) was collected from archived samples. This single core provided grid-level information for all six decades per species, creating a chronology from one tree per species per grid. The section marked 'removed' accounts for the gap between samples from 1961 and 1977. Created with BioRender.

An alternative approach to mitigate the biases associated with the STM is to create a tree-ring chronology for a specific location (e.g., a grid cell) using a multiple-tree method (MTM) in which tree cores are collected at different time points from trees of the same age (Figure 6). The MTM isolates environmental signals from the successional and physiological biases inherent in the STM, thereby keeping tree age constant and eliminating biases arising from the ecological processes mentioned above (Martínez-Sancho et al., 2020). The MTM can be achieved by utilizing archived samples, which offer a unique opportunity to select a specific age group from a particular decade, enabling the collection of cores from forests with similar age and site conditions.

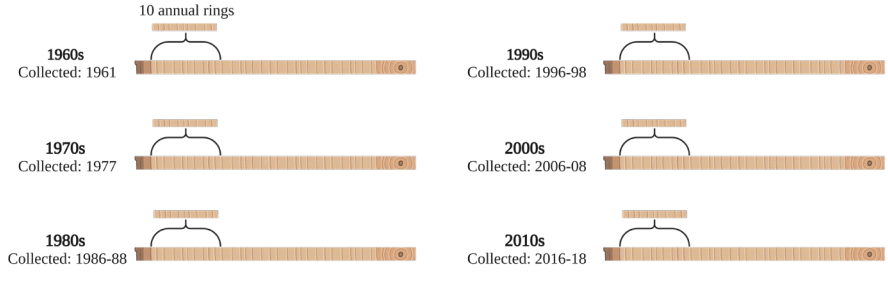

Figure 6. Alternative dendrochronological approach where 10-year segments are collected from different trees of the same age class for each decade in the grid, the multiple-tree method (MTM). Gathering one tree core from each species and different trees across the six decades at each grid location kept the age consistent. Created with BioRender.

1.4 Stemwood traits

1.4.1 Stable isotopes

In addition to differences in chemical forms, N pools are isotopically distinct. Stable isotopes act as powerful integrators of biogeochemical cycles, linking elemental fluxes across spatial and temporal scales (Bahn et al., 2012). Nitrogen has two stable isotopes: the abundant light isotope, ^{14}N (~99.63%), and the rarer heavy isotope, ^{15}N (~0.37%). The ratio of ^{15}N to ^{14}N in a sample, relative to the atmospheric N_2 standard, is expressed as $\delta^{15}N$ in per mille (‰).

Nitrogen stable isotope ratios ($\delta^{15}N$) in plant tissues over decades to centuries have served as key evidence for oligotrophication because they incorporate multiple ecosystem processes, reflecting both primary N sources and overall soil N availability (Craine et al., 2018; Mason et al., 2022a,b). Generally, higher N availability yields higher plant $\delta^{15}N$ values, while limited N availability yields lower $\delta^{15}N$ values (Robinson, 2001). This occurs because plant $\delta^{15}N$ reflects the $\delta^{15}N$ of the available soil N pool, offset by isotopic fractionation that typically favors ^{14}N during uptake, particularly under low N availability.

Isotopic fractionation, the process by which the relative abundance of ^{15}N and ^{14}N is altered through physical or chemical reactions, occurs at both the ecosystem level and during plant N uptake (Craine et al., 2015; Gerhart & McLauchlan, 2014; Hobbie & Högberg, 2012). At the ecosystem level, high N availability relative to N demand promotes the loss of ^{15}N-depleted inorganic N through processes such as volatilization (conversion of NH_4^+ to NH_3), nitrification (oxidation of NH_4^+ to NO_3^-), NO_3^- leaching and denitrification (NO_3^- reduction to N_2O and N_2). These gaseous and leaching losses preferentially remove the lighter ^{14}N, thereby enriching the remaining soil N pools in ^{15}N and subsequently increasing plant $\delta^{15}N$ (Austin & Vitousek, 1998; Craine et al., 2015; Högberg, 1997).

During plant N uptake, the acquisition mechanism directly influences isotopic signatures (Figure 7). While direct root uptake of N in natural ecosystems typically results in minimal ^{15}N discrimination (Craine et al., 2018), boreal ectomycorrhizal (EcM) fungi facilitate significant isotopic fractionation by retaining ^{15}N in their tissues while preferentially transferring ^{14}N to host trees (Hobbie & Högberg, 2012). This discrimination against ^{15}N is most pronounced under low N availability, where increased reliance on EcM fungi leads to more negative plant $\delta^{15}N$ values (Hobbie & Högberg,

2012). Furthermore, in N-limited boreal systems, plants can bypass traditional mineralization by directly acquiring LDON, such as amino acids (Näsholm et al., 1998). This organic N acquisition pathway, governed by soil-derived depolymerization rates, provides a direct link between the plant and the organic N pool, thereby shaping the vegetation's isotopic signature to closely reflect that of the source N pool (Näsholm et al., 1998).

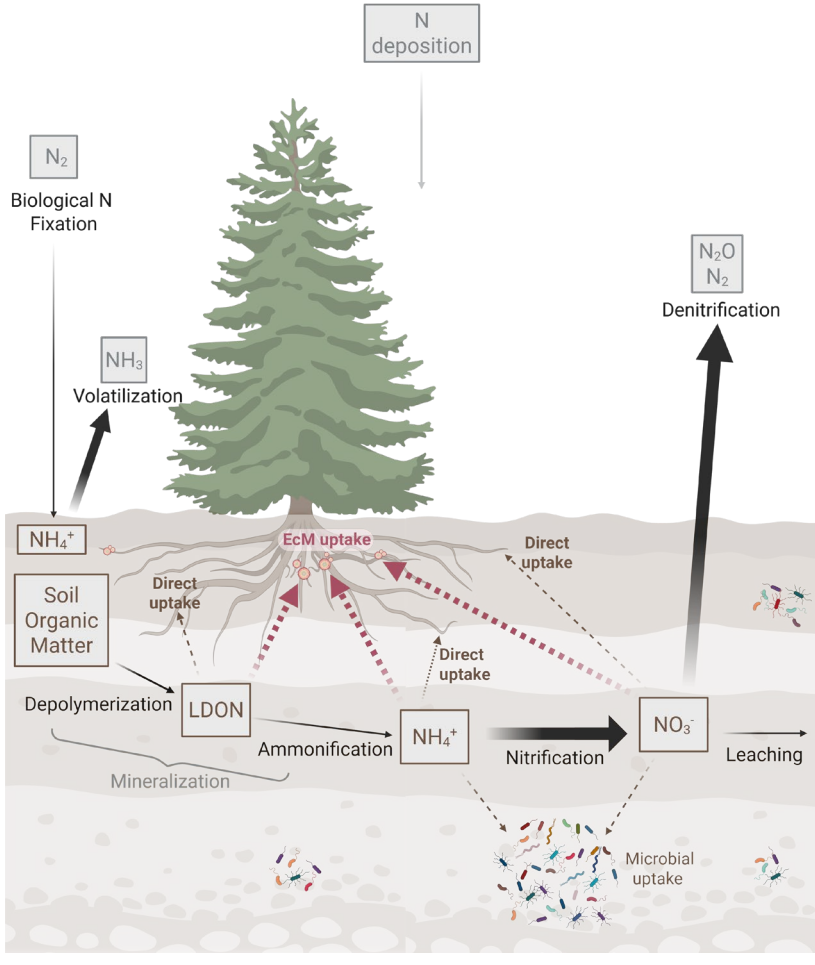

Figure 7. General representation of the terrestrial nitrogen (N) cycle, including N pools (boxes) and transformation processes (black arrows). Pathways associated with greater isotopic fractionation (i.e., stronger discrimination against ^{15}N) are indicated with wider arrows; thinner arrows represent little to no fractionation. Dashed lines represent N uptake; wider dashed arrows indicate greater fractionation during uptake; thinner dashed arrows indicate negligible fractionation. Created with BioRender.

Complementing the narrative of N availability indicated by $\delta^{15}N$, C stable isotopes ($\delta^{13}C$) can be used to track physiological changes in plant water-use strategies (Dawson et al., 2002). The ratio of the abundant light isotope, ^{12}C (~98.9%), and the rarer heavy isotope, ^{13}C (~1.1%) relative to the Vienna PeeDee Belemnite (VPDB) standard, is expressed as $\delta^{13}C$ (‰). In C_3 photosynthetic species, such as boreal conifers, C isotope discrimination (Δ) serves as an integrated measure of intrinsic water-use efficiency (*i*WUE) (Farquhar et al., 1989). This discrimination reflects the preferential uptake of ^{12}C (i.e., discrimination against ^{13}C) and is driven by the ratio of intercellular to atmospheric CO_2 concentration (C_i:C_a), which is largely regulated by stomatal conductance (g_s). When stomata close to conserve water, Δ decreases, leading to higher (less negative) $\delta^{13}C$ values in plant tissues (Figure 8). Conversely, when moisture conditions are sufficient, stomata remain open, leading to higher Δ and more negative $\delta^{13}C$ values. Consequently, wood $\delta^{13}C$ values serve as a proxy for *i*WUE, with positive deviations from the atmospheric signal indicating increasing water stress (Saurer et al., 2014).

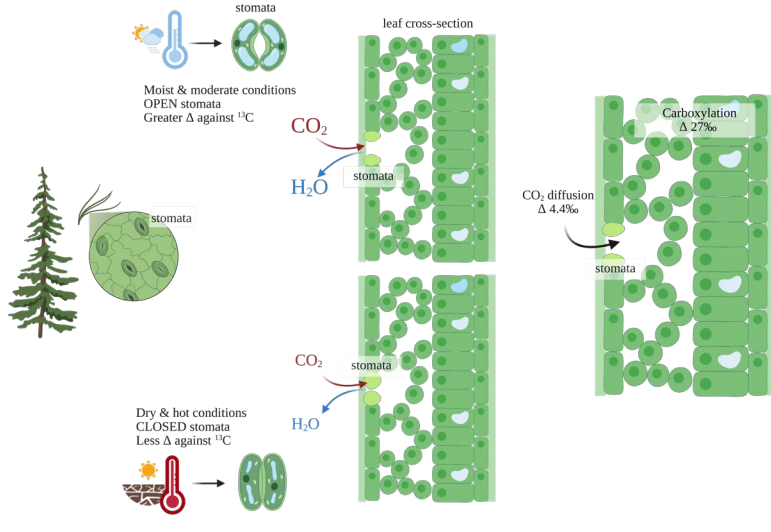

Figure 8. Representation of stomatal conductance under varying environmental conditions (left and middle), and carbon discrimination (Δ) against ^{13}C (right). Discrimination is regulated by stomatal conductance, with higher Δ against ^{13}C under favorable moisture conditions (upper left), and lower Δ during dry, hot conditions (lower left). Carbon isotope discrimination arises during CO_2 diffusion through stomata (~4.4‰) and during carboxylation by Rubisco (~27‰). Created with BioRender.

1.4.2 Element concentrations and wood density

Among aboveground biomass components, stemwood represents the dominant long-term C pool in boreal forest ecosystems (Pan et al., 2011; Marklund, 1988). Functionally, it provides mechanical support and serves as the primary conductive framework for water and nutrient transport, forming a critical link in the soil-plant-atmosphere continuum (Tyree & Zimmerman, 2002). As such, stemwood acts as both a structural tissue and a physical archive of sequestered atmospheric CO_2. The capacity of boreal forests to function as persistent C sinks is therefore closely tied to how stemwood traits—particularly wood density and elemental concentrations of C and N—respond to environmental change and anthropogenic pressures (Hyvonen et al., 2007).

Wood density, the ratio of dry mass to fresh volume (kg m^{-3}), is a key functional trait for converting forest volume data into C stocks. It is established during wood formation (xylogenesis), when cambial cells differentiate into tracheids (conifers) through phases of cell expansion, secondary wall deposition, and lignification. These processes determine cell size, wall thickness, and tissue structure, giving rise to earlywood and latewood within annual rings (Cuny et al., 2015; Rossi et al., 2006). Beyond its central role in mechanical strength and hydraulic function (Kallarackal & Ramirez, 2024), wood density strongly influences the amount of C stored per unit volume. Empirical evidence suggests a temporal correlation between accelerated growth rates and shifts in wood anatomical structure, in which environmental change or forest management can promote increased radial growth, often associated with a decline in wood density, although this relationship remains species- and context-dependent (Pretzsch, 2016; Pretzsch et al., 2016). Such variation has direct implications for C accounting, as shifts in wood density modify the C mass represented by a given stem volume.

Accurate estimation of forest C stocks also depends on the assumed chemical composition of biomass. Carbon concentration in wood is commonly approximated as ~50% of dry mass in global reporting frameworks (IPCC, 2006; Kohl et al., 2015), yet empirical studies show that C concentration varies across species, sites, and time (Martin et al., 2018; Thomas & Martin, 2012). Disregarding this variability can introduce systematic biases in forest C stock estimates, particularly in boreal regions where environmental gradients are strong. Incorporating region-specific

wood density and C concentration values is therefore essential to improve the accuracy and robustness of biomass and C accounting (Martin et al., 2018).

2. Objectives

Despite extensive research on boreal forest dynamics, gaps remain in understanding how Swedish forests respond to environmental changes. Using archived tree cores as a tool, stemwood traits such as stable isotopes, nutrient levels, and wood density can provide insights into the physiological and ecological responses of boreal forests. These methods can help assess responses to climate change; however, uncertainties about N limitation, regional differences in wood traits, and their effects on C sink estimates need to be addressed. Filling these gaps is crucial for better predicting and mitigating future declines in forest growth and C sequestration due to climate change.

The aim of this thesis is to leverage the NFI's unique tree-core archive to: compare different dendrochronological methods and evaluate their efficacy for assessing biogeochemical processes (**Paper I**); investigate changes in N availability through the evaluation of $\delta^{15}N$ across the Swedish forested landscape over multiple decades (**Paper II**); explore spatio-temporal changes in wood density and C concentration during a period of increased forest volume growth (**Paper III**); and, finally, to examine the mechanisms underlying changes in wood $\delta^{15}N$ values among species with differing nutrient acquisition strategies (**Paper IV**; Figure 9).

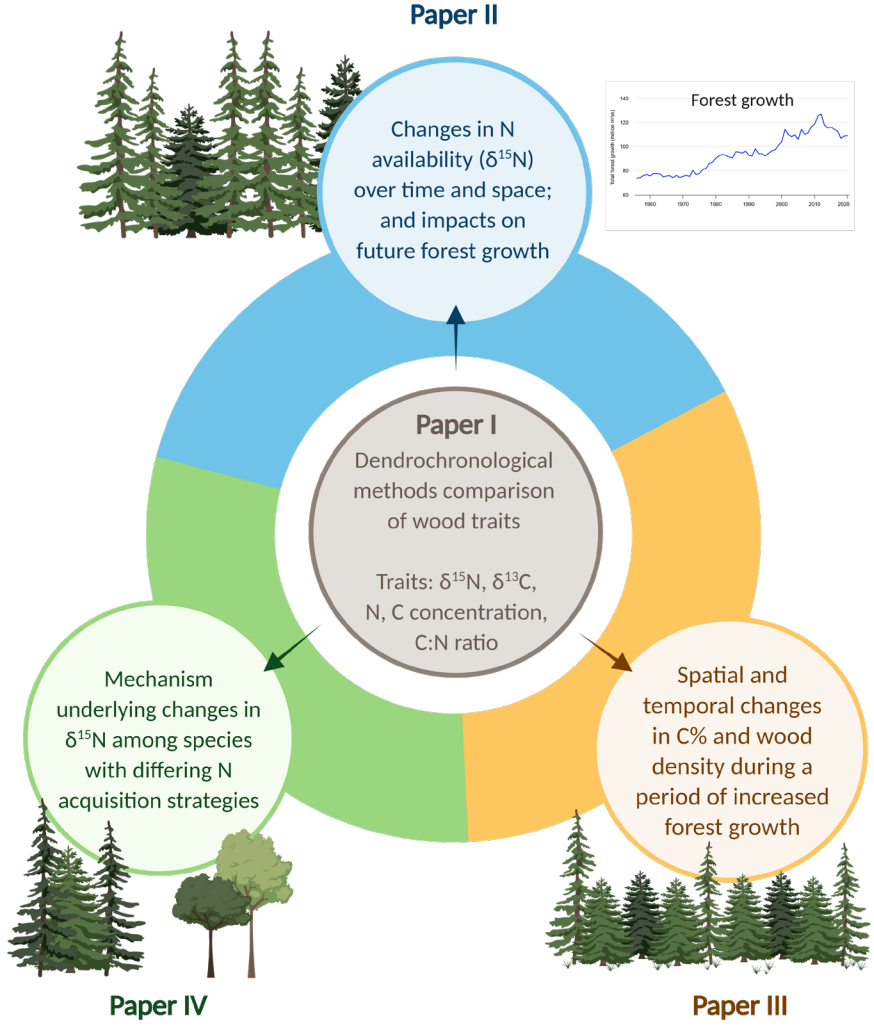

Figure 9. Overview of the four studies included in this thesis. Created with BioRender.

3. Materials and Methods

3.1 Study system and sampling design

All studies in this thesis utilize a uniform spatial distribution system, sampling criteria, and preparation protocol. Specific variation in geographic scope and filtering parameters, including age class and species is detailed in subsequent sections.

To ensure systematic and representative spatial distribution, I divided the Swedish landscape into 250 grid cells, each measuring 50 by 50 km, with each grid serving as the primary sampling unit (Figure 10). I used archived tree cores from the Swedish National Forest Inventory (NFI) collected between 1961 and 2018. Cores are 5.15 mm in diameter, extracted at breast height (1.3 m). Tree cores were selected based on the following criteria: (i) crown class of dominant or co-dominant trees and (ii) mesic, well-drained sites with a slope of 20 percent or less. A multi-temporal sampling design spanned six decades from the 1960s to the 2010s. Sampling years included 1961, 1977, 1986–1988, 1996–1998, 2006–2008, and 2016–2018. From the 1980s onward, I used three sampling years per decade to ensure sufficient numbers of tree cores. If a specific decade lacked a sample within a grid, I sampled the nearest adjacent grid. Data covered the period 1951–2017 since the most recent annual growth ring was not used. I prepared tree core samples using a standardized procedure that included removing the outer bark, cambium, and the most recent annual growth ring to avoid inconsistencies caused by timing of core collection during the growing season. Once prepped, I identified the outermost 10 years of growth using a stereo microscope at 20x magnification. I sectioned the 10 annual growth rings from the rest of the core with a No. 11 stainless steel surgical blade to an accuracy of 0.01 mm. I inspected cores for false rings; none were detected.

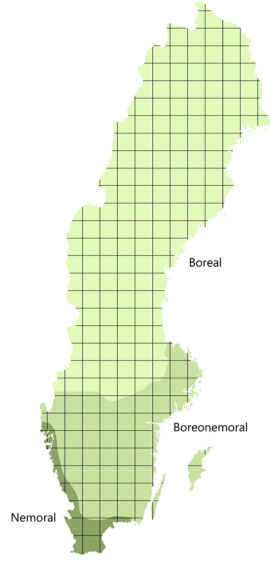

Figure 10. A spatially-distributed grid system (250–50 x 50 km grids) overlaying three major vegetation zones on the Swedish landscape applies to all studies in this thesis. Boreal (light), boreonemoral (medium), and nemoral (dark).

3.1.1 Dendrochronological methodology comparison

In **Paper I**, I examined 44 grids in central Sweden (Jämtland and Västernorrland; 61–65° N, 12–19° E; Figure 11), focusing on *P. sylvestris* and *P. abies*. I evaluated two dendrochronological methods: a multiple-tree method (MTM) with three age classes (30–40, 41–60, 61–80 years) and a single-tree method (STM) with a single age class (90–115 years). For the MTM, I collected tree cores from each species within each grid for six sampling decades, stratified into three age classes (Figure 6). The outermost 10 annual growth rings were analyzed for MTM. For the STM, I collected 10-year segments along the length of a single core from a single age class, each segment corresponding to its respective decade (1960s to 2010s; Figure 5). I measured five stemwood traits—$\delta^{15}N$, $\delta^{13}C$, N and C concentration, and C:N ratios—to assess temporal changes between 1951 and 2017 (n = 1038), to compare reconstruction methods (MTM and STM), and to assess differences among the three MTM age classes.

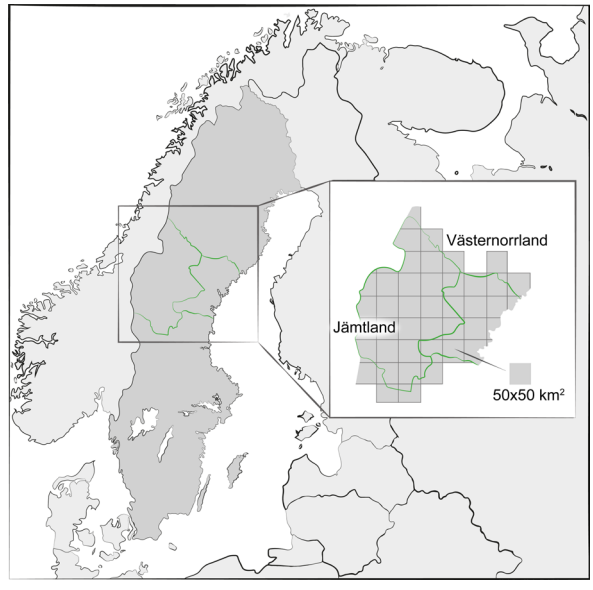

Figure 11. The study area for **Paper I** included grids in the central Swedish counties of Jämtland and Västernorrland; county borders are outlined in green. Squares indicate 50 x 50 km sampling grids.

3.1.2 Spatiotemporal drivers of $\delta^{15}N$

In **Papers II** and **IV**, I examined all grids within the Swedish forested landscape (55–69º N, 11–24º E) across six sampling decades (1960s–2010s; Figure 12). For **Paper II**, I focused on *P. sylvestris* and *P. abies* aged 41–60 years. I measured $\delta^{15}N$ to evaluate temporal trends and spatial differences across four regions with varying Nr deposition levels, ranging from the lowest rates in the north to the highest in southern regions, up to 4 times higher (n = 1609; Figure 12c,d). For **Paper IV**, I assessed temporal changes in $\delta^{15}N$ values of known N_2-fixing *Alnus* species—common alder (*Alnus glutinosa* (L.) Gaertn.) and grey alder (*Alnus incana* (L.) Moench)—as well as two potential N_2-fixing birch species, silver birch (*Betula pendula* Roth) and downy birch (*Betula pubescens* Ehrh.; total n = 979; Figure 12a,b). I compared these results with $\delta^{15}N$ values of *P. sylvestris* and *P. abies* data from **Paper II** to contrast N_2-fixing and non-N-fixing species.

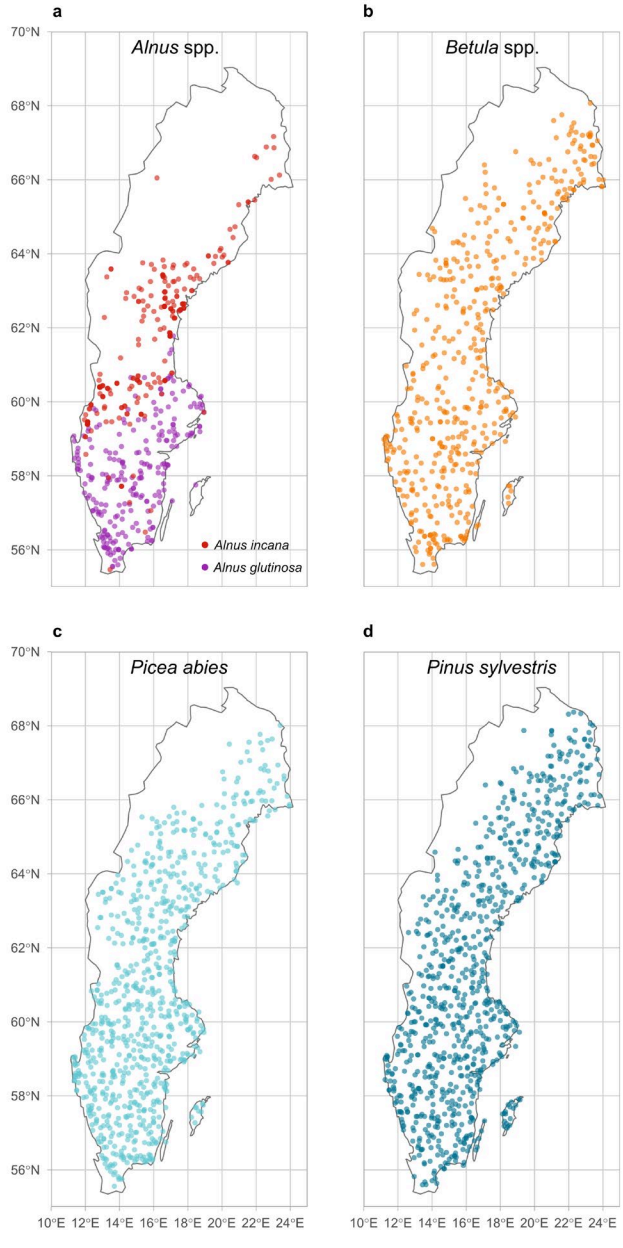

Figure 12. Sample distribution for a) *Alnus* spp. and b) *Betula* spp. (**Paper IV**); and c) *Picea abies*, and d) *Pinus sylvestris* (**Papers II**, **IV**).

3.1.3 Wood carbon concentration and density

In **Paper III**, I examined all grids in the Swedish forested landscape (55–69º N, 11–24º E) over six decades (1960s–2010s), focusing on *P. sylvestris* and *P. abies* aged 41–60 years. I analyzed the outermost 10-year segments from each core for C concentration and measured wood density (n = 1609; Figure 13a). I also collected an additional set of tree cores from each species in approximately 25% of the grids (n = 575; Figure 13b), evenly distributed across the study area to analyze C concentration and wood density of whole cores, excluding bark and the most recent year of growth, and including all rings to the pith (hereafter, 'whole cores').

Figure 13. Sample distribution of *Pinus sylvestris* (circle) and *Picea abies* (triangle) for sample types a) 10-year segments and b) whole cores used in **Paper III**.

3.2 Elemental Analysis

Elemental analyses for this thesis were performed by two independent laboratories: the Central Appalachians Stable Isotope Facility (CASIF) at the University of Maryland Center for Environmental Science Appalachian Laboratory (Frostburg, MD, USA), and the Stable Isotope Laboratory (SSIL) at the Swedish University of Agricultural Sciences (Umeå, Sweden).

Measurement of $\delta^{15}N$ and N concentration in **Papers I** and **II** was conducted at CASIF. CASIF also measured $\delta^{13}C$ and C concentration in **Paper I**, which were subsequently used to calculate C:N ratios. For **Paper III**, CASIF analyzed C concentration for 10-year segments, whereas SSIL analyzed C concentration for whole cores. In **Paper IV**, SSIL was used to measure $\delta^{15}N$ and N concentration.

3.3 Intrinsic water use efficiency

Values of *i*WUE in **Paper I** were derived from $\delta^{13}C$ measurements using established relationships between discrimination (Δ), stomatal conductance (g_s), and net photosynthetic C assimilation (A) (Ehleringer et al., 1993; Farquhar et al., 1989). Values of *i*WUE represent the ratio of net photosynthetic C assimilation to stomatal conductance (A/g_s), providing insight into how efficiently trees use water during C uptake.

3.4 Wood density

For **Paper III**, I determined wood density (D, g cm^{-3}) for both 10-year segments and whole cores. Tree cores were soaked in ultrapure water to reach a 'green' state and then weighed in air to the nearest 0.1 mg. The samples were then submerged in a liquid of known density (ultrapure water) to obtain the apparent mass, which equals the true green weight minus the buoyant force. Sample volume (cm^{-3}) was determined from these two measurements. Samples were oven-dried at 70 °C until weights stabilized. Wood density, D was calculated by dividing the oven-dry weight (g) by the green sample volume (cm^{-3}).

3.5 Climate and Nr deposition data

I utilized three external data sources to derive climate and reactive nitrogen (Nr) deposition data to support analyses. For the period 1951–2004, atmospheric CO_2 concentration (C_a; ppm) were sourced from McCarroll and Loader (2004). Data for 2005–2017 were obtained from the NOAA Global Monitoring Laboratory at Pallas-Sammaltunturi, Finland (Lan et al., 2022) for **Papers I**, **II**, and **IV**. In **Paper I**, $\delta^{13}CO_2$ values for 2005–2017 were derived using linear regression based on McCarroll and Loader (2004) data. In **Papers II** and **IV,** I computed the 10-year mean annual temperature (°C) for each sample using its geographic location and sampling decade, based on monthly temperature data from CRU TS v4.0774 (0.5° resolution; Harris et al., 2020). I also calculated relative temperature changes using a 1961 reference baseline for each grid cell. In **Papers II** and **IV**, I derived spatially explicit atmospheric Nr deposition from the Inter-Sectoral Impact Model Intercomparison Project (ISIMIP3a; Yang & Tian, 2023) at 0.5° resolution. I used monthly wet and dry deposition data for NH_x and NO_y (1951–2017) to calculate the 10-year average of four variables for each sample: NH_x, NO_y, NH_x:NO_y ratio, and total N deposition.

3.6 Swedish National Forest growth data

In **Paper II**, data from the Swedish NFI were used to estimate growth rates for both permanent and temporary plots, which are combined into a weighted mean with an estimated uncertainty of ≤1%. Permanent plots determine growth rates based on volume changes between successive inventories, using species-specific data, DBH, tree height, and crown height. Temporary plots use microscope-measured radial increments from tree cores and regression models. The total volume growth for mesic *P. sylvestris*- and *P. abies*-dominated forests was obtained from the NFI database. For each year and species, we converted total volume growth to stand-level growth by dividing it by the respective forest area.

3.7 Statistical Analysis

Statistical analyses across all four studies were conducted using R, including v.4.2.2 (R Core Team, 2022) for **Paper I**, and v.4.3.0 (R Core Team, 2023) for **Papers II, III,** and **IV**. In all studies, model residuals were tested for

normality and homoscedasticity, and statistical significance was set at $\alpha = 0.05$.

In **Paper I**, I employed three statistical approaches to analyze wood traits ($\delta^{15}N$, $\delta^{13}C$, N%, C%, C:N ratios) over time and across species. First, I used linear regressions on MTM data (comprising three age classes and decadal means) to establish baseline historical patterns for each wood trait and quantify temporal changes. Second, I applied factorial linear models with Type III analysis of variance (ANOVA) to test the effects of time, method, and their interaction on each wood trait, thereby assessing whether methodology (MTM vs. STM) significantly influenced temporal trends. Third, I conducted two-way ANOVAs with post hoc pairwise comparisons to identify specific differences in regression slopes across the methods for each species and trait. Finally, I calculated root-mean-squared error to quantify and compare method-specific prediction errors across the five traits.

In **Paper II**, I used three main statistical approaches to analyze spatiotemporal patterns of wood $\delta^{15}N$. First, I applied linear regression to estimate temporal trends in $\delta^{15}N$ for each tree species across four Swedish regions, followed by a two-way ANOVA with Tukey's post hoc tests to determine whether temporal slopes differed significantly between regions. Second, I constructed linear mixed-effects models to identify the key environmental and forest stand drivers of $\delta^{15}N$ variation. These models included atmospheric CO_2, mean annual temperature, total Nr deposition, total basal area, and tree species as fixed effects, with grid as a random effect to account for spatial autocorrelation. Stepwise selection with Akaike Information Criteria (AIC) was used to determine the optimal predictor combination, and multicollinearity was assessed using Variance Inflation Factors (VIF < 5). I calculated marginal, conditional and partial R^2 (coefficients of determination) to evaluate model performance. This process was repeated by substituting different Nr forms (NH_x, NO_y, and NH_x:NO_y) and by using Principal Component Analysis (PCA) to visualize relationships among the significant drivers. Third, I built additional linear mixed-effects models to estimate the effect of changes in forest productivity on $\delta^{15}N$, including relative forest volume growth change alongside either absolute forest volume growth or basal area as fixed effects. These models tested whether changes in growth rates beyond absolute growth levels influenced $\delta^{15}N$ values.

In **Paper III**, I examined two functional wood traits—wood density and C concentration—as response variables across different sample types (10-year segments and whole cores). I fit factorial linear models for each trait that included time, latitude, elevation, diameter, and tree species as main effects, plus species-by-time, species-by-latitude, and species-by-elevation interactions. Using Type III sum-of-squares ANOVA, I compared treatment means to assess statistical significance and determine how environmental and temporal factors influence wood trait variation. I performed Tukey's post hoc pairwise comparisons to identify specific differences in regression slopes between species. To compare sample types within each species, I used Welch's t-tests because Levene's test indicated significant heteroscedasticity among groups ($P < 0.001$). Finally, I applied Shapiro-Wilk tests to assess normality for each species-by-sample-type combination, ensuring the data met the statistical assumptions for the analyses.

In **Paper IV**, I used a combination of linear regression and mixed-effects modelling to compare N dynamics across four tree taxa. First, I analyzed temporal trends in wood $\delta^{15}N$ using linear regression for *Alnus* spp. and *Betula* spp. and compared their responses with those of *P. sylvestris* and *P. abies*. For each taxon, I estimated mean $\delta^{15}N$, standard error, and annual slope. To test whether temporal trends differed among taxa, I fitted a linear model including time-taxa interaction and evaluated main and interaction effects using Type III ANOVA. A significant interaction ($P < 0.001$) indicated heterogeneous slopes among taxa, and a post hoc comparison was applied. Second, to evaluate the explanatory power of environmental drivers, I fit linear mixed-effects models. The models included relative temperature change, total Nr deposition, total basal area, species, and the species-atmospheric CO_2 interaction as fixed effects. Grid was included as a random effect to account for spatial autocorrelation. Due to strong collinearity among Nr variables, I ran separate model variants substituting total Nr with NH_x, NO_y, and NH_x:NO_y ratio. Finally, I evaluated model performance by calculating marginal, conditional, and partial R^2 values for all model variants.

Photo: Kelley R. Bassett

4. Main results and discussion

The papers in this thesis aimed to explore whether stemwood traits changed over time across the Swedish forest landscape and, further, to better understand how anthropogenic changes may be impacting the boreal region. Here, key results are presented and discussed.

4.1 Temporal wood trait response: a methodological comparison

In **Paper I**, the alternative dendrochronological approach, MTM, revealed significant temporal shifts across all five wood traits for *P. sylvestris* and *P. abies* from 1951 to 2017, demonstrating a strong and coherent long-term signal. Wood $\delta^{15}N$ declined significantly over time in both species ($P < 0.001$), amounting to approximately 4‰ decline over the study period. This rate of decline is steeper than previously reported in comparable studies (Kranabetter et al., 2013; McLauchlan et al., 2017; Oulehle et al., 2022), indicating a pronounced shift in N dynamics within the study area.

The MTM consistently demonstrated a significant main effect of time across all traits and both species, whereas the traditional STM showed weaker, more subtle slopes. Notably, the two methods diverged substantially in the early decades, with MTM capturing values near 0‰ while STM displayed more depleted initial values (-3‰). This discrepancy highlights methodological limitations of STM in reconstructing historical N dynamics. Because N is mobile within tree stems and subject to internal redistribution, radial translocation can obscure temporal signals in tree-ring records (Mead & Preston, 1994; Nömmik, 1966; Tomlinson et al., 2014). By instead comparing wood formed at the same cambial age across different time periods, MTM minimizes the influence of internal nutrient mobility and tree ontogeny, thereby providing a more robust reconstruction of long-term environmental change.

In addition to isotopic trends, significant changes in elemental composition were observed. Wood N concentrations increased significantly over time ($P < 0.001$), while C concentrations declined ($P < 0.001$), resulting in a decreasing C:N ratio when all MTM age classes were combined. These opposing trends indicate a shift in wood stoichiometry over the study period. However, previous studies have concluded that wood N content may not

reliably reflect environmental N availability, as it is strongly influenced by internal physiological processes rather than environmental conditions (Doucet et al., 2011; Poulson et al., 1995). Consequently, the divergence between declining $\delta^{15}N$ and increasing N concentration underscores the importance of isotopic indicators for interpreting long-term changes in ecosystem N cycling.

In contrast, C isotope trends were consistent across both sampling methods. Wood $\delta^{13}C$ declined significantly over time ($P < 0.001$), with rates closely tracking with the atmospheric Suess effect—the dilution of atmospheric ^{13}C associated with fossil fuel emissions (Belmecheri & Lavergne, 2020; McCarroll & Loader, 2004). Correspondingly, *i*WUE increased significantly in both species ($P < 0.001$). The agreement between MTM and STM for $\delta^{13}C$ likely reflects the structural immobility of C once it is incorporated into woody tissues (Higuchi, 1997), thereby allowing a stable record of atmospheric and physiological signals over time.

Overall, the application of MTM demonstrates clear methodological advantages for reconstructing long-term environmental change from tree-ring archives. By reducing biases associated with internal nutrient mobility and tree aging, the approach yields a more coherent and temporally resolved signal than traditional methods. The results indicate that regional atmospheric changes have driven coordinated shifts in multiple wood traits across boreal forests, with consistent patterns observed across species. These findings highlight the value of large-scale forest inventory archives combined with improved analytical approaches for detecting long-term ecological responses to environmental change.

4.2 Drivers of $\delta^{15}N$ in boreal forests

Paper II documented a significant and spatially coherent decline in wood $\delta^{15}N$ ($P < 0.001$) across Swedish boreal forests from 1951–2017, using tree core archives to reconstruct long-term trends in ecosystem N availability. This downward trend was consistent across a broad latitudinal gradient, despite regional variation in Nr deposition and temperature. Such widespread isotopic shifts suggest a large-scale change in ecosystem N cycling rather than localized effects. Declining $\delta^{15}N$ in trees is widely interpreted as a proxy for reduced N availability, suggesting a progressive tightening of the boreal N cycle (Craine et al., 2018; Peñuelas et al., 2020).

Linear mixed models were used to evaluate the relative contributions of multiple environmental drivers. Temporal variation in anthropogenic Nr deposition did not fully account for the observed decline in $\delta^{15}N$, including in northern regions where Nr deposition has remained comparatively low and stable (Pihl Karlsson et al., 2024). In contrast, atmospheric CO_2 emerged as a key predictor of the isotopic trend, with highly significant ($P < 0.001$) results across sites, which was exhibited by substantial difference in the partial R^2 values of Nr deposition and CO_2 (partial R^2m values ≤ 0.005 versus 0.176, respectively). The spatial consistency of this relationship across a well-replicated site network indicates the influence of a large-scale driver, supporting the interpretation that rising CO_2 concentrations are influencing ecosystem N availability at large spatial scales.

I found a somewhat different pattern in wood N concentrations in **Paper I** and **II**. In **Paper I**, when restricting analysis to the 41–60-year age class, the same age class used in **Paper II**, the temporal pattern in wood N concentration differed between species, with no significant change for *P. abies* ($P = 0.181$) and a significant trend for *P. sylvestris* ($P = 0.001$). In contrast, no significant trend was found in **Paper II**. **Paper I** was based on a more limited dataset restricted to two counties, with smaller sample size and distinct geological conditions, which could influence wood chemistry and limit the generality of those patterns at broader spatial scales. In contrast, the Sweden-wide dataset used in **Paper II** is more spatially extensive and better replicated and therefore provides a stronger basis for inference. Regardless, I highlight that wood N concentration remains a poor proxy for plant N limitation due to its very low concentration and high sensitivity to variability in more abundant structural components, such as C and oxygen (O). Thus, despite some discrepancy in wood N concentration trends between the two studies, the $\delta^{15}N$ patterns were consistent, which provides a more reliable indicator of long-term changes in ecosystem N availability than bulk wood N concentration (Bukata & Kyser, 2005; Craine et al., 2015; Doucet et al., 2011; Poulson et al., 1995; Thurner et al., 2025).

The results further suggest that increasing N limitation may constrain the long-term response of boreal forests to eCO_2. Although higher CO_2 concentrations can stimulate C assimilation, sustained increases in biomass production depend on nutrient availability (Hungate et al., 2003; Peñuelas et al., 2020). A continued decline in N availability may therefore constrain boreal trees' capacity to sustain increased C uptake under rising CO_2,

suggesting that projections assuming stable nutrient availability may overestimate future C sequestration.

Within this context, shifts in plant-soil interactions may contribute to ecosystem responses to declining N availability. Boreal forests are typically dominated by EcM associations, which are central to plant N acquisition. Under increasing N limitation, greater C allocation belowground to support EcM-mediated nutrient uptake has been proposed as a response (Franklin et al., 2014; Hobbie & Högberg, 2012). Such responses are consistent with our observed system-wide decline in N availability.

Overall, the findings in **Paper II** indicate that N availability in boreal forests is declining as atmospheric CO_2 levels increase. The spatial coherence of $\delta^{15}N$ trends across Sweden suggests the influence of a dominant large-scale driver operating across diverse environmental conditions. These results highlight the importance of incorporating CO_2-driven changes in nutrient availability into Earth System Models to improve predictions of forest productivity and long-term C sink dynamics (Craine et al., 2018; Peñuelas et al., 2020).

4.3 Temporal changes in wood density and carbon concentration

Results from **Paper III** demonstrate that wood density in 10-year segments (sapwood) increased slightly but significantly over six decades ($P < 0.001$), with the increase more pronounced in *P. sylvestris* than in *P. abies*, which exhibited only a marginal increase. Both latitude and elevation exerted strong negative effects on wood density ($P < 0.001$), with lower wood density observed at higher latitudes and elevations across both species and sample types. These declines were more pronounced in *P. abies*, indicating species-specific sensitivity to environmental gradients (Swenson & Enquist, 2007; Cuny & Rathgeber, 2016). Tree diameter also had a significant negative effect ($P < 0.001$), with larger trees exhibiting lower wood density. Species differences were most evident in the 10-year segments, where *P. sylvestris* consistently showed higher density than *P. abies*. In contrast, these differences were not significant in whole cores ($P = 0.402$), suggesting that long-term developmental processes may override short-term species-specific responses (Auty et al., 2014).

Whole-core (sapwood and heartwood) wood density also increased over time ($P = 0.005$), although the trend was weaker than in 10-year segments. Mean wood density was significantly lower in whole cores (0.399 g cm^{-3}) compared to 10-year segments (0.432 g cm^{-3}; $P < 0.001$), reflecting the inclusion of lower-density heartwood (Herrero de Aza et al., 2011). The consistency of spatial patterns across both sample types indicates that environmental gradients and tree size strongly influence wood density, while temporal changes are more evident in recently formed sapwood.

The observed increase in wood density over time contrasts with findings from central Europe, where increasing forest growth has been associated with declining density (Pretzsch et al., 2018). In Swedish boreal forests, the results of **Paper III** suggest that increases in forest productivity have not been accompanied by reductions in wood density, potentially reflecting differences in forest management, genetics, or climatic conditions (Lucas et al., 2016). The pronounced spatial gradients further underscore the importance of temperature and site conditions in wood-forming processes (Swenson & Enquist, 2007; Cuny & Rathgeber, 2016).

In contrast to wood density, C concentration exhibited contrasting patterns between sample types. In 10-year segments, C concentration declined slightly but significantly over time ($P < 0.001$) and with elevation ($P < 0.001$), but showed no significant relationships with latitude, tree diameter, or species. This decline is consistent with broader findings that higher mean annual temperature is associated with reduced wood C content (Paroshy et al., 2021). In contrast, whole-core C concentration showed no significant temporal trend but increased modestly with latitude ($P = 0.047$) and tree diameter ($P = 0.089$) and remained unaffected by elevation. Mean C concentration was lower in whole cores (48.9%) than in 10-year segments (49.9%; $P < 0.001$), reflecting the integration of sapwood and heartwood with differing chemical composition (Galibina et al., 2024). Species differences in C concentration were small and only evident in sapwood segments, with *P. abies* showing slightly lower values than *P. sylvestris*.

These results align with findings from **Paper I**, which show a significant decline in wood C concentration over time across both species in the 41–60-year age class, the same age class used in **Paper III**. Together, the studies indicate that a decline in C concentration is a robust feature of sapwood formation. However, **Paper III** further demonstrates that this temporal signal is largely absent from whole-core samples, highlighting how integrating

sapwood and heartwood can mask changes detected in earlywood alone. The decline in C concentration may partly reflect a shift toward a higher proportion of latewood, which has a lower C concentration than earlywood (Lamlom & Savidge, 2003), a mechanism that is consistent with the lower mean C values observed in whole cores in **Paper III**.

The divergence between 10-year segments and whole cores highlights the importance of sampling strategy in interpreting wood traits and C dynamics. Ten-year segments capture recent physiological responses to environmental change, whereas whole cores integrate signals across the tree's lifespan, and are also more relevant for forest C stock estimation (Schweingruber, 1996). These differences indicate that temporal changes are more readily detected in sapwood, whereas whole-core values provide more stable estimates for large-scale C accounting.

These findings have direct implications for forest C accounting. Current Swedish reporting uses fixed C concentration values (48.0–48.8%) and assumes constant wood density (Skogsstyrelsen, 2000), yet both traits have been shown to vary significantly across space and time. Whole-core C concentrations were slightly higher than Swedish default values; however, they remained below the global default of 50% (IPCC, 2013), suggesting that national estimates may slightly underestimate and global defaults may slightly overestimate boreal forest C stocks.

Overall, the results demonstrate that wood density and C concentration vary systematically across temporal and spatial gradients in Swedish boreal forests. These findings challenge the assumption of constancy in forest C models and highlight the need for regionally derived, sampling-specific values to improve the accuracy of C stock estimates and assessments of boreal forest contributions to the global C cycle (Martin et al., 2018; Mensah & Petersson, 2024; IPCC, 2021).

4.4 Divergent wood $\delta^{15}N$ trends reveal increasing nitrogen limitation under rising CO_2

In **Paper IV**, wood $\delta^{15}N$ chronologies revealed contrasting responses among four boreal tree genera related to their N acquisition strategies. Non-N-fixing taxa (*Betula* spp., *P. sylvestris*, *P. abies*) exhibited significant long-term declines in $\delta^{15}N$ ($P < 0.001$), whereas no temporal trend was observed for N_2-fixing *Alnus* ($P = 0.191$). This stability, along with low inter-decadal

variability, likely reflects *Alnus'* reliance on atmospheric N_2 fixation for most of its N, which buffers its isotopic signature against fluctuations in soil N cycling (Scott, Perakis & Hibbs, 2008). In contrast, the consistent declines observed in non-N-fixing taxa indicate increasing sensitivity to changes in soil N supply over time.

Linear mixed-effects models identified atmospheric CO_2 as a significant negative predictor of $\delta^{15}N$ across all taxa, consistent with earlier findings for *P. sylvestris* and *P. abies* (**Paper II**). However, the magnitude of this effect differed among taxa. The strongest responses occurred in conifers, while *Betula* showed an intermediate decline and *Alnus* exhibited only a weak CO_2 effect, explaining only a very small portion of the overall model. This suggests that although N_2-fixing taxa are not fully decoupled from environmental change, they appear much more buffered than non-N-fixing taxa. In *Alnus*, N_2 fixation likely provides a steady source of N that balances variability in soil N uptake under rising CO_2, with plant $\delta^{15}N$ reflecting integrated ecosystem processes due to microbial transformation and fractionation of fixed N within soil pools (Craine et al., 2015; Robinson, 2001). Experimental evidence indicates that eCO_2 can stimulate biological N_2 fixation (Hoosbeek et al., 2011; Millett et al., 2012), although this response is likely constrained in boreal systems by N limitation and tightly conserved N cycling (Sponseller et al., 2016).

In contrast, the pronounced declines in $\delta^{15}N$ observed in *P. sylvestris* and *P. abies*, and to a lesser extent in *Betula*, are consistent with PNL, whereby rising CO_2 stimulates plant growth and N demand, leading to tighter N cycling and reduced isotopic discrimination (Craine et al., 2009; Luo et al., 2004). The weaker response in *Betula* relative to conifers may reflect partial buffering through associations with free-living N_2-fixing microbes (Smolander, 1990), suggesting that PNL effects vary among functional groups.

The contrasting responses between N_2-fixing and non-N-fixing species provide a critical test of the mechanisms underlying declining $\delta^{15}N$ chronologies. If increased photosynthetic nitrogen use efficiency (PNUE) were the dominant driver, similar isotopic trends would be expected across all taxa (Hiltbrunner et al., 2019; Olff et al., 2022). Instead, the absence of a temporal decline in *Alnus*, alongside consistent declines in non-N-fixing species, supports PNL as the primary mechanism (Stocker et al., 2025; Bassiouni et al., 2025). Although eCO_2 can enhance PNUE and reduce foliar

N concentrations (Bassiouni et al., 2025; Perkowski et al., 2025), these responses remain constrained by N availability at the whole-plant level and do not provide a mechanistic explanation for long-term declines in $\delta^{15}N$ (Perkowski et al., 2025; Stocker et al., 2025). Moreover, PNUE-driven reductions in plant N demand would be expected to increase soil N availability and promote N losses, leading to increasingly positive $\delta^{15}N$ values over time (BassiriRad et al., 2003), contrary to the observed patterns. Declining aquatic N exports from boreal ecosystems further support increasingly tight N cycling under rising CO_2 (Lucas et al., 2016; Nilsson et al., 2024).

Collectively, these results demonstrate that declining $\delta^{15}N$ chronologies in boreal forests are primarily driven by PNL rather than physiological downregulation of foliar N. Non-N-fixing species reflect long-term declines in N availability, whereas N_2-fixing species such as *Alnus* remain comparatively buffered, responding to rising CO_2 through shifts in N acquisition strategies rather than sustained N limitation.

5. Conclusions and implications

Trees act as long-term biological indicators, capturing environmental changes through their annual growth rings (Speer, 2010). This thesis used a unique tree-core archive to assess stemwood traits as indicators of boreal forest responses to environmental change and to evaluate their capacity to function as future C sinks. The main conclusions are:

I. The MTM is preferred for reconstructing long-term nutrient trends because it more effectively separates environmental signals from biological noise while maintaining biological age. Because N is sensitive to age-related processes due to its mobility in the stemwood, the STM can confound physiological and environmental signals. In contrast, both methods yield similar results for $\delta^{13}C$. This highlights MTM as the more reliable sampling approach for detecting long-term ecosystem change for certain nutrients.

II. Wood $\delta^{15}N$ declined consistently across Sweden's 1500-km latitudinal gradient, indicating a widespread reduction in N availability despite regional differences in Nr deposition. Rising atmospheric CO_2 was the primary driver, increasing N demand beyond supply and supporting PNL. This suggests boreal forests may not sustain the increased growth predicted by climate models, constraining their future role as C sinks.

III. Average C concentrations were higher than those used in Swedish accounting models but lower than the global default, indicating a slight underestimation nationally and an overestimation globally. Ten-year segments (sapwood) were more sensitive to recent environmental changes, whereas whole cores (sapwood and heartwood) better represent long-term trends.

IV. The N_2-fixing species *Alnus* showed no temporal change in wood $\delta^{15}N$, consistent with its primary reliance on atmospheric N_2 and indicating that declines in other species are driven by soil processes rather than internal physiology. In contrast, non-N-fixing *Betula*, *Pinus*, and *Picea* spp. exhibited declining wood $\delta^{15}N$, contradicting the PNUE, which was not a suitable explanation for declining $\delta^{15}N$ trends. Instead, the data support PNL as the driver of ecosystem-scale nutrient limitation, with implications for future forest productivity.

Photo: Kelley R. Bassett

6. Future perspectives

The findings in this thesis improve our understanding of N cycling in the boreal forest and the implications for future forest growth and C sequestration. Specifically, it clarifies how rising atmospheric CO_2 and climate change alter the structural and chemical properties of wood—key factors that are fundamentally tied to the forest's future as a C sink. While this work offers a necessary framework for understanding how these ecosystems may respond to future environmental stressors, there are knowledge gaps that could be addressed:

I. Could forest fertilization be a reasonable approach to counter the declines in N availability and promote sustained forest growth and sequestration in the boreal forest? Moreover, which sites would be suitable candidates, and which sites could have deleterious impacts on other ecosystem properties (e.g., biodiversity)?

II. Would mixed-species forest practices help alleviate N limitation in the boreal forest? Are there additional forest management strategies that could be implemented?

III. Does PNL occur across all types of site characteristics, such as across all soil moisture gradients?

IV. Would wood $\delta^{13}C$, a proxy for *i*WUE, help illuminate the potential role of drought in the observed decline in forest growth, and at what temporal resolution can these relationships be robustly evaluated?

V. How does genetically improved growing stock respond to declining N availability, and can this be better understood by incorporating DNA analysis of the cores?

VI. How can we build upon the systematic sampling protocols conducted by the NFI, e.g., expanding the archive to include larger-diameter cores for biogeochemical analyses in anticipation of advancements in other techniques and methodologies?

References

Ainsworth, E. A., & Rogers, A. (2007). The response of photosynthesis and stomatal conductance to rising CO_2: Mechanisms and environmental interactions. *Plant, Cell & Environment*, 30, 258–270.

Austin, A. T., & Vitousek, P. M. (1998). Nutrient dynamics on a precipitation gradient in Hawai'i. *Oecologia*, 113(4), 519–529.

Auty, D. et al. (2014). Models for predicting wood density variation in Scots pine. *Forestry: An International Journal of Forest Research*, 87(3), 449–458.

Bahn, M., Buchmann, N., & Knohl, A. (2012). Stable isotopes and biogeochemical cycles in terrestrial ecosystems. *Biogeosciences*, 9, 3979–3981.

Bassiouni, M., Smith, N. G., Reu, J. C., Penuelas, J., & Keenan, T. F. (2025). Observed declines in leaf nitrogen explained by photosynthetic acclimation to CO_2. *Proceedings of the National Academy of Sciences*, 122, e2501958122.

BassiriRad, H. et al. (2003). Widespread foliage $\delta^{15}N$ depletion under elevated CO_2: Inferences for the nitrogen cycle. *Global Change Biology*, 9, 1582–1590.

Belmecheri, S., & Lavergne, A. (2020). Compiled records of atmospheric CO_2 concentrations and stable carbon isotopes to reconstruct climate and derive plant ecophysiological indices from tree rings. *Dendrochronologia*, 63, 125748.

Binkley, D., Cromack, K., & Baker, D. (1994). Nitrogen fixation by red alder: Biology, rates, and controls. In D. E. Hibbs, D. S. DeBell, & R. F. Tarrant (Eds.), *The biology and management of red alder* (pp. 57–72). OSU Press.

Binkley, D., & Högberg, P. (1997). Does atmospheric deposition of nitrogen threaten the efficiency of grazing, recycling, and regeneration of northern forests? *Plant and Soil*, 191(1), 35–51.

Bobbink, R. et al. (2010). Global assessment of nitrogen deposition effects on terrestrial plant diversity: A synthesis. *Ecological Applications*, 20(1), 30–59.

Bonan, G. B., & Shugart, H. H. (1989). Ecological processes in boreal forests. *Annual Review of Ecology and Systematics*, 20, 1–28.

Bond-Lamberty, B., Gower, S. T., Wang, C., Cyr, P., & Veldhuis, H. (2006). Nitrogen dynamics of a boreal black spruce wildfire chronosequence. *Biogeochemistry*, 81, 1–16.

Brandt, J. P. (2009). The extent of the North American boreal zone. *Environmental Reviews*, 17, 101–161.

Boonstra, R. et al. (2016). Why do the boreal forest ecosystems of northwestern Europe differ from those of western North America? *BioScience*, 66(9), 722–734.

Bukata, A. R., & Kyser, T. K. (2005). Response of the nitrogen isotopic composition of tree-rings following tree-clearing and land-use change. *Environmental Science & Technology,* 39, 7777–7783.

Bunn, R. A. et al. (2024). What determines transfer of carbon from plants to mycorrhizal fungi? *New Phytologist*, 244, 1199–1215.

Canadell, J. G. et al. (2007). Contributions to accelerating atmospheric CO_2 growth from economic activity, carbon intensity, and efficiency of natural sinks. *Proceedings of the National Academy of Sciences*, 104, 18866–18870.

Chave, J., Coomes, D., Jansen, S., Lewis, S. L., Swenson, N. G., & Zanne, A. E. (2009). Towards a worldwide wood economics spectrum. *Ecology Letters*, 12, 351–366.

Craine, J. M. et al. (2015). Ecological interpretations of nitrogen isotope ratios of terrestrial plants and soils. *Plant and Soil*, 396, 1–26.

Craine, J. M. et al. (2018). Isotopic evidence for oligotrophication of terrestrial ecosystems. *Nature Ecology & Evolution*, 2, 1735–1744.

Cuny, H. E. et al. (2015). Woody biomass production lags stem-girth increase by over one month in coniferous forests. *Nature Plants*, 1, 15160.

Cuny, H. E., & Rathgeber, C. B. K. (2016). Xylogenesis: Coniferous trees of temperate forests are listening to the climate tale during the growing season but only remember the last words! *Plant Physiology*, 171(1), 306–317.

Dawson, T. E., Mambelli, S., Plamboeck, A. H., Templer, P. H., & Tu, K. P. (2002). Stable isotopes in plant ecology. *Annual Review of Ecology and Systematics*, 33, 507–559.

Deluca, T. H., Zackrisson, O., Nilsson, M.-.C., & Sellstedt, A. (2002). Quantifying nitrogen-fixation in feather moss carpets of boreal forests. *Nature*, 419, 917–920.

Deluca, T. H., Zackrisson, O., Gundale, M. J., & Nilsson, M.-.C. (2008). Ecosystem feedbacks and nitrogen fixation in boreal forests. *Science*, 320, 1181.

DeLuca, T. H., & Boisvenue, C. (2012). Boreal forest soil carbon: Distribution, function and modelling. *Forestry: An International Journal of Forest Research*, 85, 161–184.

Díaz, S. et al. (2016). The global spectrum of plant form and function. *Nature*, 529, 167–171.

Doucet, A., Savard, M. M., Bégin, C., & Smirnoff, A. (2011). Is wood pre-treatment essential for tree-ring nitrogen concentration and isotope analysis? *Rapid Communications in Mass Spectrometry*, 25, 469–475.

Ehleringer, J. R., Hall, A. E., & Farquhar, G. D. (Eds.). (1993). *Stable isotopes and plant carbon-water relations*. Academic Press.

Eriksson, B. (1985). The Swedish National Forest Inventory. In *National Forest Inventory systems in Europe* (conference meeting). Albert Ludwigs Universität, Freiburg, Germany.

Erisman, J. W., Galloway, J., Seitzinger, S., Bleeker, A., & Butterbach-Bahl, K. (2011). Reactive nitrogen in the environment and its effect on climate change. *Current Opinion in Environmental Sustainability*, 3(5), 281–290.

Esseen, P.-.A., Enhnström, B., Ericson, L., & Sjöberg, K. (1997). Boreal forests. *Ecological Bulletins*, 46, 16–47.

Farquhar, G., Ehleringer, J. R., & Hubick, K. T. (1989). Carbon isotope discrimination and photosynthesis. *Annual Review of Plant Physiology and Plant Molecular Biology*, 40, 503–537.

Finzi, A. C. et al. (2006). Progressive nitrogen limitation of ecosystem processes under elevated CO_2 in a warm temperate forest. *Ecology*, 87, 15–25.

Firestone, M. K., & Davidson, E. A. (1989). Microbiological basis of NO and N_2O production and consumption in soils. In M. O. Andreae & D. S. Schimel (Eds.), *Exchange of trace gases between terrestrial ecosystems and the atmosphere* (pp. 7–21). John Wiley & Sons.

Forrester, D. I. (2019). Linking forest growth with stand structure: Tree size inequality, tree growth or resource partitioning and the asymmetry of competition. *Forest Ecology and Management*, 447, 139–157.

Franklin, O., Näsholm, T., Högberg, P., & Högberg, M. N. (2014). Forests trapped in nitrogen limitation: An ecological market perspective on ectomycorrhizal symbiosis. *New Phytologist*, 203, 657–666.

Fridman, J., Holm, S., Nilsson, M., Nilsson, P., Ringvall, A. H., & Ståhl, G. (2014). Adapting national forest inventories to changing requirements: The case of the Swedish National Forest Inventory at the turn of the 20th century. *Silva Fennica*, 48(3), 1095. https://doi.org/10.14214/sf.1095

Friedlingstein, P. et al. (2022). Global carbon budget 2022. *Earth System Science Data*, 14(11), 4811–4900.

Fritts, H. C. (1976). *Tree rings and climate*. Academic Press.

Galibina, N. A., Nikerova, K. M., Moshnikov, S. A., & Kryshen, A. M. (2024). Assessment of the heartwood contribution to carbon accumulation in *Pinus sylvestris* L. trees under different forest site conditions. *Forest Ecosystems*, 12, 100274.

Galloway, J. N. et al. (2004). Nitrogen cycles: Past, present, and future. *Biogeochemistry*, 70, 153–226.

Gauthier, S., Bernier, P., Kuuluvainen, T., Shvidenko, A. Z., & Schepaschenko, D. G. (2015). Boreal forest health and global change. *Science*, 349(6250), 819–822.

Gerhart, L. M., & McLauchlan, K. K. (2014). Reconstructing terrestrial nutrient cycling using stable nitrogen isotopes in wood. *Biogeochemistry*, 120, 1–21.

Giorgi, F. (2006). Climate change hot-spots. *Geophysical Research Letters*, 33, L08707.

Gundale, M. J., From, F., Bach, L. H., & Nordin, A. (2011). Anthropogenic nitrogen deposition in boreal forests has a minor impact on the global carbon cycle. *Global Change Biology*, 17(1), 276–286.

Guo, P., Zhao, X., Wang, X., Feng, Q., Li, X., & Tan, Y. (2024). Wood density and carbon concentration jointly drive wood carbon density of five Rosaceae tree species. *Forests*, 15(7), 1102.

Harris, I. et al. (2020). Version 4 of the CRU TS monthly high-resolution gridded multivariate climate dataset. *Scientific Data*, 7, 1–18.

Hasselquist, N.J. et al. (2016). Greater carbon allocation to mycorrhizal fungi reduces tree nitrogen uptake in a boreal forest. *Ecology*, 97, 1012–1022.

Hart, S. C., & Classen, A. T. (2003). Potential for assessing long-term dynamics in soil nitrogen availability from variations in $\delta^{15}N$ of tree rings. *Isotopes in Environmental and Health Studies*, 39, 15–28.

Herrero de Aza, C., Turrión, M. B., Pando, V., & Bravo, F. (2011). Carbon in heartwood, sapwood and bark along the stem profile in three Mediterranean *Pinus* species. *Annals of Forest Science*, 68, 1067.

Higuchi, T. (1997). *Biochemistry and molecular biology of wood*. Springer-Verlag.

Hiltbrunner, E., Körner, C., Meier, R., Braun, S., & Kahmen, A. (2019). Data do not support large-scale oligotrophication of terrestrial ecosystems. *Nature Ecology & Evolution*, 3, 1285–1286.

Hobbie, E. A., & Högberg, P. (2012). Nitrogen isotopes link mycorrhizal fungi and plants to nitrogen dynamics. *New Phytologist*, 196, 367–382.

Högberg, P. (1997). Tansley Review No. 95: ^{15}N natural abundance in soil–plant systems. *New Phytologist*, 137, 179–203.

Högberg, M.N., Myrold, D. D., Giesler, R., & Högberg, P. (2006). Contrasting patterns of soil N-cycling in model ecosystems of Fennoscandian boreal forests. *Oecologia*, 147, 96–107.

Hoosbeek, M. R., Lukac, M., Velthorst, E., Smith, A. R., & Godbold, D. L. (2011). Free atmospheric CO_2 enrichment increased above ground biomass but did not affect symbiotic N_2-fixation and soil carbon dynamics in a mixed deciduous stand in Wales. *Biogeosciences*, 8, 353–364.

Hungate, B. A., Dukes, J. S., Shaw, M. R., Luo, Y. Q., & Field, C. B. (2003). Nitrogen and climate change. *Science*, 302(5650), 1512–1513.

Hupperts, S.F. et al. (2025). A meta-regression of 18 wildfire chronosequences reveals key environmental drivers and knowledge gaps in the boreal nitrogen balance. *Global Change Biology*, 31(e70398).

Hyvönen, R. et al. (2007). The likely impact of elevated CO_2, nitrogen deposition, increased temperature and management on carbon sequestration in temperate and boreal forest ecosystems: A literature review. *New Phytologist*, 173, 463–480.

Intergovernmental Panel on Climate Change (IPCC). (2013). Climate change 2013: The physical science basis. Contribution of Working Group I to the Fifth Assessment Report of the Intergovernmental Panel on Climate Change (T. F. Stocker et al., Eds.). Cambridge University Press.

IPCC. (2018). Global warming of 1.5°C: An IPCC special report on the impacts of global warming of 1.5°C above pre-industrial levels and related global greenhouse gas emission pathways, in the context of strengthening the global response to the threat of climate change, sustainable development, and efforts to eradicate poverty (V. Masson-Delmotte et al., Eds.). Cambridge University Press.

IPCC. (2021). Climate change 2021: The physical science basis. Contribution of Working Group I to the Sixth Assessment Report of the Intergovernmental Panel on Climate Change (V. Masson-Delmotte et al., Eds.). Cambridge University Press.

IPCC. (2023). Climate change 2023: Synthesis report. Contribution of Working Groups I, II and III to the Sixth Assessment Report of the Intergovernmental Panel on Climate Change (Core Writing Team, H. Lee, & J. Romero, Eds.). IPCC.

Kallarackal, J., & Ramírez, F. (2024). Wood density and biomass. In *Wood density: Functional trait in plants* (pp. 75–88). Springer Nature.

Kellomäki, S., Peltola, H., Nuutinen, T., Korhonen, K. R., & Strandman, H. (2008). Sensitivity of managed boreal forests in Finland to climate change, with implications for adaptive management. *Philosophical Transactions of the Royal Society of London*, 363, 2341–2351.

Köhl, M. et al. (2015). Changes in forest production, biomass and carbon: Results from the 2015 UN FAO Global Forest Resource Assessment. *Forest Ecology and Management*, 352, 21–34.

Korhonen, J. F. J. et al. (2013). Nitrogen balance of a boreal Scots pine forest. *Biogeosciences*, 10, 1083–1095.

Kranabetter, J. M., Saunders, S., MacKinnon, J. A., Klassen, H., & Spittlehouse, D. L. (2013). An assessment of contemporary and historic nitrogen availability in contrasting coastal Douglas-fir forests through $\delta^{15}N$ of tree rings. *Ecosystems*, 16, 111–122.

Lagerström, A., Nilsson, M. C., Zackrisson, O., & Wardle, D.A.(2007). Ecosystem input of nitrogen through biological fixation in feather mosses during ecosystem retrogression. *Functional Ecology*, 21, 1027–1033.

Lamlom, S.H. & Savidge, R.A. (2003). A reassessment of carbon content in wood: variation within and between 41 North American species. *Biomass Bioenergy*, 25, 381–388.

Lan, X. et al. (2022). Atmospheric carbon dioxide dry air mole fractions from the NOAA GML Carbon Cycle Cooperative Global Air Sampling Network, 1968–2021 (Version 2022-11-21).

LeBauer, D. S., & Treseder, K. K. (2008). Nitrogen limitation on net primary productivity in terrestrial ecosystems is globally distributed. *Ecology*, 89, 371–379.

Lindo, Z., Nilsson, M.-C., & Gundale, M. J. (2013). Bryophyte-cyanobacteria associations as regulators of the northern latitude carbon balance in response to global change. *Global Change Biology*, 19, 2022–2035.

Lövblad, G. (2000). Nitrogen deposition now and in the future. In U. Bertills & T. Näsholm (Eds.), *Effects of nitrogen deposition on forest ecosystems*. Swedish Environmental Protection Agency.

Lucas, R. W. et al. (2016). Long-term declines in stream and river inorganic nitrogen (N) export correspond to forest change. *Ecological Applications*, 26(2), 545–556.

Lundström, U. S., van Breemen, N., & Bain, D. (2000). The podzolization process: A review. *Geoderma*, 94(2–4), 91–107.

Luo, Y. et al. (2004). Progressive nitrogen limitation of ecosystem responses to rising atmospheric CO_2. *BioScience*, 54, 731–739.

Maljanen, M., Alm, J., Martikainen, P. J., & Repo, T. (2010). Prolongation of soil frost resulting from reduced snow cover increases nitrous oxide emissions from boreal forest soil. *Boreal Environment Research*, 15, 34–42.

Manzoni, S., Jackson, R. B., Trofymow, J. A., & Porporato, A. (2008). The global stoichiometry of litter nitrogen mineralization. *Science*, 321, 684–686.

Marklund, L. G. (1988). Biomass functions for pine, spruce and birch in Sweden (Report No. 45). Swedish University of Agricultural Sciences, Department of Forest Survey.

Martin, A. R., Doraisami, M., & Thomas, S. C. (2018). Global patterns in wood carbon concentration across the world's trees and forests. *Nature Geoscience*, 11(12), 915–920.

Martínez-Sancho, E. et al. (2020). The GenTree dendroecological collection, tree-ring and wood density data from seven tree species across Europe. *Scientific Data*, 7, 1.

Mason, R. E. et al. (2022a). Evidence, causes, and consequences of declining nitrogen availability in terrestrial ecosystems. *Science*, 376, 1–11.

Mason, R. E. et al. (2022b). Explanations for nitrogen decline—Response. *Science*, 376, 1170.

McCarroll, D., & Loader, N. J. (2004). Stable isotopes in tree rings. *Quaternary Science Reviews*, 23, 771–801.

McLauchlan, K. K. et al. (2017). Centennial-scale reductions in nitrogen availability in temperate forests of the United States. *Scientific Reports*, 7, 7856.

McLaren, J. R., & Turkington, R. (2013). Boreal forest ecosystems. In S. A. Levin (Ed.), *Encyclopedia of biodiversity* (2nd ed.). Academic Press.

Mead, D. J., & Preston, C. M. (1994). Distribution and retranslocation of ^{15}N lodgepole pine over eight growing seasons. *Tree Physiology*, 4, 389–402.

Mensah, A. A., & Petersson, H. (2024). Carbon concentration of living tree biomass of *Pinus sylvestris*, *Picea abies*, *Betula pendula* and *Betula pubescens* in Sweden. *Scandinavian Journal of Forest Research*, 39(3–4), 145–155.

Millett, J., Godbold, D., Smith, A. R., & Grant, H. (2012). N_2 fixation and cycling in *Alnus glutinosa*, *Betula pendula* and *Fagus sylvatica* woodland exposed to free air CO_2 enrichment. *Oecologia*, 169(2), 541–552.

Näsholm, T., Ekblad, A., Nordin, A., Giesler, R., Högberg, M., & Högberg, P. (1998). Boreal forest plants take up organic nitrogen. *Nature*, 392(6679), 914–916.

National Oceanic and Atmospheric Administration. (2022, June 3). Carbon dioxide now more than 50% higher than pre-industrial levels.

Nikolov, N., & Helmisaari, H. (1992). Silvics of the circumpolar boreal forest tree species. In H. H. Shugart, R. Leemans, & G. B. Bonan (Eds.), *A systems analysis of the global boreal forest* (pp. 13–84). Cambridge University Press.

Nilsson, J. L., Camiolo, S., Huser, B., Agstam-Norlin, O., & Futter, M. (2024). Widespread and persistent oligotrophication of northern rivers. *Science of the Total Environment*, 955, 177261.

Nömmik, H. (1966). The uptake and translocation of fertilizer N^{15} in young trees of Scots pine and Norway spruce. *Studia Forestalia Suecica*, 35.

Norby, R.J., Warren, J. M., Iversen, C. M., Medlyn, B. E., & McMurtrie, R. E. (2010). CO_2 enhancement of forest productivity constrained by limited nitrogen availability. *Proceedings of the National Academy of Sciences*, 107, 19368–19373.

Oulehle, F. et al. (2022). Changes in forest nitrogen cycling across deposition gradient revealed by $\delta^{15}N$ in tree rings. *Environmental Pollution*, 304, 119104.

Olff, H. et al. (2022). Explanations for nitrogen decline. *Science*, 376, 1169–1170.

Pan, Y. et al. (2011). A large and persistent carbon sink in the world's forests. *Science*, 333, 988–993.

Paroshy, N. J., Doraisami, M., Kish, R., & Martin, A.R. (2021). Carbon concentration in the world's trees across climatic gradients. *New Phytologist*, 232(1), 123–133.

Peñuelas, J. et al. (2020). Increasing atmospheric CO_2 concentrations correlate with declining nutritional status of European forests. *Communications Biology*, 3, 125.

Perkowski, E. A., Ezekannagha, E., & Smith, N. G. (2025). Nitrogen demand, availability, and acquisition strategy control plant responses to elevated CO_2. *Journal of Experimental Botany*, 76(10), 2908–2923.

Peuke, A. D. (2010). Correlations in concentrations, xylem and phloem flows, and partitioning of elements and ions in intact plants: A summary and statistical reevaluation of modelling experiments in *Ricinus communis*. *Journal of Experimental Botany*, 61, 635–655.

Pihl Karlsson, G., Akselsson, C., Hellsten, S., & Karlsson, P.E. (2011). Reduced European emissions of S and N—Effects on air concentrations, deposition and soil water chemistry in Swedish forests. *Environmental Pollution*, 159(12), 3571–3582.

Pihl Karlsson, G., Akselsson, C., Hellsten, S., & Karlsson, P.E. (2024). Atmospheric deposition and soil water chemistry in Swedish forests since 1985-Effects of reduced emissions of sulphur and nitrogen. *Science of the Total Environment*, 913, 169734.

Poulson, S. R., Chamberlain, C. P., & Friedland, A. J. (1995). Nitrogen isotope variation of tree rings as a potential indicator of environmental change. *Chemical Geology*, 125, 307–315.

Prescott, C. E. (2010). Litter decomposition: What controls it and how can we alter it to sequester more carbon in forest soils? *Biogeochemistry*, 101(1–3), 133–149.

Pretzsch, H. (2016). Ertragstafel-Korrekturfaktoren für Umwelt- und Mischungseffekte. AFZ-Wald, 187, 47–50.

Pretzsch, H., Biber, P., Schiitze, G., Kemmerer, J., & Uh, E. (2018). Wood density reduced while wood volume growth accelerated in central European forests since 1870. *Forest Ecology and Management*, 429, 589–616.

R Core Team. (2022). R: A language and environment for statistical computing. R Foundation for Statistical Computing.

R Core Team. (2023). R: A language and environment for statistical computing. R Foundation for Statistical Computing.

Rawson, H. M., Begg, J. E., & Woodward, R. G. (1977). The effect of atmospheric humidity on photosynthesis, transpiration and water use efficiency of leaves of several plant species. *Planta*, 134, 5–10.

Reich, P. et al. (2006). Nitrogen limitation constrains sustainability of ecosystem response to CO_2. *Nature*, 440, 922–925.

Riksskogstaxeringen. (2025). Swedish National Forest Inventory. Swedish University of Agricultural Sciences.

Robinson, D. (2001). $\delta^{15}N$ as an integrator of the nitrogen cycle. *Trends in Ecology & Evolution*, 3, 153–162.

Rossi, S., Deslauriers, A., & Anfodillo, T. (2006). Assessment of cambial activity and xylogenesis by microsampling tree species: An example at the alpine timberline. *IAWA Journal*, 27(4), 383–394.

Saurer, M. et al. (2014). Spatial variability and temporal trends in water-use efficiency of European forests. *Global Change Biology*, 20, 3700–3712.

Schimel, J. P., & Bennett, J. (2004). Nitrogen mineralization: Challenges of a changing paradigm. *Ecology*, 85, 591–602.

Schweingruber, F. H. (1996). *Tree rings and environmental dendroecology*. Paul Haupt.

Scott, E. E., Perakis, S. S., & Hibbs, D. E. (2008). $\delta^{15}N$ patterns of Douglas-fir and red alder riparian forests in the Oregon Coast Range. *Forest Science*, 54(2), 140–147.

Sémhur. (2010). Map of the circumpolar boreal forests (taiga). Wikimedia Commons. https://commons.wikimedia.org/wiki/File:Taiga.png

Skogsstyrelsen. (2000). Klimatförändringar och Sveriges skogar (Rapport No. 2). Skogsstyrelsen.

Smith, S. E., & Read, D. J. (2008). Mycorrhizal Symbiosis (3rd ed.). Academic Press.

Smolander, A. (1990). *Frankia* populations in soils under different tree species—with special emphasis on soils under *Betula pendula*. *Plant and Soil*, 121(1), 1–10.

Speer, J. (2010). *Fundamentals of tree-ring research*. University of Arizona Press.

Sponseller, R. A., et al. (2016). Nitrogen dynamics in managed boreal forests: Recent advances and future research directions. *Ambio*, 45, 175–187.

Stein, L. Y., & Klotz, M. G. (2016). The nitrogen cycle. *Current Biology*, 26(3), R94–R98.

Stocker, B. D. et al. (2025). Empirical evidence and theoretical understanding of ecosystem carbon and nitrogen cycle interactions. *New Phytologist*, 245(1), 49–68.

Tamm, C. O. (1991). *Nitrogen in terrestrial ecosystems: Questions of productivity, vegetational changes, and ecosystem stability*. Springer.

Taylor, B. R., Parkinson, D., & Parsons, W. F. J. (1989). Nitrogen and lignin content as predictors of litter decay rates: A microcosm test. *Ecology*, 70, 97–104.

Terrer, C., Vicca, S., Hungate, B. A., Phillips, R. P., & Prentice, I. C. (2016). Mycorrhizal association as a primary control of the CO_2 fertilization effect. *Science*, 353(6294), 72–74.

Thiffault, E. (2019). Boreal forests and soils. In *Global change and forest soils: Cultivating stewardship of a finite natural resource* (Vol. 36, pp. 59–82).

Thomas, D. S., & Martin, A. R. (2012). Carbon content of tree tissues: A synthesis. *Forests*, 3, 332–352.

Thorell, K. E., & Östlin, E. O. (1931). The National Forest Survey of Sweden. *Journal of Forestry*, 29, 585–591.

Threatt, S. D., & Rees, D. C. (2023). Biological nitrogen fixation in theory, practice, and reality: A perspective on the molybdenum nitrogenase system. *FEBS Letters*, 597, 45–58.

Thurner, M. et al. (2025). Nitrogen concentrations in boreal and temperate tree tissues vary with tree age/size, growth rate and climate. *Biogeosciences*, 22, 1475–1493.

Tomlinson, G. et al. (2014). The mobility of nitrogen across tree-rings of Norway spruce (*Picea abies* L.) and the effect of extraction method on tree-ring $\delta^{15}N$ and $\delta^{13}C$ values. *Rapid Communications in Mass Spectrometry*, 27, 1258–1264.

Tyree, M. T., & Zimmermann, M. H. (2002). *Xylem structure and the ascent of sap* (2nd ed.). Springer.

Vallotton, J. D., & Unc, A. (2024). Soil carbon in the boreal region under climate and land use change. *Soil Use and Management*, 40, e13108.

Vitousek, P. M., & Howarth, R. W. (1991). Nitrogen limitation on land and in the sea: How can it occur? *Biogeochemistry*, 13(2), 87–115.

Walker, A. P., et al. (2021). Integrating the evidence for a terrestrial carbon sink caused by increasing atmospheric CO_2. *New Phytologist*, 229(5), 2413–2445.

Yang, H. et al. (2024). Global patterns of tree wood density. *Global Change Biology*, 30(3), e17224.

Yang, J., & Tian, H. (2023). ISIMIP3a N-deposition input data (Version 1.3). ISIMIP. https://doi.org/10.48364/ISIMIP.759077.3

Yuan, W. et al. (2019). Increased atmospheric vapor pressure deficit reduces global vegetation growth. *Science Advances*, 5, 1–12.

Yue, K., Peng, Y., Peng, C., Yang, W., Peng, X. & Wu, F. (2016). Stimulation of terrestrial ecosystem carbon storage by nitrogen addition: A meta-analysis. *Scientific Reports*, 6, 19895.

Popular science summary

Human-created carbon dioxide (CO_2) emissions from fossil fuels are a major contributor to current climate change. Terrestrial ecosystems offset a substantial portion of this CO_2 through photosynthesis, as plants take up CO_2 from the atmosphere and use it for growth. Boreal forests play a crucial role by capturing and storing a significant amount of global carbon in tree biomass, such as wood, roots, and leaves, as well as in forest soils. In recent decades, boreal forest growth has increased, sparking growing interest in the processes that control this carbon uptake. However, the ability of boreal forests to continue sequestering carbon depends on the availability of essential nutrients, particularly nitrogen, which is widely considered limiting because demand exceeds supply.

Trees act as natural records of environmental change by capturing conditions in their annual growth rings. In this thesis, I used an extensive archive of tree cores—cylindrical samples extending from the outer bark to the tree's center (pith)—collected over the past several decades by the National Forest Inventory across Swedish boreal forests to evaluate long-term environmental changes.

Because nitrogen is mobile within wood—being redistributed from areas of low demand to areas of higher demand in the tree—it can be influenced by age-related processes within the stem. As a result, measurements spanning several decades from a single core can make it difficult to distinguish biological effects from environmental signals. This motivated me to evaluate alternative sampling approaches for reconstructing long-term nutrient trends in wood. The results show that building a chronology (a time series) using multiple tree cores—one core per decade, of the same age—provides a more reliable method than using on a single tree core to retrieve all decades. Using multiple tree cores from the archive better distinguishes environmental changes from age-related effects. In contrast, carbon remains more stable in wood and is largely unaffected by the method, indicating that nutrients respond differently to the sampling approach.

Using this alternative method, I then analyzed stable nitrogen isotopes in wood, which serve as an indicator of nitrogen availability. The results revealed a consistent long-term decline in nitrogen availability across Sweden's approximately 1500-km north-to-south gradient. This pattern, evident over several decades, occurred despite regional differences in

atmospheric nitrogen deposition, which historically follows a gradient of low in the north to high in the south. Instead, the pattern was primarily associated with rising atmospheric CO_2, which is thought to increase plant nitrogen demand beyond available supply, leading to progressive nitrogen limitation. This suggests that nutrient constraints may limit sustained increases in forest growth under elevated CO_2, thereby reducing the future strength of boreal forests as carbon sinks.

Further comparisons among different boreal tree species helped clarify the mechanisms behind the decline in wood nitrogen isotope values. The nitrogen-fixing genus Alder (*Alnus*) showed no change in wood isotope values over time, consistent with its ability to obtain nitrogen directly from the atmosphere and its reduced dependence on soil nitrogen. In contrast, non-fixing species—birch, Scots pine, and Norway spruce *(Betula*, *Pinus sylvestris*, and *Picea abies*)—showed clear declines in wood nitrogen isotope values. This comparison allowed me to distinguish between two proposed explanations for the observed trends. One explanation is that trees increase nitrogen use efficiency under rising atmospheric CO_2, which would lead to similar isotopic trends across all species. However, this alone cannot account for the contrasting responses I observed among species. The alternative explanation is that nitrogen availability is declining due to changes in soil nitrogen cycling, which would primarily affect species that rely on soil nitrogen. In the results, I show support for the second explanation: the absence of a temporal trend in *Alnus*, combined with clear declines in non-N-fixing species, indicates that the observed patterns are mainly driven by changes in soil nitrogen cycling and availability. Together, these results support the idea that increasing nitrogen limitation is shaping forest responses to elevated CO_2, with important implications for future forest growth and carbon storage.

Finally, I investigated changes in wood density and carbon concentration—two key properties used to estimate forest carbon storage—using 10-year segments from the outermost part of the tree near the bark and whole cores that included all wood to the center (pith). Using tree cores from Scots pine and Norway spruce, I found that these wood traits vary across time and space, as well as with latitude, elevation, and tree diameter. Wood density increased slightly over time, while carbon concentration declined in the outermost, younger wood but remained stable in whole cores. This shows that short-term samples capture recent environmental changes, whereas

whole cores reflect longer-term patterns. These results highlight that assuming constant wood properties can lead to errors in carbon estimates and emphasize the need for regionally specific values to improve assessments of forest carbon storage.

The goal of this thesis was to provide a clearer picture of how nutrients in boreal forests change over time. My results indicate a large-scale reduction in nitrogen availability, which could slow forest growth and thus limit how much carbon boreal forests can store in the future. Overall, this work improves our understanding of how boreal forests function and helps us better predict their role in the carbon cycle as the climate continues to change.

Populärvetenskaplig sammanfattning

De koldioxidutsläpp (CO_2) som orsakas av människan genom användning av fossila bränslen är en av de främsta orsakerna till dagens klimatförändringar. Landekosystemen neutraliserar en betydande del av denna koldioxid genom fotosyntesen, då växterna tar upp koldioxid från atmosfären och använder den för sin tillväxt. Boreala skogar spelar en avgörande roll genom att binda och lagra en betydande mängd globalt kol i trädbiomassan, såsom i ved, rötter och blad, samt i marken. Under de senaste decennierna har tillväxten i de boreala skogarna ökat, vilket har väckt ett växande intresse för de processer som styr detta kolupptag. De boreala skogarnas förmåga att fortsätta binda kol beror dock på tillgången på viktiga näringsämnen, särskilt kväve, som allmänt anses vara en begränsande faktor eftersom efterfrågan överstiger tillgången.

Träd fungerar som naturliga arkiv över miljöförändringar genom att de registrerar förhållandena i sina årsringar. I denna avhandling använde jag ett omfattande arkiv av borrkärnor – cylindriska prover som sträcker sig från den yttre barken till trädets centrum (märgen)—som samlats in under de senaste decennierna av Riksskogstaxeringen i svenska boreala skogar för att utvärdera långsiktiga miljöförändringar.

Eftersom kväve är rörligt i veden—det omfördelas från områden med lågt behov till områden med högre behov i trädet – kan det påverkas av åldersrelaterade processer i stammen. Följaktligen kan mätningar som omfattar flera decennier och som hämtats från en enda borrkärna göra det svårt att skilja mellan biologiska effekter och miljömässiga signaler. Detta motiverade till mig att utvärdera alternativa provtagningsmetoder för att rekonstruera långsiktiga näringstrender i trä. Resultaten visar att det är en mer tillförlitlig metod att bygga upp en kronologi (en tidsserie) med hjälp av flera borrkärnor – en kärna per årtionde, alla av samma ålder—än att använda en enda borrkärna för att få fram data för alla årtionden. Genom att använda flera borrkärnor från arkivet kan man bättre skilja miljöförändringar från åldersrelaterade effekter. Däremot är kol mer stabilt i borrkärnorna och påverkas i stort sett inte av metoden, vilket tyder på att näringsämnena reagerade olika på provtagningsmetoden.

Med hjälp av denna alternativa metoden analyserade jag sedan stabila kväveisotoper i borrkärnorna, vilket fungerar som en indikator på kvävetillgången. Resultaten visade på en konsekvent långsiktig minskning

av kvävetillgången längs Sveriges cirka 1 500 km långa nord-sydliga gradient. Detta mönster, som varit tydligt under flera decennier, uppstod trots regionala skillnader i kvävedeposition från atmosfären, vilka historiskt sett följer en gradient från låga nivåer i norr till höga i söder. I stället var mönstret främst kopplat till stigande atmosfärisk koldioxidhalt, vilket tros öka växternas kvävebehov utöver det tillgängliga utbudet, vilket leder till en gradvis kvävebegränsning. Detta tyder på att näringsbegränsningar kan hämma en hållbar ökning av skogstillväxten vid förhöjda koldioxidhalter, vilket därmed minskar de boreala skogarnas framtida förmåga att fungera som kolsänkor i jämförelse med vad man tidigare trott.

Ytterligare jämförelser mellan olika boreala trädslag bidrog till att klarlägga mekanismerna bakom nedgången i kväveisotopvärdena i borrkärnorna. Det kvävefixerande släktet al (*Alnus*) uppvisade inga förändringar i isotopvärdena i veden över tid, vilket stämmer överens med dess förmåga att ta upp kväve direkt från atmosfären och dess minskade beroende av kväve i marken. Däremot visade icke-kvävefixerande arter—björk, tall och gran (*Betula*, *Pinus sylvestris* och *Picea abies*)—tydliga minskningar i kväveisotopvärdena i veden. Denna jämförelse gjorde det möjligt för mig att skilja mellan två föreslagna förklaringar till de observerade trenderna. En förklaring är att träd ökar sin kväveanvändningseffektivitet vid stigande atmosfärisk koldioxidhalt, vilket skulle leda till likartade isotopiska trender hos alla arter. Detta kan dock inte ensamt förklara de kontrasterande responserna som jag observerade mellan arterna. Den alternativa förklaringen är att kvävetillgången minskar på grund av förändringar i kvävecykeln i marken, vilket främst skulle påverka arter som är beroende av markkväve. I resultaten visar jag stöd för den andra förklaringen: avsaknaden av en tidsmässig trend hos *Alnus*, i kombination med tydliga minskningar hos icke-kvävefixerande arter, indikerar att de observerade mönstren huvudsakligen drivs av förändringar i kvävecykeln och av kvävetillgången i marken. Sammantaget stöder dessa resultat idén att ökande kvävebegränsning formar skogens respons på förhöjda koldioxidhalter, med viktiga implikationer för framtida skogstillväxt och koldioxidlagring.

Slutligen undersökte jag förändringar i veddensiteten och kolkoncentrationen i trä—två viktiga egenskaper som används för att uppskatta skogens kollagring—med hjälp av 10-årssegment från trädets yttersta del nära barken och hela borrkärnor, vilket inkluderade all ved, till

mitten (märgen). Med hjälp av borrkärnor från tall och gran fann jag att dessa vedegenskaper varierar över tid och rum samt över latitud, höjd och träddiameter. Veddensiteten ökade något över tid, medan kolkoncentrationen minskade i den yttersta, yngre veden men förblev stabil i hela borrkärnor. Detta visar att kortsiktiga prover fångar aktuella miljöförändringar, medan hela kärnor återspeglar långsiktiga mönster. Dessa resultat belyser att antagandet av konstanta vedegenskaper kan leda till fel i koluppskattningar och betonar behovet av regionalt specifika värden för att förbättra bedömningarna av skogens kollagring.

Acknowledgements

First, I want to thank my main supervisor, Sandra Jämtgård, along with co-supervisors Lars Östlund and Jonas Fridman. I believe the key to this thesis's success was your willingness to give me space to explore and develop, to find my own path (and truly shape this thesis), and to step in with guidance when I needed it most. Sandra, thank you for always being there to discuss both science and everything else, and for jumping in with help or solutions whenever I needed them. I appreciated your curiosity and your readiness to learn new things alongside me. Lars, thank you for your insights, for always keeping the big picture in mind—and for the lovely autumn days spent among the trees in the beautiful northern forests, which offered a much-needed break from my time in the archive. And Jonas, thank you for being someone I could rely on all my NFI-related issues and Swedish translations (at record speed!), and for reminding me to go skiing.

Also, a very big thank you to my co-authors Stefan Hupperts, Steve Perakis (USGS), and Michael Gundale for helping me work through problems and find solutions, providing valuable input on manuscripts, and always finding a way for me to spend more time coding in R! Things were rarely 'quickly solved' when R was involved, but it always made the manuscript better.

Thanks to Tuwa S., Petra E., Karoline S., Ilse V., Riccardo C., Valeria C., and Morgan K., who agreed to work with me (and sometimes on their own) in the archive and then with sample prep afterwards. Collecting samples for weeks/months in a windowless cellar in the middle of the Swedish summer was no small request. I'd still be in the cellar if it weren't for all your help.

I also want to thank all my colleagues at the Department of Forest Ecology and Management. There are far too many to thank individually here, but I will say that I feel lucky to work with so many great people. Special thanks to Clydecia for giving the best PhD advice, helping me keep perspective, and showing up for morning 'tea', which always included a lot of laughter (sorry for the noise, Johannes). To Inger for always greeting me with a warm smile and a friendly chat. And a huge thanks to Jenny, Jonas, Meredith, Ingrid, and Johannes T. at SLU's Stable Isotope Lab—you saved my sanity when reviewer demands meant running samples under tight deadlines.

I have tremendous gratitude for the NFI—past and present. It is hard to put into words how grateful I am to the many crew members who, since the 1960s, have spent their days walking through Sweden's forests collecting the tree cores that make up this unique archive. I feel honored to have been entrusted by the NFI with this incredible resource and to have had the chance to give it new life after so many years. And to Fredrik J., you made the archive make sense—turning chaos into order (I have photos to confirm the mess). Thank you!

While it often felt like I was living in a bubble during this thesis, it certainly couldn't have happened without the support and encouragement of many others. To my friend Karyn, for showing up at SLU on weekends with fika in hand, providing me with much-needed distraction at just the right times. You kept track of me, and I can't thank you enough for that. To my best friend and sister, Guthrie, for her reassuring words, care packages, and for living in such wonderful places I could escape to, even if I didn't escape as much as I would have liked. To my families in Minnesota and Ireland, all of you, but especially the matriarchs. Linda, for offering me an Irish writing retreat (even if I never made it); Marlene, who never failed to tell me how proud she was of me for taking on this challenge (*' we made it!'*); and my mom, Michele, for always being supportive and proud. You helped me to keep perspective and remember to breathe, even when I didn't realize I was holding my breath. Also, a special shout into the ether, to my dad, who gave me my first increment borer back when I was an undergrad. Throughout my PhD, I often wondered to myself, *'Who knew it would come to this, Dad?'* I suppose maybe you did.

Finally, to the three stars who complete the constellation of my life. Brule and Stellan, this journey required me to become someone new and different, and I know that did not go unnoticed. You met me with grace and gave me space you weren't used to giving (and I wasn't used to taking). This thesis marks a great achievement, but you are my greatest work—my living, growing story. And to Michael, I could not—and would not—have wanted to do this without you in my corner. *'...I would meet you anywhere the western sun meets the air, we'll hit the road, never looking behind…'* I think it's time.

I

Science of the Total Environment 900 (2023) 165795

Contents lists available at ScienceDirect

Science of the Total Environment

journal homepage: www.elsevier.com/locate/scitotenv

Forest inventory tree core archive reveals changes in boreal wood traits over seven decades

Kelley R. Bassett [a,*], Lars Östlund [a], Michael J. Gundale [a], Jonas Fridman [b], Sandra Jämtgård [a]

[a] Department of Forest Ecology and Management, Swedish University of Agricultural Sciences, SE901-83 Umeå, Sweden
[b] Department of Forest Resource Management, Swedish University of Agricultural Sciences, SE901-83 Umeå, Sweden

ARTICLE INFO

Editor: Elena Paoletti

Keywords:
Carbon isotopes
Nitrogen isotopes
Tree rings
Wood traits
Wood carbon content
Isotope natural abundance

ABSTRACT

Boreal forests play an important role in the global carbon (C) cycle, and there is great interest in understanding how they respond to environmental change, including nitrogen (N) and water limitation, which could impact future forest growth and C storage. Utilizing tree cores archived by the Swedish National Forest Inventory, we measured stemwood traits, including stable N and C isotope composition which provides valuable information related to N availability and water stress, respectively, as well as N and C content, and C/N ratio over 1950–2017 in two central Swedish counties covering an area of ca. 55,000 sq. km ($n = 1038$). We tested the hypothesis that wood traits are changing over time, and that temporal patterns would differ depending on alternative dendrochronological reconstruction methods, i.e. the commonly applied "single tree method" (STM) or a conceptually stronger "multiple tree method" (MTM). Averaged across all MTMs, our data showed that all five wood traits for *Picea abies* and *Pinus sylvestris* changed over time. Wood $\delta^{15}N$ strongly declined, indicating progressive nitrogen limitation. The decline in $\delta^{13}C$ tracked the known atmospheric $\delta^{13}CO_2$ signal, suggesting no change in water stress occurred. Additionally, wood N significantly increased, while C and C/N ratios declined over time. Furthermore, wood trait patterns sometimes differed between dendrochronological methods. The most notable difference was for $\delta^{15}N$, where the slope was much shallower for the STM compared to MTMs for both species, indicating that mobility of contemporary N is problematic when using the STM, resulting in substantially less sensitivity to detect historical signals. Our study indicates strong temporal changes in boreal wood traits and also indicates that the field of dendroecology should adopt new methods and archiving practices for studying highly mobile element cycles, such as nitrogen, which are critical for understanding environmental change in high latitude ecosystems.

1. Introduction

Boreal forests play an important role in the global carbon (C) cycle due to their capacity to take up and store a considerable amount of global C (Pan et al., 2011; DeLuca and Boisvenue, 2012; Lucas et al., 2016). As the world's largest vegetation type, this circumpolar forest belt covers about 11 % of the Earth's land surface, and stores roughly 272 ± 23 petagrams (1 Pg = 1 billion metric tons) of C, accounting for 32 % of the total terrestrial C stocks (Pan et al., 2011). Since the start of the Industrial Era, anthropogenic activities such as fossil fuel combustion, cement production, and land use changes (Canadell et al., 2007) have caused atmospheric carbon dioxide (CO_2) to rise dramatically. Presently, approximately 11 Pg C of CO_2 are emitted to the atmosphere annually (Friedlingstein et al., 2022) and according to some IPCC (2013) models, atmospheric CO_2 levels are predicted to more than double by the end of the century. Present-day boreal forests not only grow in an atmosphere with >50 % higher CO_2 concentrations compared to pre-industrial levels (NOAA, 2022), but increasing atmospheric CO_2 is also responsible for rising global surface temperatures and associated changes in precipitation (IPCC, 2007) that alter the land-atmosphere vapor pressure deficit, VPD (Yuan et al., 2019), the driving force of water loss through evaporation and transpiration (Rawson et al., 1977). Additionally, the Progressive Nitrogen Limitation (PNL) hypothesis (Hungate et al., 2003; Luo et al., 2004) predicts that increased CO_2 levels may lead to the enrichment of plants with C relative to N (higher C/N ratio) leading to reduced N cycling and availability to forests (Luo et al., 2004). Numerous models predict future climate change will continue to enhance C uptake; however, these predictions are highly uncertain

* Corresponding author.
E-mail address: kelley.bassett@slu.se (K.R. Bassett).

https://doi.org/10.1016/j.scitotenv.2023.165795
Received 1 June 2023; Received in revised form 21 July 2023; Accepted 23 July 2023
Available online 25 July 2023

(Hungate et al., 2003; Koca et al., 2006; Fang et al., 2014; Ehlers et al., 2017) because they may not consider the development of resource limitations that could gradually constrain forest growth through time (Pretzsch et al., 2018), or changes in the C concentration of major forest C compartments, such as wood.

Given their important role in the global C cycle, there is great interest in evaluating how boreal forests are responding to environmental and management changes. One monitoring tool used to assess forest growth, C stocks, and forest response to change is the systematic collection of stemwood cores by national forest inventories in many forested countries. Trees serve as long-term biological indicators that record the environmental factors that limit or enhance growth in a given period of time (Speer, 2010). So, while tree cores are often collected to measure annual growth increment, they are also used to evaluate a variety of other traits, including wood N content, C content, C/N ratio, as well as N and C isotope values.

Classical dendrochronological protocols involve reconstructing time from individual trees (hereafter referred to as the "single tree method", STM; Fig. 1), which are often selected from extreme sites where stress is greatest, in order to maximize climatic signals found in the annual growth rings (Fritts, 1976). The STM is relevant to address certain types of dendrochronological questions; however, it may have limitations when used in other contexts such as assessing forest-level responses to environmental change. For example, tree cores are increasingly being promoted as tools to provide spatial and temporal resolution of key wood traits related to forest C and N cycling (e.g. wood C and N content; Evans et al., 2022). Stable isotope values can further serve as powerful tools for understanding biogeochemical cycles by integrating element flux processes that play out over spatial and temporal scales (Bahn et al., 2012). Wood $\delta^{13}C$ values serve as an indicator for intrinsic water use efficiency (iWUE), with values deviating positively from the atmospheric signal indicating increasing water stress (Saurer et al., 2014). Additionally, the $\delta^{15}N$ of plant tissues is indicative of N availability (Poulson et al., 1995; Craine et al., 2018; Mason et al., 2022a), where decreasing $\delta^{15}N$ values are considered indicative of slowing or tightening of the N cycle, suggesting lower N availability to plants (McLauchlan et al., 2007; Craine et al., 2018). When chronologies are established from single trees (STM) within forests, both the age of the tree and the forest has changed through time. This may be problematic because the competitive ability of trees for resources, such as N or water, is known to change as trees age (Forrester, 2019); further, nutrient limitation is known to intensify during forest successional time (Bond-Lamberty et al., 2006; DeLuca et al., 2008; Gundale et al., 2011; Gundale et al., 2012). Thus, the STM approach may introduce substantial bias when a project goal is to infer about the average forest's response to long-term environmental change at the landscape scale. An alternative to the STM is to utilize national forest inventory (NFI) archival collections to create tree ring chronologies from multiple trees collected at different points in time from trees of the same age class (i.e. a "multiple tree method", MTM; Fig. 1), which would allow tree age to be held constant, and thus would eliminate biases caused by the above-mentioned ecological processes (Martínez-Sancho et al., 2020). Yet, while the MTM may be conceptually better, a potential drawback of the method is that it might introduce substantial noise associated with incorporating greater site-to-site variation, making temporal trends more difficult to detect.

To address this knowledge gap, we investigated whether five stemwood traits: $\delta^{15}N$, $\delta^{13}C$, N content, C content, and C/N ratios have changed over the period of 1950 to 2017 over a large land area (ca. 55,000 sq. km) in central Sweden. Further, we evaluated whether temporal patterns differed depending on which dendrochronological reconstruction method we employed, i.e. STM vs. MTM. Regarding the MTM, we also evaluated whether patterns differed across three different age classes of trees (Fig. 1). Our project utilized a unique tree core archive resource collected as part of the Swedish NFI, established in 1923 (Thorell and Östlin, 1931) and evolved to include over 30,000 permanent plots measured at 5-year intervals and 910,000 temporary sampling plots measured since 1953, all with corresponding data

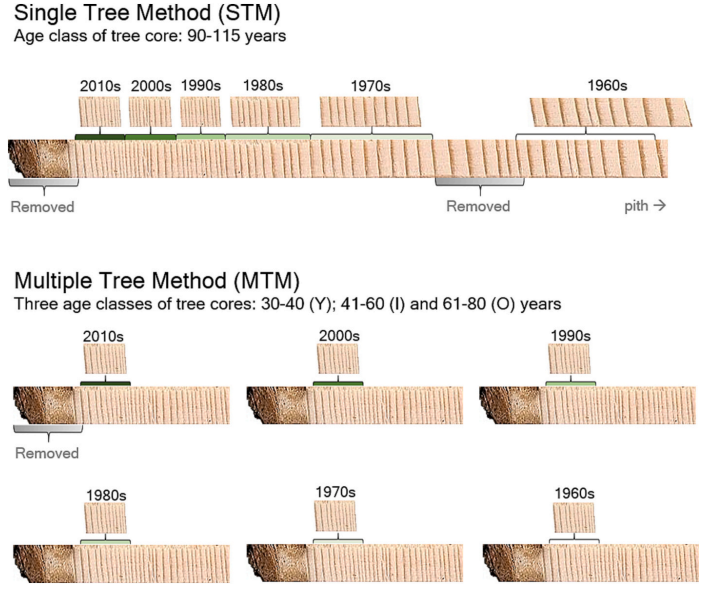

Fig. 1. Representation of sampling for the four alternative methods: STM and MTM-Y, MTM-I, and MTM-O. * Bark, cambium and most recent growth ring were removed from all cores for both methods.

maintained in the NFI database (Fridman et al., 2014). The present-day NFI tree core archive contains systematically collected and archived wood cores from 1961 onward. We isolated and analyzed contemporary and historical cores at the decade scale (10-year segments) from the archive to test the following hypotheses. First, we hypothesized that wood traits: $\delta^{15}N$, $\delta^{13}C$, N and C content, and C/N ratios, would change over time. Specifically, we hypothesized that wood $\delta^{15}N$ and N content would decrease with time as a result of PNL, and C content and C/N ratios would increase in association with rising atmospheric CO_2 concentrations. With respect to wood $\delta^{13}C$, we hypothesized a decrease through time, but expected this negative slope to be less steep than the well-known decrease in atmospheric $\delta^{13}C$, which would contribute to increasing iWUE as a response to water stress. Secondly, we hypothesized that the four methods (STM and three age classes of MTM) would differ in their representation of time, with the further expectation that method differences would be more pronounced for N versus C traits, due to greater mobility of N that could obscure historic signals (Nömmik, 1966; Mead and Preston, 1994). To our knowledge, no previous study has directly compared the commonly used STM to the conceptually stronger MTM as an alternative tool for reconstruction of temporal wood trait patterns. Testing these hypotheses will not only provide novel data on how boreal forest properties are changing across a large temporal and spatial scale, but will also provide new insights into the importance of method choice for revealing these patterns.

2. Materials and methods

2.1. Study area and sample selection

The study area includes two counties, Jämtland and Västernorrland (range: 61–65°N, 12–19°E; 0–1796 m.a.s.l.) in central Sweden, and spans an area of 55,687 sq. km. (Fig. 2). This region is characterized by coniferous boreal forest covering coastal, inland, and montane environments. We used 5.15 mm diameter tree core samples collected at breast height (1.3 m), archived by the Swedish NFI as part of its annual surveys. We spatially subdivided the study area by creating a 44-cell grid system; each grid measured 50 × 50 sq. km (Fig. 2), and was either fully or partially within county boundaries. From each 50 × 50 sq. km grid, we selected tree cores from each of the two most abundant and economically important tree species in Sweden: Norway spruce (*Picea abies* L. Karst) and Scots pine (*Pinus sylvestris* L.). Cores were selected from six archived decades, 1960s to the 2010s, which allowed us to evaluate a date range from 1950 to 2017 (described further below). Tree cores were randomly selected from the NFI archive database using the following criteria: i) dominant or co-dominant trees; ii) mesic, well-drained sites; and iii) sites with 20 % slope or less (n = 1038). We prepared each core by removing the outer bark and cambium, as well as the most recent annual ring to avoid including an incomplete year of growth due to variability in the timing of core collection during the growing season (Fig. 1). We then sectioned the target 10-year growth segment(s) using a No.11 stainless steel surgical blade under a stereo microscope with a 20× magnification, which had an accuracy of 0.01 mm. No false rings were observed. For the purposes of this study, we compared four alternative collection methods: one STM and three MTMs (Fig. 1). The STM consisted of archived tree cores that were collected from 90 to 115 year old trees that were cored in the most recent decade (2010s); thereby, all six representative decade segments in a given grid location were derived from a single tree core. Alternatively, for the MTM, a different tree core was removed from the archive to represent each decade in each grid such that the tree age could be held constant (Fig. 1). We employed this approach for three different tree age classes: 30–40 (young, Y), 41–60 (intermediate, I) and 61–80 (old, O) years old, hereafter referred to as MTM-Y, MTM-I, and MTM-O, respectively. To obtain sufficient tree cores for the STM method, we gathered cores originally collected in 2016–2018 and for each of the MTM age classes, we used cores that were originally collected in 2016–2018, 2006–2008, 1996–1998, 1986–1988, 1977 and 1961 (Table 1). Samples were then categorized according to the 'average growth year' of the decadal period. For example, for a core collected in 2017, analysis was done for increment period 2006–2016, and was assigned an 'average growth year' of 2011. For decades where cores were utilized from multiple collection years (i.e., 2016–2018), the middle of those three years (i.e., 2017) was used for classification. In order to create an identical time series between the STM and MTMs, we removed a five-year section of tree rings (1961–1965) from the STM to correspond with the offset in sampling years for the 1960s (1961) and 1970s (1977; Fig. 1).

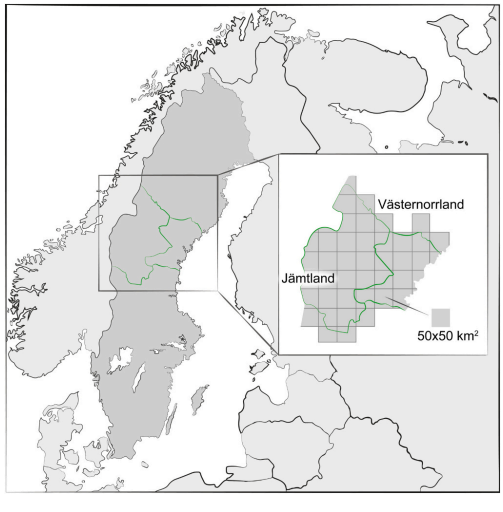

Fig. 2. A map of the study area, Jämtland and Västernorrland counties in central Sweden. The gray squares represent 50 × 50 sq. km sampling grids. The green lines are the approximate boundaries of the two counties.

2.2. Nitrogen and carbon stable isotope analysis

Measurement of nitrogen ($\delta^{15}N$) and carbon ($\delta^{13}C$) isotope ratios, and N and C content were analyzed at the Central Appalachians Stable Isotope Facility (CASIF), University of Maryland Center for Environmental Science (UMCES) Appalachian Laboratory (Frostburg, MD, USA) with a Carlo Erba NC2500 elemental analyzer (CE Instruments Ltd., Wigan, UK) interfaced with a Thermo Finnigan Delta V+ isotope-ratio mass spectrometer (IRMS, Waltham, MA, USA). The Carlo Erba NC2500 Elemental Analyzer with Costech zero-blank autosampler modifications permits for analysis of N and C isotopes in solid organic samples with <0.5 % N such as wood (Elmore et al., 2016; R. Paulman, personal communication, 2023). For each core, a radial slice was precisely sectioned to represent each 10-year segment. Approximately 10 and 1 mg of wood from the core segment was weighed for analysis of $\delta^{15}N$ and $\delta^{13}C$, respectively. For $\delta^{15}N$ analysis, a Carbosorb trap was used to remove CO_2 in advance of removing water vapor with $MgClO_4$; whereas, for $\delta^{13}C$ analysis, an $MgClO_4$ trap was used to remove water vapor before the transfer of sample gases to the IRMS. The $\delta^{15}N$ and $\delta^{13}C$ data were normalized to the Ambient Inhalable Reservoir (AIR) and Vienna Pee Dee Belemnite (VPDB) scales, respectively, using a two-point normalization curve with internal standards, including ground corn, cocoa, and caffeine powder calibrated against international standards, USGS40 and USGS41. Analytical precision (1σ) of an internal wood standard (ground pine powder) analyzed alongside samples was 0.3 ‰ for $\delta^{15}N$ and 0.1 ‰ for $\delta^{13}C$; atropine powder was used for determining N and C content values.

Table 1
The number of samples for each method: single tree (STM) and multiple tree (MTM) by method, species (*Pinus sylvestris*, *Picea abies*), average growth year, and sampling years.

Average growth year		1955	1971	1981			1991			2001			2011			
Sampling years		1961	1977	1986	1987	1988	1996	1997	1998	2006	2007	2008	2016	2017	2018	**Total (*n*)**
Method	Species															
STM	*P. sylvestris*	–	–		–			–			–		18	66	36	120
	P. abies	–	–		–			–			–		36	42	48	126
MTM-Y	*P. sylvestris*	8	22	9	8	1	6	10	6	6	9	6	6	11	7	115
	P. abies	12	20	7	2	4	3	7	5	4	4	10	8	5	7	98
MTM-I	*P. sylvestris*	19	26	13	6	2	6	13	3	4	8	9	11	10	6	136
	P. abies	18	32	9	11	7	6	12	4	6	6	8	9	11	4	143
MTM-O	*P. sylvestris*	25	29	8	15	4	12	8	3	5	8	5	4	10	3	139
	P. abies	26	32	13	12	5	13	12	5	4	10	10	6	10	3	161
	Total (*n*)	108	161	59	54	23	46	62	26	29	45	48	98	165	114	**1038**

2.3. Analysis of stable nitrogen and carbon isotope ratios

The ratio of heavy to light isotopes of N samples, ^{15}N:^{14}N and C samples, ^{13}C:^{12}C samples are expressed in standard delta (δ) notation with reference to a standard of known isotopic ratio.

$$\delta^{15}N = \left(\left[R_{sample}/R_{standard}\right] - 1\right) \times 1000$$

and

$$\delta^{13}C = \left(\left[R_{sample}/R_{standard}\right] - 1\right) \times 1000$$

where R_{sample} and $R_{standard}$ are the ratios of the heavy to light isotopes in the sample and standard, respectively and are expressed in units of parts per thousand or per mil (‰). The chosen standard for N and C are AIR and VPDB, respectively.

2.4. Carbon isotope discrimination (Δ) and iWUE calculations

In C3 plants, carbon isotope discrimination (Δ) can serve as an integrated measure of iWUE (Farquhar et al., 1989) and is written as (Farquhar et al., 1982):

$$\Delta = \frac{\delta^{13}C_{AIR} - \delta^{13}C_P}{\left(1 + \left[\frac{\delta^{13}C_P}{1000}\right]\right)} \quad (1)$$

where Δ is carbon discrimination by the plant; $\delta^{13}C_{AIR}$ is the carbon isotope value of the atmosphere (‰); and $\delta^{13}C_P$ is the carbon isotope value of the plant material (‰). The $\delta^{13}C_{AIR}$ values and the CO_2 concentration in the atmosphere, C_a, for the period of 1950–2004 were taken from McCarroll and Loader (2004); this data was then used to derive values for the period 2005–2017 by adding the rate of change over time taken from the linear regression of the data (0.0252 ‰) per year. The derived rate of change for $\delta^{13}C_{AIR}$ was most consistent with the Scripps data for the period 2004–2017 (−0.0244 ‰ per year) and determined suitable for this application. C_a for the period of 2005–2017 was obtained from the National Oceanic and Atmospheric Administration (NOAA) Global Monitoring Laboratory recorded at PAL: Pallas-Sammaltunturi, GAW Station, Finland (67.9733°N, 24.1157°E; 565 masl; Lan et al., 2022), the monitoring station most similar to the study area in terms of latitude and climate. Δ was calculated using the measured $\delta^{13}C_P$ values from tree rings. Furthermore, Δ is also a function of the intercellular and atmospheric CO_2:

$$\Delta = a + (b - a) \times \left(\frac{C_i}{C_a}\right) \quad (2)$$

where a is the isotopic discrimination associated with diffusion of CO_2 from the atmosphere into the intercellular leaf spaces via the stomata (~4.4 ‰); b is the net fractionation occurring during carboxylation (~27 ‰); and $\frac{C_i}{C_a}$ are the intercellular (C_i) and atmospheric (C_a) CO_2 concentrations. Intercellular CO_2 concentrations, C_i are obtained based on Eqs. (1) and (2); and iWUE is calculated as follows (Ehleringer et al., 1993):

$$iWUE = \frac{A}{g_s} = C_a \times \left[\left(1 - \frac{C_i}{C_a}\right) \div 1.6\right] \quad (3)$$

where $\frac{A}{g_s}$ is the ratio of net photosynthetic assimilation rate, A to stomatal conductance, g_s for water vapor; and 1.6 is the constant representing the ratio of diffusivity of water vapor and CO_2 in the air.

2.5. Statistical methods

Statistical analysis was performed using R v.4.2.2 (R Core Team, 2022). We first performed separate linear regressions for each species (*P. sylvestris* and *P abies*) and wood trait using only the MTM data (i.e. 3 age classes) including the mean for each decade to establish baseline historical patterns from data derived from the conceptually stronger approach; further, we performed linear regressions examining iWUE as a function of time on the MTM data for each species to determine if significant change occurred. We then performed a factorial linear model for each trait and tree species (*P. sylvestris* and *P. abies*) with time, method, and their interaction serving as fixed factors using Type III sum of squares, ANOVA (package 'tidyverse'). Further, we performed separate follow-up two-way ANOVAs with post-hoc pairwise comparisons ($p = 0.05$) to identify differences in regression slopes between the four methods for each species and trait (package 'emmeans'). And lastly, we calculated the root mean squared error, RMSE (package 'rmse') of the different methods for each of the five traits to compare prediction errors.

3. Results

3.1. Mean temporal response of wood traits

The MTM data showed a significant main effect of time for both *P. sylvestris* and *P. abies* for all five wood traits measured (Table 2, Fig. 3). Both $\delta^{15}N$ and $\delta^{13}C$ showed a significant decrease over time for both species, and a 95 % confidence interval of our $\delta^{13}C$ slope indicates that the decline was equal to or slightly steeper than the rate of atmospheric $\delta^{13}C$ decline (approximately 0.025 ‰ per year) for *P. sylvestris* (−0.025 to −0.033 ‰) and *P. abies* (−0.028 to −0.037 ‰). There was a significant increase in N content, while C content and C/N ratio showed a significant decrease over time for each of the species. Additionally, iWUE showed a significant increase over time for both *P. sylvestris* and *P. abies* (Fig. 4).

Table 2
Tests of between-subjects effects for traits: $\delta^{15}N$, N content, C content, C/N ratio, and, $\delta^{13}C$ for *Pinus sylvestris* and *Picea abies*.

Variable			$\delta^{15}N$ (‰)		N (%)		C (%)		C/N ratio		$\delta^{13}C$ (‰)	
Source	Species	*df*	*F*	*p*	*F*	*p*	*F*	*p*	*F*	*p*	*F*	*p*
Time	*P. sylvestris*	1	**123.435**	**<0.001**	**50.955**	**<0.001**	**81.701**	**<0.001**	**86.289**	**<0.001**	**239.293**	**<0.001**
	P. abies	1	**50.939**	**<0.001**	**33.742**	**<0.001**	**85.629**	**<0.001**	**73.049**	**<0.001**	**208.579**	**<0.001**
Method	*P. sylvestris*	3	**5.467**	**0.0011**	1.827	0.1413	1.079	0.3576	0.796	0.4968	2.049	0.1061
	P. abies	3	**3.323**	**0.0196**	**4.527**	**0.0038**	**7.399**	**<0.001**	**3.788**	**0.0104**	0.240	0.8683
Time: method	*P. sylvestris*	3	**5.293**	**0.0013**	1.802	0.1458	1.0689	0.3620	0.783	0.5040	2.069	0.1034
	P. abies	3	**3.251**	**0.0216**	**4.4123**	**0.0045**	**7.305**	**<0.001**	**0.368**	**0.01215**	0.244	0.8658

P. sylvestris residual *df* = 502; *P. abies* residual *df* = 520. $\delta^{15}N$ (‰): *P. sylvestris*: $R^2 = 0.2736$; adjusted $R^2 = 0.2635$; *P. abies*: $R^2 = 0.1247$; adjusted $R^2 = 0.1129$. N content (%): *P. sylvestris*: $R^2 = 0.1164$; adjusted $R^2 = 0.104$; *P. abies*: $R^2 = 0.1346$; adjusted $R^2 = 0.123$. C content (%): *P. sylvestris*: $R^2 = 0.1458$; adjusted $R^2 = 0.1339$; *P. abies*: $R^2 = 0.1876$; adjusted $R^2 = 0.1767$. C/N ratio: *P. sylvestris*: $R^2 = 0.1636$; adjusted $R^2 = 0.1519$; *P. abies*: $R^2 = 0.1953$; adjusted $R^2 = 0.1844$. $\delta^{13}C$ (‰): *P. sylvestris*: $R^2 = 0.3364$; adjusted $R^2 = 0.3271$; *P. abies*: $R^2 = 0.296$; adjusted $R^2 = 0.2866$. ***F* and *p* values in bold show significant differences at $p < 0.05$.**

3.2. Comparison of sampling methods

For *P. abies*, four of five traits ($\delta^{15}N$, N and C content and C/N ratio) responded signficantly to the interaction between time and method, while $\delta^{13}C$ was unresponsive to a method by time interaction (Fig. 5). For the variable $\delta^{15}N$, this interaction occured because the STM had a signficantly shallower slope than all three MTMs. For N content, the STM exhibited a steeper slope, with values of the first decade starting at a lower value than for the MTMs (see STM, Fig. 5). For C content, the slope of STM was shallower than MTM-Y, MTM-I and MTM-O, which all exhibited a strongly significant decline through time. Regarding the C/N ratio, the STM exhibited a steeper slope and higher starting value during the first decade than all three MTMs.

For *P. sylvestris*, $\delta^{15}N$ responded significantly to the interaction between time and method between all four methods; whereas, $\delta^{13}C$, N and C content, or C/N ratio were not affected by method (Fig. 6). For the variable $\delta^{15}N$, this interaction occured because the STM method had a signficantly shallower slope and a much lower starting value compared to all three MTMs.

4. Discussion and conclusions

Our aim was to provide novel data on how wood traits in boreal forests are changing through time, and to evaluate the traditional dendrochronological STM approach against a conceptually stronger MTM approach. We found that all wood traits we measured, $\delta^{15}N$, N and C content, C/N ratio, and $\delta^{13}C$ have changed over time (1950–2017) for both *P. sylvestris* and *P. abies* (Fig. 3), and that these patterns sometimes differed between methods (Figs. 5, 6).

4.1. Mean temporal response of wood traits

In support of our first hypothesis, we found a significant decline in wood $\delta^{15}N$ for both *P. sylvestris* and *P. abies* ($p < 0.01$; $p < 0.01$, respectively) over the period of 1950–2017. Several previous studies have provided evidence that wood (Poulson et al., 1995; McLauchlan et al., 2007; McLauchlan and Craine, 2012) or foliar (Craine et al., 2009; Craine et al., 2018) $\delta^{15}N$ values are declining with time; however, it is notable that the magnitude change we observed using the MTM (ca. 4 ‰ decline over 70 years) is much steeper than previously reported (e.g., Kranabetter et al., 2013; McLauchlan et al., 2017; Oulehle et al., 2022). Several mechanisms have been proposed to explain these temporal declines in $\delta^{15}N$. First, isotopic signature of $\delta^{15}N$ of soil and plants are considered to be sensitive to N cycling and availability in forests (Poulson et al., 1995; Högberg, 1997; Craine et al., 2009). Specifically, ecosystems with low mineralization rates have lower N loss rates, e.g. via nitrification, denitrification, and leaching which lead to greater loss of ^{14}N relative to ^{15}N, and are thus associated with lower $\delta^{15}N$ values. Reductions in the $\delta^{15}N$ signature through time have been interpreted as evidence of the Progressive Nitrogen Limitation (PNL) hypothesis, which results from elevated CO_2 and subsequent ecosystem N limitation (Luo et al., 2004; Mason et al., 2022a). Thus, a tightening of N cycling and reduction in N losses in response to elevated CO_2 (i.e. PNL hypothesis) may explain the decline in $\delta^{15}N$ signatures we observed through time. In addition to PNL, another non-mutually exclusive mechanism that could explain the observed decline in wood $\delta^{15}N$ values is greater reliance of trees on mycorrhizal fungi for acquiring N in response to elevated CO_2 (Näsholm et al., 2013; Franklin et al., 2014; Hasselquist et al., 2016). Mycorrhizal fungi are known to retain the heavier ^{15}N atom and pass the depleted N onto the plant (Hobbie and Högberg, 2012) resulting in lower $\delta^{15}N$ values in plant tissues. Finally, a counter-argument to the PNL explanation for declining $\delta^{15}N$ values is that the total amount and $\delta^{15}N$ signature of anthropogenic N deposition has declined for approximately three to four decades (Olff et al., 2022). However, we note that the decline in $\delta^{15}N$ we observed in our wood data started at least one decade prior to peak atmospheric N deposition rates in Sweden, which occurred in the early 1980s (Lajtha and Jones, 2013; Ferm et al., 2019). We also note that atmospheric N deposition rates in our study area are relatively low (<4 kg N ha^{-1} yr^{-1}), and experimental work in northern Sweden has shown that long-term anthropogenic N inputs at this rate do not alleviate N limitation (Gundale et al., 2014). Finally, nutrient discharge data from Swedish streams has shown long-term declines in inorganic N, including areas far north of our study area, where atmospheric N deposition rates are <1 kg ha^{-1} yr^{-1} (Lucas et al., 2016), indicating that terrestrial N limitation is increasing, independent of temporal trends in N deposition. While changes in atmospheric N deposition may be partly responsible for the declining wood $\delta^{15}N$ signatures we observe, these studies suggest other change factors, such as increasing atmospheric CO_2, are likely key drivers of this pattern (Mason et al., 2022a, 2022b).

Contrary to expectations, our data did not show a significant decrease in N content with time for either species, but rather, we observed a significant increase. One potential explanation for this pattern is that rising atmospheric CO_2 has stimulated trees to invest more energy into N uptake via mycorrhizae, which could potentially result in both higher wood N and lower $\delta^{15}N$ values. However, several previous studies on stemwood N concentrations have concluded that wood N content may not serve as a useful indicator of ecosystem N availability, but rather is more responsive to internal physiological drivers versus environmental conditions (Poulson et al., 1995; Doucet et al., 2011). Because N accounts for such a small fraction of wood mass (i.e., 0.03–0.10 % N; Cowling and Merrill, 1966), wood N content may inversely respond to changes in other constituents of wood. In fact, several studies have shown that wood N content is unresponsive to fertilizer addition, whereas $\delta^{15}N$ values are highly responsive (Schleppi et al., 1999; Hart and Classen, 2003; Balster et al., 2009). Furthermore, Gerhart and McLauchlan (2014) highlighted that wood $\delta^{15}N$ and N concentration are not consistently correlated across studies, and concluded that $\delta^{15}N$ is a more sensitive measure of temporal changes in N availability.

In addition to N content, an additional unexpected pattern we observed was that wood C content decreased over time, rather than

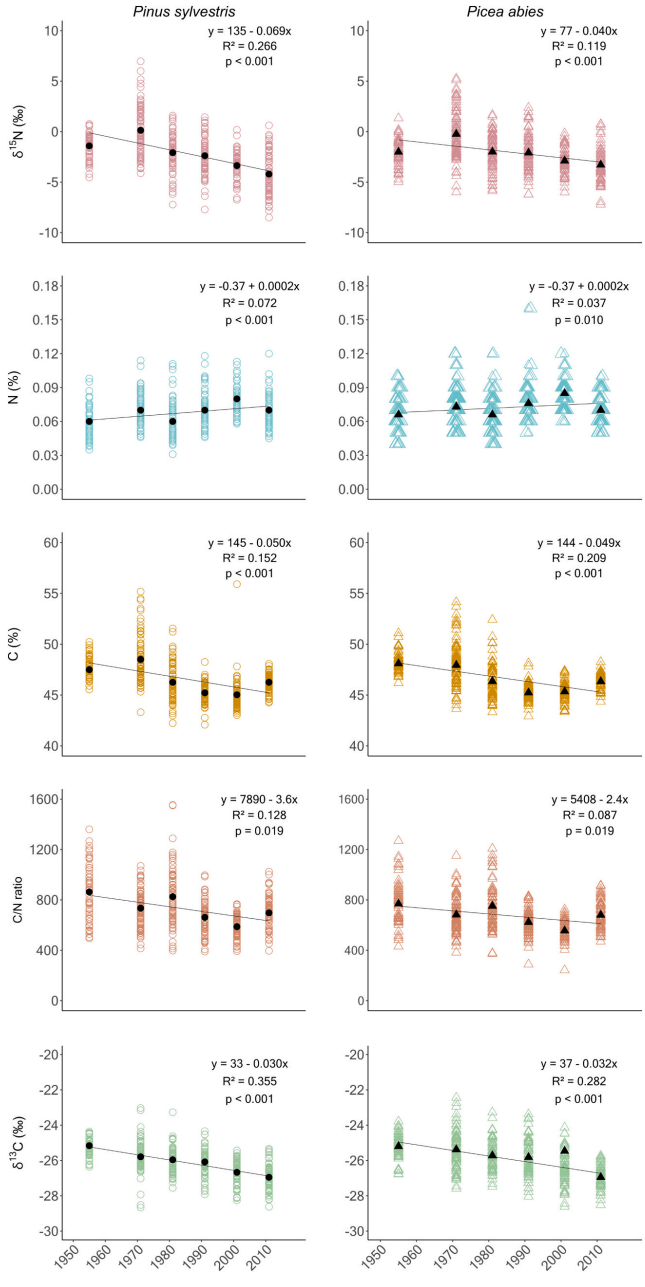

Fig. 3. The composite temporal response of five wood traits, $\delta^{15}N$, N content, C content, C/N ratio, and $\delta^{13}C$ for species *Pinus sylvestris* (left-hand panels) and *Picea abies* (right-hand panels) for the three MTMs (young, intermediate and old). Means per decade for each trait and species are indicated by the black symbols. Note: The R ggplot jitter function was applied for N content (*P. abies*) to horizontally offset overlapping data points.

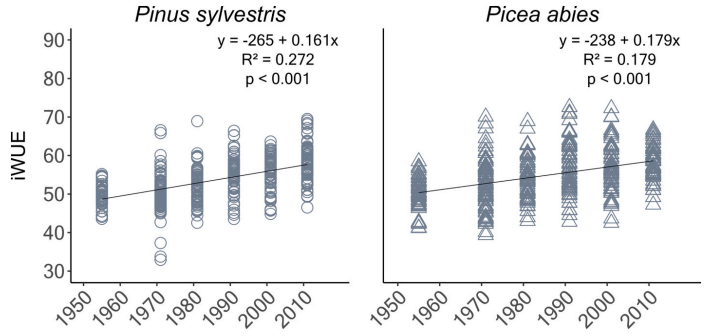

Fig. 4. The composite temporal response of iWUE for *Pinus sylvestris* and *Picea abies* for the three MTMs (young, intermediate and old).

increased, which partially explained the decline in the C/N ratio. The reduction in wood C content, which accounts for nearly 50 % of the mass of wood, may also partially explain the observed increase in N, given that a ca. 7 % change in the most abundant wood element (i.e., C) would cause other elements to become more concentrated. However, the percent increase in N contents we observed were greater than the decrease in wood C contents, at least for *P. sylvestris*. Hence, other factors may also be important for explaining increases in wood N content, such as changes in wood oxygen (O) content. One possible explanation for the decline in wood C content could be a shift towards a higher proportion of latewood versus earlywood in our samples; the former having a lower C content than the latter (Lamlom and Savidge, 2003). In support of this mechanism, several studies have shown that climate change has corresponded with an increase total production of latewood (Arzac et al., 2019), as well as earlier seasonal transition from earlywood to latewood production (Buttò et al., 2021).

Another concurrent change that could potentially explain a decrease in wood C is a reduction in lignin and an increase in cellulose content, which differ in their percent C (ca. 40–45 % and 26–34, respectively; Zobel and van Buijtenen, 1989; Lamlom and Savidge, 2003; Rowell et al., 2012). Finally, N fertilization studies have shown that higher C content in earlywood production (van Buijtenen, 2004) increases in response to N; thus, the long-term reduction in N availability (i.e., PNL) may contribute to a greater portion of lower C content of latewood versus earlywood. Future analysis of the earlywood and latewood transition on individual annual rings, as well as analysis of lignin/cellulose ratio could provide additional clarity on the mechanisms driving the changes in wood N, C, and C/N ratio we observed.

Our data also showed that $\delta^{13}C$ values have declined over time for both species, (*P. sylvestris*: $p < 0.01$; *P. abies*: $p < 0.01$); however, this rate of change is consistent with declining $\delta^{13}C$ values observed in atmospheric CO_2 worldwide (Mook, 1983; Keeling et al., 1984). Inconsistent with our hypothesis, the rate of change we observed was not significantly less steep than the average decline over time in the $\delta^{13}C$ of atmospheric CO_2, (approximately 0.025 ‰ per year) as a result of the addition of $\delta^{13}C$-depleted fossil fuel-derived CO_2 inputs to the atmosphere (Suppl. Table 1; McCarroll and Loader, 2004; Belmecheri and Lavergne, 2020). Calculations of iWUE are based on atmospheric and plant $\delta^{13}C$ values, as well as atmospheric CO_2 concentration (Adams et al., 2020; Mathias and Thomas, 2021), which indicate an increase in iWUE through time in our study area (Fig. 4). This increase in iWUE was entirely driven by the change in the atmospheric CO_2 concentration that has occurred over our analysis period, rather than a change in $\delta^{13}C$ fractionation processes during photosynthesis. This suggests that while forests may use water more efficiently per unit of CO_2 acquired, this does not appear to part of a tree stress response (Saurer et al., 2014), as has been observed in some studies of northern temperate forests of North America and Europe (Keenan et al., 2013). Our hypothesis of increased water stress is based on predictions that despite increases in annual precipitation for the period of 1950–2018 (SMHI, 2022), a shift towards less frequent and more intense summer precipitation events are occurring. This may eventually lead to increased run-off and less water retained by forests (IPCC, 2013; Lucas et al., 2016) which could potentially constrain growth and limit C storage. Likewise, climate warming is gradually increasing the land-atmosphere vapor pressure deficit, VPD, which is the driving force of water loss through evaporation and transpiration (Yuan et al., 2019). Increases in VPD have been shown to decrease photosynthetic rates (Fletcher et al., 2007); however, while increasing VPD is emerging as a trend in forests globally (Yuan et al., 2019), our data suggest increasing VPD has not yet crossed a threshold that is clearly impacting the photosynthetic fractionation processes of trees in our study area. In fact, the relative change in total volume growth for our study area (Västernorrland and Jämtland counties) was +3 and +21 %, respectively, between 2005 and 2012; whereas between 2012 and 2016 total volume growth changed by 0 %. This may indicate that volume growth is slowing, potentially due to PNL, but that growth has not yet turned negative as a result of severe drought. In contrast, drought events have been relatively more severe in southern Swedish counties during this period, and annual growth decreased by an average of −8 % during the 2012–2016 period (range −15 to +2 % among the counties in the region; Fridman et al., 2022).

4.2. Difference in methodological sampling approaches

Our analysis indicated that temporal patterns of several traits we measured were sensitive to method choice (i.e. MTM-Y, MTM-I, and MTM-O and STM). We found that $\delta^{15}N$ was far more impacted by method choice, whereas $\delta^{13}C$ data was not responsive to method choice, which is consistent with our hypothesis. The lack of $\delta^{13}C$ response to method is likely due to the non-mobile nature of C once fixed into long-term tissues and compounds, making contamination from contemporary C (e.g. sugars) very minor compared to the pool of C fixed into these long-term pools (Higuchi, 1997). Regarding $\delta^{15}N$, temporal trends never differed between the three different MTMs, whereas the STM almost always differed from the MTMs for both *P. sylvestris* and *P. abies*. We found that all four methods converged on a similar final $\delta^{15}N$ value (approx. −4 ‰) in the most recent decade (2010s), while the starting values for the earliest decade (1950s) for the STM and MTMs were much different, −3 ‰ and 0 ‰, respectively. Nitrogen demonstrates high mobility among tree rings of different ages including remobilization of N to active growth regions as well as translocation within stems into older tree rings via ray parenchyma cells (Nömmik, 1966; Mead and Preston, 1994; Schleppi et al., 1999; Tomlinson et al., 2014), thus, the most parsimonious explanation for the relative flatness of the STM slopes is

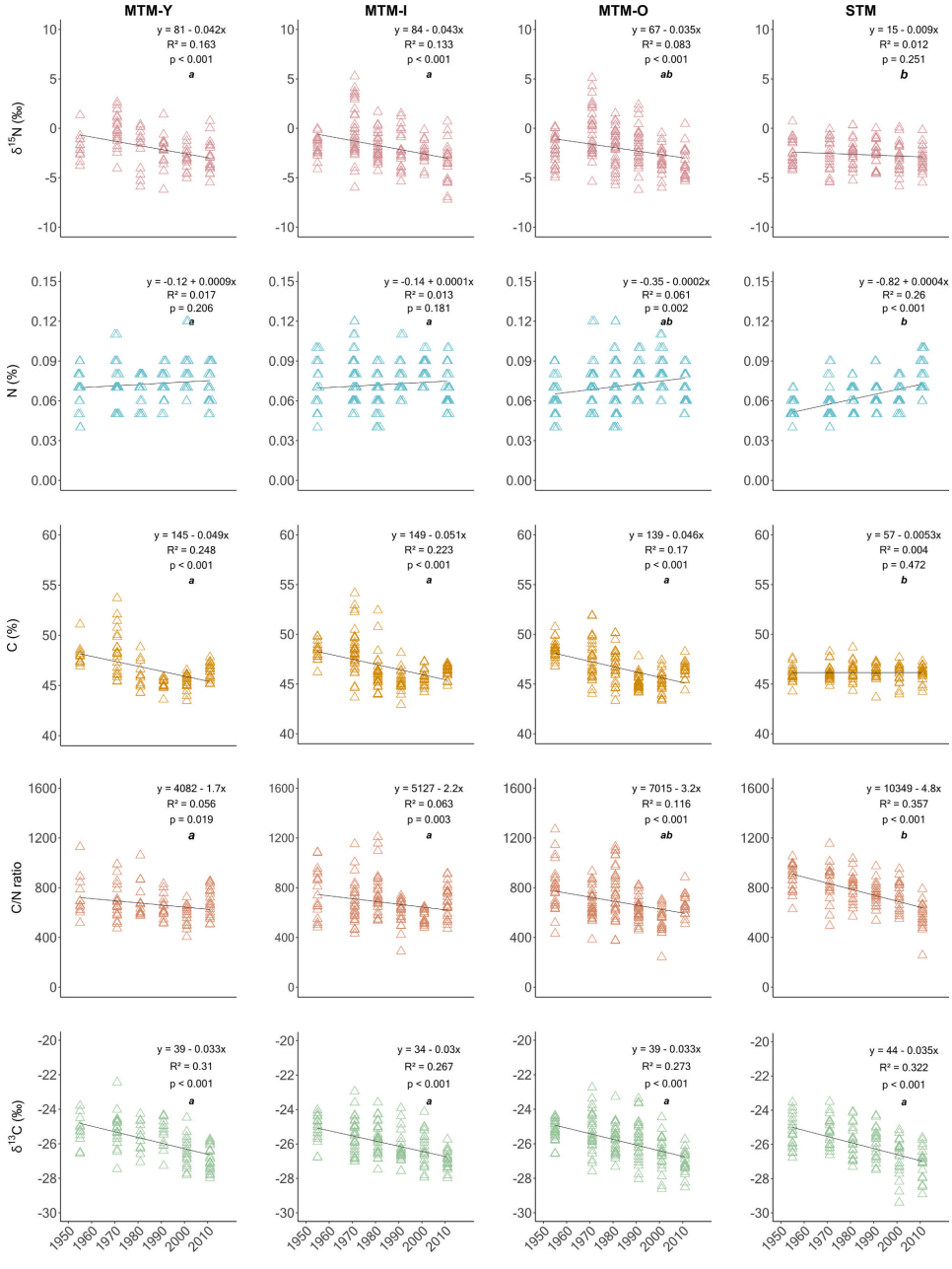

Fig. 5. Linear regression for five wood traits by method: $\delta^{15}N$, N content, C content, C/N ratio, and $\delta^{13}C$ over six decades for *Picea abies* with pairwise comparisons of the methods. Pairwise differences between the slopes of each method for each trait (in rows) are indicated by **bold**, *italicized* letters in each panel. Note: The R ggplot jitter function was applied for N content to horizontally offset overlapping data points.

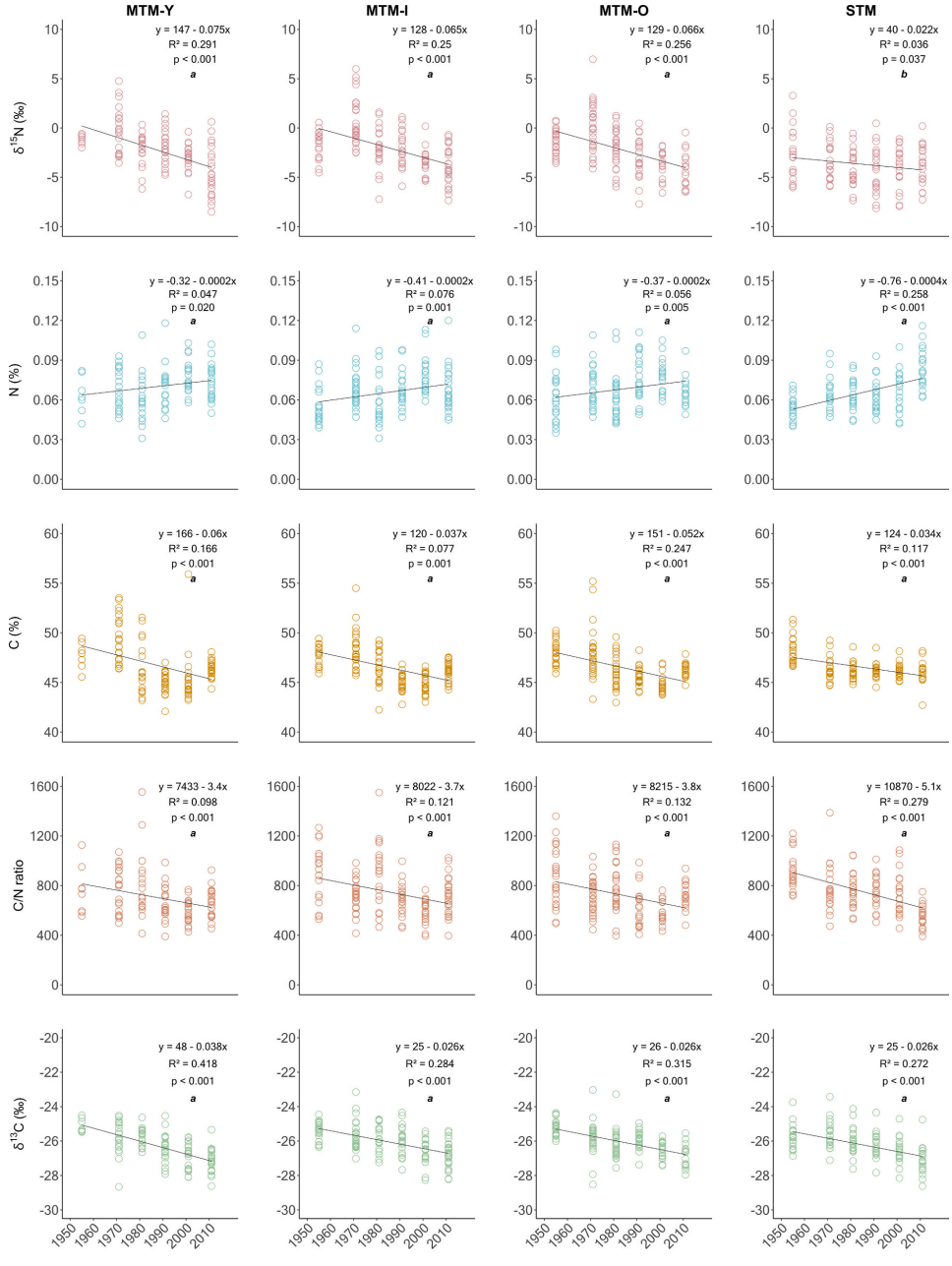

Fig. 6. Linear regression for five wood traits by method: $\delta^{15}N$, N content, C content, C/N ratio, and $\delta^{13}C$ over six decades for *Pinus sylvestris* with pairwise comparisons of the methods. Pairwise differences between the slopes of each method for each trait (in rows) are indicated by **bold**, *italicized* letters in each panel.

that the oldest segments (1950s) are contaminated by contemporarily-acquired N transported in the xylem water (Peuke, 2010) at the time of sampling. Thus, the STM appears to be an inherently limited and insensitive approach to evaluate temporal changes in $\delta^{15}N$, because of the greater opportunity for contemporary physiological and ecological processes to obscure historical signals.

In addition to $\delta^{15}N$, we observed significant differences in temporal patterns among the methods for N, C and C/N ratio, but only for *P. abies*. Interestingly, temporal responses for these three traits exhibited much shallower slopes for MTM than the STM, which contrasts the response described above for $\delta^{15}N$, where responses were stronger for the MTM. This may suggest that *P. abies* wood undergoes stronger changes in wood anatomy or chemistry during aging compared to *P. sylvestris*. Wood C and N content, and C/N ratios can have important implications for ecosystem properties and process, such as estimation of forest C stocks, or as predictors of wood decomposition rates. In regards to forest C, stock estimates often assume a wood C content of 50 % (Doraisami et al., 2022). It is notable that our data suggests a substantially lower and decreasing C content with time, at least for the outer sapwood, which was the focus of our study. While both STM and MTM methods found similar temporal patterns, our comparison of methods suggests that reliance on the classical STM approach would likely exaggerate temporal change in these traits.

While conceptually the MTM is a better approach to evaluate changes in wood traits because it removes the potential influence of tree aging or forest succession on growth and nutrient acquisition, we also considered the potential drawback that using the MTM might have by introducing excessive noise that could make temporal trends difficult to observe. However, our results of the root mean squared error (RMSE) do not show a consistent increase in noise associated with the MTMs across the traits for the two species (Suppl. Table 1). This indicates that there appears to be no major downside for using the MTM approach.

Over 100 countries across Europe, Asia, Africa, and the Americas, accounting for a large amount of the Earth's forested landscape (Suppl. Fig. 1), actively conduct, have capacity in place, or are receiving technical support to develop national forest inventories (Schelhaas et al., 2006; Magnussen et al., 2007; Tomppo et al., 2010; Romijn et al., 2015; UNFAO, n.d.). Clearly, this illustrates the tremendous potential that tree core archiving could provide if incorporated into NFI protocols. Tree cores provide critical benefits to NFIs by providing an unbiased sample, representative of climate and other environmental conditions, which offers insight into the effect of climate on tree growth; and by design, NFIs are well-suited for upscaling, which allows for better and more accurate C accounting (Evans et al., 2022). Wood traits are a tremendous tool for understanding response to climate, and our results show that methodology is clearly important for reconstructing $\delta^{15}N$, which may account for why other studies have found very subtle (Kranabetter et al., 2013; McLauchlan et al., 2017; Oulehle et al., 2022) or no temporal patterns (Tomlinson et al., 2014). Our results show for the first time that the MTM provides a more sensitive window into environmental change for certain biogeochemical cycles that exhibit high intra-wood mobility, i.e. nitrogen, and that systematic archiving of wood cores within already existing NFIs has great potential to provide a long-term record of forest responses to changes in our Earth system.

Supplementary data to this article can be found online at https://doi.org/10.1016/j.scitotenv.2023.165795.

Author contributions

All authors developed the experimental design/conceived the study; K.R.B prepared all samples and wrote the first draft of the manuscript; and all authors interpreted and discussed the ideas and results and provided input on each draft of the manuscript.

CRediT authorship contribution statement

Kelley R. Bassett: Conceptualization, Methodology, Formal analysis, Investigation, Resources, Data curation, Writing – original draft, Writing – review & editing, Visualization, Project administration, Funding acquisition. **Lars Östlund:** Conceptualization, Methodology, Writing – review & editing, Supervision. **Michael J. Gundale:** Conceptualization, Methodology, Writing – review & editing, Funding acquisition. **Jonas Fridman:** Conceptualization, Methodology, Writing – review & editing, Supervision. **Sandra Jämtgård:** Conceptualization, Methodology, Writing – review & editing, Supervision.

Declaration of competing interest

The authors declare that they have no known competing financial interests or personal relationships that could have appeared to influence the work reported in this paper.

Data availability

Data will be made available on request.

Acknowledgements

We thank Fredrik Johansson for organization of the Swedish NFI archive samples and interpretation of archival coding; Petra Edlund, Morgan Karlsson, Karoline Spies, Tuwa Sundvall, and Ilse Van Duuren for sample collection and measurements; and the Swedish NFI field crews over the decades for field sample collection. We thank Jonatan Klaminder for helpful comments on a previous draft of this manuscript. Additionally, we wish to acknowledge David Nelson and Robin Paulman at Central Appalachians Stable Isotope Facility (CASIF) located at the University of Maryland Center for Environmental Science (UMCES) Appalachian Laboratory for providing analytical results. This research was supported by grants from Stiftelsen Gunnar och Birgitta Nordins fond (KSLA), Brattås Stiftelsen, VR (2020-03908), TC4 and the Knut and Alice Wallenberg Foundation (2018.0259).

References

Adams, M.A., Buckley, T.N., Turnbull, T.L., 2020. Diminishing CO_2-driven gains in water-use efficiency of global forests. Nat. Clim. Chang. 10, 466–471.

Arzac, A., Popkova, M., Anarbekova, A., Olano, J.M., Gutiérrez, E., Nikolaev, A., Shishov, V., 2019. Increasing radial and latewood growth rates of *Larix cajanderi* Mayr. and *Pinus sylvestris* L. in the continuous permafrost zone in Central Yakutia (Russia). Ann. For. Sci. 76, 1–15.

Bahn, M., Buchmann, N., Knohl, A., 2012. Stable isotopes and biogeochemical cycles in terrestrial ecosystems. Biogeosciences 9, 3979–3981.

Balster, N.J., Marshall, J.D., Clayton, M., 2009. Coupling tree-ring $\delta^{13}C$ and $\delta^{15}N$ to test the effect of fertilization on mature Douglas-fir (*Pseudotsuga menziesii* var. *glauca*) stands across the Interior Northwest, USA. Tree Physiol. 29, 1491–1501.

Belmecheri, S., Lavergne, A., 2020. Compiled records of atmospheric CO_2 concentrations and stable carbon isotopes to reconstruct climate and derive plant ecophysiological indices from tree rings. Dendrochronologia 63, 125748.

Bond-Lamberty, B., Gower, S.T., Wang, C., Cyr, P., Veldhuis, H., 2006. Nitrogen dynamics of a boreal black spruce wildfire chronosequence. Biogeochemistry 81, 1–16.

Buttò, V., Khare, S., Drolet, G., Sylvain, J., Gennaretti, F., Deslauriers, A., Morin, H., Rossi, S., 2021. Region-wide temporal gradients of carbon allocation allow for shoot growth and latewood formation in boreal black spruce. Glob. Ecol. Biogeogr. 30, 1657–1670.

Canadell, J.G., Le Quéré, C., Raupach, M.R., Field, C.B., Buitenhuis, E.T., Ciais, P., Conway, T.J., Gillett, N.P., Houghton, R.A., Marland, G., 2007. Contributions to accelerating atmospheric CO_2 growth from economic activity, carbon intensity, and efficiency of natural sinks. Proc. Natl. Acad. Sci. U. S. A. 104, 18866–18870.

Cowling, E.B., Merrill, W., 1966. Nitrogen in wood and its role in wood deterioration. Can. J. Bot. 44, 1539–1554.

Craine, J.M., Elmore, A.J., Aidar, M.P.M., Bustamante, M., Dawson, T.E., Hobbie, E.A., Kahmen, A., Mack, M.C., McLauchlan, K.K., Michelsen, A., Nardoto, G.B., Pardo, L. H., Peñuelas, J., Reich, P.B., Schuur, E.A.G., Stock, W.D., Templer, P.H., Virginia, R. A., Welker, J.M., Wright, I.J., 2009. Global patterns of foliar nitrogen isotopes and their relationships with climate, mycorrhizal fungi, foliar nutrient concentrations, and nitrogen availability. New Phytol. 183, 980–992.

Craine, J.M., Elmore, A.J., Aranibar, J., Bauters, M., Boeck, P., Crowley, B.E., Dawes, M. A., Delzon, S., Fajardo, A., Fang, Y., Fujiyoshi, L., Gray, A., Guerrieri, R., Gundale, M. J., Hawke, D.J., Hietz, P., Jonard, M., Kearsley, E., Kenzo, T., Makarov, M., Marañón-Jiménez, S., McGlynn, T.P., McNeil, B.E., Mosher, S.G., Nelson, D.M., Peri, P.L., Roggy, J.C., Sanders-DeMott, R., Song, M., Szpak, P., Templer, P.H., Van der Colff, D., Wang, L., Werner, C., Xu, X., Yang, Y., Yu, G., Zmudczyńska-Skarbek, K., 2018. Isotopic evidence for oligotrophication of terrestrial ecosystems. Nature Ecology and Evolution 2, 1735–1744.

Deluca, T.H., Boisvenue, C., 2012. Boreal forest soil carbon: distribution, function and modelling. Forestry: An International Journal of Forest Research 85, 161–184.

DeLuca, T.H., Zackrisson, O., Gundale, M.J., Nilsson, M.-C., 2008. Ecosystem feedbacks and nitrogen fixation in boreal forests. Science 320, 1181.

Doraisami, M., Kish, R., Paroshy, N.J., Domke, G.M., Thomas, S.C., Martin, A.R., 2022. A global database of woody tissue carbon concentrations. Scientific Data 9, 284.

Doucet, A., Savard, M.M., Bégin, C., Smirnoff, A., 2011. Is wood pre-treatment essential for tree-ring nitrogen concentration and isotope analysis? Rapid Commun. Mass Spectrom. 25, 469–475.

Ehleringer, J.R., Hall, A.E., Farquhar, G.J. (Eds.), 1993. Stable Isotopes and Plant Carbon-Water Relations. Academic Press.

Ehlers, I., August, A., Betson, T.R., Nilsson, M.B., Marshall, J.D., 2017. Detecting long-term metabolic shifts using isotopomers: CO_2-driven suppression of photorespiration in C3 plants over the 20th century. Proceedings of the National Academy of Sciences of the United States 112, 15585–15590.

Elmore, A.J., Nelson, D.M., Craine, J.M., 2016. Earlier springs are causing reduced nitrogen availability in North American eastern deciduous forests. Nature Plants 2, 16133.

Evans, M.E.K., DeRose, R.J., Klesse, S., Girardin, M.P., Heilman, K.A., Alexander, M.R., Arsenault, A., Babst, F., Bouchard, M., Cahoon, S.M.P., Campbell, E.M., Dietze, M., Duchesne, L., Frank, D.C., Giebink, C.L., Gómez-Guerrero, A., Gutiérrez García, G., Hogg, E.H., Metsaranta, J., Ols, C., Rayback, S.A., Reid, A., Ricker, M., Schaberg, P. G., Shaw, J.D., Sullivan, P.F., Villela GaytÁn, S.A., 2022. Adding tree rings to North America's National Forest Inventories: an essential tool to guide drawdown of atmospheric CO_2. BioScience 72, 233–246.

Fang, J., Kato, T., Guo, Z., Yang, Y., Hu, H., Shen, H., Zhao, X., Kishimoto-Mo, A.W., Tang, Y., Houghton, R.A., 2014. Evidence for environmentally enhanced forest growth. Proc. Natl. Acad. Sci. U. S. A. 111, 9527–9532.

Farquhar, G., O'Leary, M., Berry, J., 1982. On the relationship between carbon isotope discrimination and the intercellular carbon dioxide concentration in leaves. Aust. J. Plant Physiol. 9, 121–137.

Farquhar, G., Ehleringer, J.R., Hubick, K.T., 1989. Carbon isotope discrimination and photosynthesis. Annual Review of Plant Physiology Plant Molecular Biology 40, 503–537.

Ferm, M., Granat, L., Engardt, M., Pihl Karlsson, G., Danielsson, H., Karlsson, P.E., Hansen, K., 2019. Wet deposition of ammonium, nitrate and non-sea-salt sulphate in Sweden 1955 through 2017. Atmospheric Environment: X 2, 100015.

Fletcher, L., Sinclair, T.R., Allen Jr., L.H., 2007. Transpiration responses to vapor pressure deficit in well-watered 'slow-wilting' and commercial soybean. Environ. Exp. Bot. 61, 145–151.

Forrester, D.I., 2019. Linking forest growth with stand structure: tree size inequality, tree growth or resource partitioning and the asymmetry of competition. For. Ecol. Manag. 447, 139–157.

Franklin, O., Näsholm, T., Högberg, P., Högberg, M.N., 2014. Forests trapped in nitrogen limitation – an ecological market perspective on ectomycorrhizal symbiosis. New Phytol. 203, 657–666.

Fridman, J., Holm, S., Nilsson, M., Nilsson, P., Hedström Ringvall, A., Ståhl, G., 2014. Adapting National Forest Inventories to changing requirements – the case of the Swedish National Forest Inventory at the turn of the 20th century. Silva Fennica 48, 1095.

Fridman, J., Westerlund, B., Mensah, A.A., 2022. Volymtillväxten för träd i Sverige under 00-talet Ett faktaunderlag med anledning av den minskande nettotillväxten. Arbetsrapport/ Sveriges lantbruksuniversitet, Institutionen för skoglig resurshushållning, p. 540.

Friedlingstein, P., O'Sullivan, M., Jones, M.W., Andrew, R.M., Gregor, L., Hauck, J., Le Quéré, C., Luijkx, I.T., Olsen, A., Peters, G.P., Peters, W., Pongratz, J., Schwingshackl, C., Sitch, S., Canadell, J.G., Ciais, P., Jackson, R.B., Alin, S.R., Alkama, R., Arneth, A., Arora, V.K., Bates, N.R., Becker, M., Bellouin, N., Bittig, H.C., Bopp, L., Chevallier, F., Chini, L.P., Cronin, M., Evans, W., Falk, S., Feely, R.A., Gasser, T., Gehlen, M., Gkritzalis, T., Gloege, L., Grassi, G., Gruber, N., Gürses, Ö., Harris, I., Hefner, M., Houghton, R.A., Hurtt, G.C., Iida, Y., Ilyina, T., Jain, A.K., Jersild, A., Kadono, K., Kato, E., Kennedy, D., Klein Goldewijk, K., Knauer, J., Korsbakken, J.I., Landschützer, P., Lefèvre, N., Lindsay, K., Liu, J., Liu, Z., Marland, G., Mayot, N., McGrath, M.J., Metzl, N., Monacci, N.M., Munro, D.R., Nakaoka, S.I., Niwa, Y., O'Brien, K., Ono, T., Palmer, P.I., Pan, N., Pierrot, D., Pocock, K., Poulter, B., Resplandy, L., Robertson, E., Rödenbeck, C., Rodriguez, C., Rosan, T.M., Schwinger, J., Séférian, R., Shutler, J.D., Skjelvan, I., Steinhoff, T., Sun, Q., Sutton, A.J., Sweeney, C., Takao, S., Tanhua, T., Tans, P.P., Tian, X., Tian, H., Tilbrook, B., Tsujino, H., Tubiello, F., van der Werf, G.R., Walker, A.P., Wanninkhof, R., Whitehead, C., Willstrand Wranne, A., Wright, R., Yuan, W., Yue, C., Yue, X., Zaehle, S., Zeng, J., Zheng, B., 2022. Global carbon budget 2022. Earth System Science Data 14, 4811–4900.

Fritts, H.C., 1976. Tree Rings and Climate. Academic Press, London; New York.

Gerhart, L.M., McLauchlan, K.K., 2014. Reconstructing terrestrial nutrient cycling using stable nitrogen isotopes in wood. Biogeochemistry 120, 1–21.

Gundale, M.J., Fajardo, A., Lucas, R.W., Nilsson, M.-C., Wardle, D.A., 2011. Resource heterogeneity does not explain the diversity-productivity relationship across a boreal island fertility gradient. Ecography 34, 887–896.

Gundale, M.J., Hyodo, F., Nilsson, M.-C., Wardle, D.A., 2012. Nitrogen niches revealed through species and functional group removal in a boreal shrub community. Ecology 93, 1695–2005.

Gundale, M.J., From, F., Back-Holmen, L., Nordin, A., 2014. Nitrogen deposition in boreal forests has a minor impact on the global carbon cycle. Glob. Chang. Biol. 20, 276–286.

Hart, S.C., Classen, A.T., 2003. Potential for assessing long-term dynamics in soil nitrogen availability from variations in $\delta^{15}N$ of tree rings. Isot. Environ. Health Stud. 39, 15–28.

Hasselquist, N.J., Metcalfe, D.B., Inselsbacher, E., Stangl, Z., Oren, R., Näsholm, T., Högberg, P., 2016. Greater carbon allocation to mycorrhizal fungi reduces tree nitrogen uptake in a boreal forest. Ecology 97, 1012–1022.

Higuchi, T., 1997. Biochemistry and Molecular Biology of Wood. Springer-Verlag, Timell, T.E., Berlin Heidelberg New York.

Hobbie, E.A., Högberg, P., 2012. Nitrogen isotopes link mycorrhizal fungi and plants to nitrogen dynamics. New Phytol. 196, 367–382.

Högberg, P., 1997. Nitrogen impacts on forest carbon. Nature 447, 781–782.

Hungate, B.A., Dukes, J.S., Shaw, M.R., Luo, Y., Field, C.B., 2003. Nitrogen and climate change. Science 302, 1512–1513.

IPCC, 2007. Climate Change 2007: The Physical Science Basis. Contribution of Working Group I to the Fourth Assessment Report of the Intergovernmental Panel on Climate Change. Cambridge University Press, Cambridge, United Kingdom and New York, NY, USA.

IPCC, 2013. Climate Change 2013: The Physical Science Basis. Contribution of Working Group I to the Fifth Assessment Report of the Intergovernmental Panel on Climate Change. Cambridge University Press, Cambridge, United Kingdom and New York, NY, USA.

Keeling, C.D., Carter, A.F., Morek, W.G., 1984. Seasonal, latitudinal and secular variations in the abundance and isotopic ratios of atmospheric CO_2. J. Geophys. Res. 88, 10 915-10 933.

Keenan, T., Hollinger, D.Y., Bohrer, G., Dragoni, D., Munger, J.W., Schmid, H.P., Richardson, A.D., 2013. Increase in forest water-use efficiency as atmospheric carbon dioxide concentrations rise. Nature 499, 324–327.

Koca, D., Smith, B., Sykes, M.T., 2006. Modelling regional climate change effects on potential natural ecosystems in Sweden. Clim. Chang. 78, 381–406.

Kranabetter, J.M., Saunders, S., MacKinnon, J.A., Klassen, H., Spittlehouse, D.L., 2013. An assessment of contemporary and historic nitrogen availability in contrasting coastal Douglas-fir forests through $\delta^{15}N$ of tree rings. Ecosystems 16, 111–122.

Lajtha, K., Jones, J., 2013. Trends in cation, nitrogen, sulfate and hydrogen ion concentrations in precipitation in the United States and Europe from 1978 to 2010: a new look at an old problem. Biogeochemistry 116, 303–334.

Lamlom, S.H., Savidge, R.A., 2003. A reassessment of carbon content in wood: variation within and between 41 North American species. Biomass Bioenergy 25, 381–388.

Lan, X., Dlugokencky, E.J., Mund, J.W., Crotwell, A.M., Crotwell, M.J., Moglia, E., Madronich, M., Neff, D., Thoning, K.W., 2022. Atmospheric Carbon Dioxide Dry Air Mole Fractions from the NOAA GML Carbon Cycle Cooperative Global Air Sampling Network, 1968–2021. Version: 2022-11-21. https://doi.org/10.15138/wkgj-f215.

Lucas, R.W., Sponseller, R.A., Gundale, M.J., Stendahl, J., Fridman, J., Högberg, P., Laudon, H., 2016. Long-term declines in stream and river inorganic nitrogen (N) export correspond to forest change. Ecol. Appl. 26, 545–556.

Luo, Y., Su, B., Currie, W.S., Dukes, J.S., Finzi, A., Hartwig, U., Hungate, B., McMurtrie, R.E., Oren, R., Parton, W.J., Pataki, D.E., Shaw, M.R., Zak, D.R., Field, C. B., 2004. BioScience 54, 731–739.

Magnussen, S., Smith, B., Uribe, A.S., 2007. National Forest Inventories in North America for monitoring forest tree species diversity. Plant Biosystems - An International Journal Dealing with all Aspects of Plant Biology 141, 113–122.

Martínez-Sancho, E., Slámová, L., Morganti, S., Grefen, C., Carvalho, B., Dauphin, B., Rellstab, C., Gugerli, F., Opgenoorth, L., Heer, K., Knutzen, F., von Arx, G., Valladares, F., Cavers, S., Fady, B., Alía, R., Aravanopoulos, F., Avanzi, C., Bagnoli, F., Barbas, E., Bastien, C., Benavides, R., Bernier, F., Bodineau, G., Bastias, C.C., Charpentier, J., Climent, J.M., Corréard, M., Courdier, F., Danusevicius, D., Farsakoglou, A., García Del Barrio, J.M., Gilg, O., González-Martínez, S.C., Gray, A., Hartleitner, C., Hurel, A., Jouineau, A., Kärkkäinen, K., Kujala, S.T., Labriola, M., Lascoux, M., Lefebvre, M., Lejeune, V., Le-Provost, G., Liesebach, M., Malliarou, E., Mariotte, N., Matesanz, S., Michotey, C., Milesim, P., Myking, T., Notivol, E., Pakull, B., Piotti, A., Plomion, C., Pringarbem, M., Pyhäjärvi, T., Raffin, A., Ramírez-Valiente, J.A., Ramskogler, K., Robledo-Arnuncio, J.J., Savolainen, O., Schueler, S., Semerikov, V., Spanu, I., Thévenet, J., Tollefsrud, M.M., Turion, N., Veisse, D., Vendramin, G.G., Villar, M., Westin, J., Fonti, P., 2020. The GenTree Dendroecological collection, tree-ring and wood density data from seven tree species across Europe. Scientific Data 7, 1.

Mason, R.E., Craine, J.M., Lany, N.K., Jonard, M., Ollinger, S.V., Groffman, P.M., Fulweiler, R.W., Angerer, J., Read, Q.D., Reich, P., Templer, P.H., Elmore, A.J., 2022a. Evidence, causes, and consequences of declining nitrogen availability in terrestrial ecosystems. Science 376, 1–11.

Mason, R.E., Craine, J.M., Lany, N.K., Jonard, M., Ollinger, S.V., Groffman, P.M., Fulweiler, R.W., Angerer, J., Read, Q.D., Reich, P.B., Templer, P.H., Elmore, A.J., 2022b. Explanations for nitrogen decline - response. Science 376, 1170.

Mathias, J.M., Thomas, R.B., 2021. Global tree intrinsic water use efficiency is enhanced by increased atmospheric CO_2 and modulated by climate and plant functional types. Proc. Natl. Acad. Sci. 1187, e2014286118.

McCarroll, D., Loader, N.J., 2004. Stable isotopes in tree rings. Quat. Sci. Rev. 23, 771–801.

McLauchlan, K.K., Craine, J.M., 2012. Species-specific trajectories of nitrogen isotopes in Indiana hardwood forests, USA. Biogeosciences 9, 867–874.

McLauchlan, K.K., Craine, J.M., Oswald, W.W., Leavitt, P.R., Likens, G.E., 2007. Changes in nitrogen cycling during the past century in a northern hardwood forest. Proceedings of the National Academy of Sciences of the United States 104, 7466–7470.
McLauchlan, K.K., Gerhart, L.M., Battles, J.J., Craine, J.M., Elmore, A.J., Higuera, P.E., Mack, M.C., McNeil, B.E., Nelson, D.M., Pederson, N., Perakis, S.S., 2017. Centennial-scale reductions in nitrogen availability in temperate forests of the United States. Sci. Rep. 7, 7856.
Mead, D.J., Preston, C.M., 1994. Distribution and retranslocation of ^{15}N lodgepole pine over eight growing seasons. Tree Physiol. 4, 389–402.
Mook, W.G., 1983. ^{13}C in atmospheric CO_2. Neth. J. Sea Res. 20, 211–223.
Näsholm, T., Högberg, P., Franklin, O., Metcalfe, D., Keel, S.G., Campbell, C., Hurry, V., Linder, S., Högberg, M.N., 2013. Are ectomycorrhizal fungi alleviating or aggravating nitrogen limitation of tree growth in boreal forests? New Phytol. 198, 214–221.
National Oceanic and Atmospheric Administration (NOAA), National Centers for Environmental Information, 2022. Carbon dioxide now more than 50% higher than pre-industrial levels. https://www.noaa.gov/news-release/carbon-dioxide-now-more-than-50-higher-than-pre-industrial-levels [June 13, 2022].
Nömmik, H., 1966. The uptake and translocation of fertilizer N15 in young trees of scots pine and Norway spruce. *Stockholm: predecessors to SLU > Royal School of Forestry, Sveriges* lantbruksuniversitet. Studia forestalia Suecica 35.
Olff, H., Aerts, R., Bobbink, R., Cornelissen, J.H.C., Erisman, J.W., Galloway, J.N., Stevens, C.J., Sutton, M.A., de Vries, F.T., Wieger Wamelink, G.W., Wardle, D.A., 2022. Explanations for nitrogen decline. Science 376, 1169–1170.
Oulehle, F., Tahovská, K., Ač, A., Kolář, T., Rybníček, M., Čermák, P., Štěpánek, P., Trnka, M., Urban, O., Hruška, J., 2022. Changes in forest nitrogen cycling across deposition gradient revealed by $\delta^{15}N$ in tree rings. Environ. Pollut. 304, 119104.
Pan, Y., Birdsey, R.A., Fang, J., Houghton, R., Kauppi, P.E., Kurz, W.A., Phillips, O.L., Shvidenko, A., Lewis, S.L., Canadell, J.G., Ciais, P., Jackson, R.B., Pacala, S.W., McGuire, A.D., Piao, S., Rautianen, A., Sitch, S., Hayes, D., 2011. A large and persistent carbon sink in the world's forests. Science 333, 988–993.
Peuke, A.D., 2010. Correlations in concentrations, xylem and phloem flows, and partitioning of elements and ions in intact plants. A summary and statistical re-evaluation of modelling experiments in *Ricinus communis*. J. Exp. Bot. 61, 635–655.
Poulson, S.R., Chamberlain, C.P., Friedland, A.J., 1995. Nitrogen isotope variation of tree rings as a potential indicator of environmental change. Chem. Geol. 125, 307–315.
Pretzsch, H., Biber, P., Schütze, G., Kemmerer, J., Uhl, E., 2018. Wood density reduced while wood volume growth accelerated in central European forests since 1870. For. Ecol. Manag. 429, 589–616.
R Core Team, 2022. R: A Language and Environment for Statistical Computing. R Foundation for Statistical Computing, Vienna, Austria.
Rawson, H.M., Begg, J.E., Woodward, R.G., 1977. The effect of atmospheric humidity on photosynthesis, transpiration and water use efficiency of leaves of several plant species. Planta 134, 5–10.
Romijn, E., Lantican, C.B., Herold, M., Lindquist, E., Ochieng, R., Wijaya, A., Murdiyarso, D., Verchot, L., 2015. Assessing change in national forest monitoring capacities of 99 tropical countries. For. Ecol. Manag. 352, 109–123.
Rowell, R.M., Pettersen, R., Tshabalala, M.A., 2012. Cell wall chemistry. In: Rowell, R.M. (Ed.), Handbook of Wood Chemistry and Wood Composites. CRC Press, Boca Raton, pp. 37–72.
Saurer, M., Spahni, R., Frank, D.C., Joos, F., Leuenberger, M., Loader, N.J., McCarroll, D., Gagen, M., Poulter, B., Siegwolf, R.T.W., Andreu-Hayles, L., Boettger, T., Dorado Liñán, I., Fairchild, I.J., Friedrich, M., Gutierrez, E., Haupt, M., Hilasvuori, E., Heinrich, I., Helle, G., Grudd, H., Jalkanen, R., Levanič, T., Linderholm, H.W., Robertson, I., Sonninen, E., Treydte, K., Waterhouse, J.S., Woodley, E.J., Wynn, P. M., Young, G.H.F., 2014. Spatial variability and temporal trends in water-use efficiency of European forests. Glob. Chang. Biol. 20, 3700–3712.
Schelhaas, M.J., Varis, S., Schuck, A., Nabuurs, G.J., 2006. EFISCEN Inventory Database. European Forest Institute, Joensuu, Finland. http://www.efi.int/portal/virtual_library/databases/efiscen/.
Schleppi, P., Bucher-Wallin, L., Siegwolf, R.T.W., Saurer, M., Muller, N., Bucher, J., 1999. Simulation of increased nitrogen deposition to a montane forest ecosystem: partitioning of the added ^{15}N. Water Air Soil Pollut. 116, 129–134.
Speer, J., 2010. Fundamentals of Tree Ring Research. University of Arizona Press.
Swedish Meteorological and Hydrological Institute (SMHI), 2022. Climate indicator – precipitation. https://www.smhi.se/en/climate/climate-indicators/climate-indicators-precipitation-1.91462 [2023-04-10].
Thorell, K.E., Östlin, E.O., 1931. The National Forest Survey of Sweden. J. For. 29, 585–591.
Tomlinson, G., Siegwolf, R.T.W., Buchmann, N., Schleppi, P., Waldner, P., Weber, P., 2014. The mobility of nitrogen across tree-rings of Norway spruce (*Picea abies* L.) and the effect of extraction method on tree-ring $\delta^{15}N$ and $\delta^{13}C$ values. Rapid Commun. Mass Spectrom. 27, 1258–1264.
Tomppo, E., Gschwantner, T., Lawrence, M., McRoberts, R.E., Gabler, K., Schadauer, K., Vidal, C., Lanz, A., Ståhl, G., Cienciala, E., 2010. National forest inventories. Pathways for common reporting. European Science Foundation 1, 541–553.
United Nations Food and Agriculture Organization (UN FAO) (n.d.). National Forest Inventory. https://www.fao.org/national-forest-monitoring/areas-of-work/nfi/en/. [2023-05-10].
van Buijtenen, J.P., 2004. Tree breeding practices, genetics and improvement of wood properties. In: Encyclopedia of Forest Sciences. Elsevier Ltd., pp. 1466–1472
Yuan, W., Zheng, Y., Piao, S., Ciais, P., Lombardozzi, D., Wang, Y., Ryu, Y., Chen, G., Dong, W., Hu, Z., Jain, A.K., Jiang, C., Kato, E., Li, S., Lienert, S., Liu, S., Nabel, J.E. M.S., Qin, Z., Quine, T., Sitch, S., Smith, W.K., Wang, F., Wu, C., Xiao, Z., Yang, S., 2019. Increased atmospheric vapor pressure deficit reduces global vegetation growth. Sci. Adv. 5, 1–12.
Zobel, B.J., van Buijtenen, J.P., 1989. Wood variation and wood properties. In: Wood Variation. Springer, Berlin Heidelberg, pp. 1–32.

II

Article

Rising atmospheric CO_2 reduces nitrogen availability in boreal forests

https://doi.org/10.1038/s41586-025-10039-5

Received: 12 December 2024

Accepted: 11 December 2025

Published online: 18 February 2026

Open access

Check for updates

Kelley R. Bassett[1]✉, Stefan F. Hupperts[1], Sandra Jämtgård[1], Lars Östlund[1], Jonas Fridman[2], Steven S. Perakis[3] & Michael J. Gundale[1]

Anthropogenic nitrogen (N) pollution is a cause of eutrophication globally[1]. However, recent datasets indicate that some ecosystems may be experiencing widespread oligotrophication—declining N availability—which is suggested to be a response to elevated atmospheric carbon dioxide (CO_2)[2]. Plant N isotope ($\delta^{15}N$) chronologies have served as primary evidence for oligotrophication, but there is wide disagreement whether rising CO_2 or temporal changes in N deposition explain these patterns[3–6]. Here we construct $\delta^{15}N$ tree-ring chronologies using archived samples from Sweden's 23.5-million-hectare forest area from 1961 to 2018. The study area spans a 1,500-km latitudinal distance where N deposition varies fourfold, but where rising CO_2 is spatially uniform. Our data show declining $\delta^{15}N$ chronologies throughout Sweden, including forests in the far north where atmospheric N deposition rates are very low. Linear mixed-effects models showed that rising CO_2 is the strongest predictor of $\delta^{15}N$ values, whereas N deposition variables, temperature and forest basal area had lower explanatory power. Our findings suggest that elevated atmospheric CO_2 is causing oligotrophication in boreal forests, which has implications for predicting their future role as sinks in the global carbon cycle[7–9].

Human-induced environmental change has approached or exceeded several planetary Earth-system process boundaries[10], in part owing to substantial alterations to both the global nitrogen (N) and carbon (C) cycles. Since 1960, humans have increased the rate of reactive nitrogen (Nr) creation by a factor of 10 owing to the industrial Haber–Bosch process, expansion of leguminous crops and fossil fuel combustion; and Nr creation is expected to increase by a factor of 18 by 2050 (ref. 11). In addition, considerable atmospheric Nr emissions and subsequent deposition of NH_x and NO_y to Earth's surface occur as a consequence of global energy and food production[12]. These changes have enriched terrestrial and aquatic ecosystems with N, causing well-documented eutrophication and acidification problems in many regions with high-Nr inputs[13]. At the same time, human activities have increased atmospheric carbon dioxide (CO_2) concentrations by more than 50% since the start of the industrial age, which has been shown to enhance terrestrial net primary productivity (NPP)[14,15]. Furthermore, enhanced NPP from rising atmospheric CO_2 has been proposed to interact with the N cycle, potentially reducing N availability and intensifying N limitation of terrestrial NPP (referred to as progressive N limitation (PNL)[16] or ecosystem oligotrophication[2,17]). PNL may occur if rising CO_2 stimulates plant growth and N uptake that reduces soil N availability for further plant growth, or if CO_2 increases the plant C:N ratio that stimulates microbial N immobilization during detrital decomposition, thus also reducing soil N availability. Consequently, although it is well known that Nr deposition causes eutrophication in some regions, it is plausible that rising CO_2 may have an opposing effect, leaving substantial uncertainty in the trajectory of terrestrial N limitation, which has implications for Earth-system model predictions of the future terrestrial C sink[18].

Although eutrophication owing to excess N has been an active focus of research over many decades in natural ecosystems, several recent datasets instead indicate that widespread oligotrophication may be occurring. Chronologies (that is, time series) of N stable isotope ratios ($\delta^{15}N$) in plant tissues that span decades to centuries have served as key evidence for oligotrophication because they integrate multiple N-cycling processes in ecosystems, yet the interpretation of these chronology datasets has been the subject of ongoing debate[2–6]. The $\delta^{15}N$ values of plants broadly reflect sources of plant N as well as soil and ecosystem N availability, with higher N availability yielding elevated plant $\delta^{15}N$ values[19]. This pattern arises from $^{15}N/^{14}N$ isotopic fractionation that occurs at both the ecosystem level and during plant N uptake[20–22]. At the ecosystem level, high N availability relative to plant N demand promotes losses of soil inorganic N with low $\delta^{15}N$ values (for example, ammonia volatilization, nitrification, nitrate leaching and denitrification), which increases the $\delta^{15}N$ of remaining soil N pools and of the ecosystem as a whole, thus increasing plant $\delta^{15}N$ (ref. 22). During plant N uptake in forests, the primary fractionation mechanism is through the production of ^{15}N-enriched mycorrhizal tissue and preferential transfer of ^{14}N to host plants, with the greatest fractionation occurring at low N availability and for ectomycorrhizal associations[20]. In contrast to the above, only small N-isotope discrimination occurs by direct root N uptake at levels present in natural ecosystems, and N-isotope ratios are generally well correlated among plant tissues (leaves, stems and roots)[22]. Thus, when N limitation intensifies, reduced N losses and

[1]Department of Forest Ecology and Management, Swedish University of Agricultural Sciences, Umeå, Sweden. [2]Department of Forest Resource Management, Swedish University of Agricultural Sciences, Umeå, Sweden. [3]US Geological Survey, Forest and Rangeland Ecosystem Science Center, Corvallis, OR, USA. ✉e-mail: kelley.bassett@slu.se

greater plant reliance on mycorrhizal fungi can steer plant $\delta^{15}N$ values more negative.

The spatial relationship between plant $\delta^{15}N$ values, foliar N content and N availability is now well established and accepted[2,23,24], and as a result, $\delta^{15}N$ values have more recently been used as a proxy to indicate changes in N limitation through time[21], where $\delta^{15}N$ plant chronologies with negative slopes have been interpreted as evidence for oligotrophication[2,4,25]. Notably, wood samples from forests across the continental USA showed a slight temporal decline of $\delta^{15}N$ (about -0.009 ± 0.002‰ yr^{-1}, 1850 to 2010)[25]; furthermore, a meta-regression of published foliar $\delta^{15}N$ data found a temporal decline of $\delta^{15}N$ globally (-0.043 ± 0.014‰ yr^{-1}, 1980 to 2017)[2]. Most recently, ref. 4 compiled a range of evidence for widespread ecosystem oligotrophication, including temporal $\delta^{15}N$ declines for several sample types, namely, foliar, wood, lake sediment and herbarium samples, as well as other N-cycling response variables, for example, direct measurement of watershed N exports and soil N mineralization. Corresponding datasets showing temporal declines of foliar N content provide further support for interpretations of reported $\delta^{15}N$ chronologies[2,26].

In response to these findings, alternative interpretations of declining $\delta^{15}N$ trends have been proposed. First, it is proposed that increasing N limitation over the past three decades is instead the result of declining Nr deposition rates (that is, declining eutrophication), which reached peak levels in North America and Europe in the 1980s[3,6]. Furthermore, it is suggested that the decline in N deposition rates during recent decades has been driven by policy-regulated reductions in the oxidized forms of Nr deposition (NO_y), which are derived from fossil organic matter combustion and typically have higher $\delta^{15}N$ values[6], whereas reduced forms (NH_x) have increased[3]. Shifting $\delta^{15}N$ values of Nr deposition owing to a change in the NH_x:NO_y ratio is therefore an additional alternative explanation for the observed declining $\delta^{15}N$ values of plants, instead of CO_2-induced oligotrophication. Furthermore, a study[27] applying an ecosystem ^{15}N fractionation model concluded that several other factors in addition to increasing CO_2 can plausibly explain declining $\delta^{15}N$ values, including the amount and signature of Nr deposition inputs, and changes in temperature. Consequently, there remains wide disagreement regarding the drivers of reported $\delta^{15}N$ chronologies, and thus uncertainty in their interpretation.

Constructing $\delta^{15}N$ chronologies

To address this debate, we analysed $\delta^{15}N$ values from 1,609 independent, archived tree cores collected between 1961 and 2018 (Fig. 1a); decadal increments from tree cores representing the time span 1950 to 2017 across Sweden's 23.5-million-hectare forest area. We focused on $\delta^{15}N$ rather than %N, given that %N of wood is not considered a good indicator of plant N limitation owing to its very low concentration and subsequent sensitivity to concentration variability of more abundant wood elements (for example, C and oxygen (O))[22,28–31]. Swedish forests span a 1,500-km latitudinal gradient of Nr deposition, with southern Sweden experiencing around fourfold higher Nr deposition during the industrial age, as well as stronger reductions in total and NO_y deposition in response to emissions-reduction policy[32,33]. In contrast, Nr deposition rates in northern Sweden have been consistently low and stable[33] (Fig. 1a,b). Compared with the strong gradients in Nr deposition across Sweden, rising atmospheric concentrations of CO_2 gas are generally well mixed and show relatively negligible spatial variation (about 0.5% variation regionally)[34].

Owing to the independent spatio-temporal relationship between atmospheric Nr deposition and rising CO_2 across Sweden (Extended Data Fig. 1), the Swedish forest landscape is an ideal large-scale study system to separate the debated drivers of $\delta^{15}N$ chronologies and thus reconcile their interpretation. Furthermore, we use a sampling approach that yields more robust $\delta^{15}N$ chronologies than previous efforts. First, we acquired wood samples for two tree species, *Picea abies* (L.) H. Karst and *Pinus sylvestris* L., from the Swedish National Forest Inventory (NFI) tree-core archive for which sample collection occurred between 1961 and 2018, using a stratified random sampling approach (Methods). This systematic approach has several advantages. First, although using wood cores can be problematic for establishing $\delta^{15}N$ chronologies owing to tree ageing and N translocation across xylem[35–37], our use of archived samples allows us to sample trees of the same age class across space and through time, eliminating these inherent problems[38]. Second, this systematic approach allows us to control for spatial or temporal variation in the species sampled, as well as tree and site characteristics, factors that have not been held constant in previous analyses[2,25,39]. Finally, our focus on wood $\delta^{15}N$ avoids concerns raised regarding the interpretation of foliar %N chronologies as an indicator of PNL, which have alternatively been suggested to result from photosynthetic down-regulation instead of PNL, as this alternative explanation would not directly affect wood N-isotope ratios[3].

We first analysed our data by dividing Sweden into four regions—north, central, southeast and southwest—which represent a large gradient of atmospheric Nr deposition levels ranging from very low in the north (≤3 N kg ha^{-1} yr^{-1}) to their maximum rates in the southwest (regional mean approximately 12 kg N ha^{-1} yr^{-1}; Fig. 1b) when at their peak in the late 1990s[40]. The $\delta^{15}N$ chronologies for each of these regions were negative for both *P. sylvestris* and *P. abies* (between −0.01‰ yr^{-1} and −0.07‰ yr^{-1}; Fig. 1c–j). These $\delta^{15}N$ chronologies were markedly more negative and less variable than some previously published $\delta^{15}N$ chronologies[25,32,41,42], because our methodology was not confounded by tree age or N translocation across tree rings, thus making our measurements more sensitive to detect temporal changes in ecosystem N-cycle processes[38]. Our data also showed that pairwise comparisons of the $\delta^{15}N$ chronology slopes never differed between the low- and high-Nr-deposition northern and southern regions, respectively, for both *P. sylvestris* and *P. abies*, indicating that N deposition was not strongly influential on $\delta^{15}N$.

Drivers of forest $\delta^{15}N$ variation

We constructed linear mixed-effects models to directly compare the explanatory power of CO_2 versus atmospheric Nr deposition variables on the spatial and temporal variation of tree-ring $\delta^{15}N$ values, while controlling for additional factors of mean annual temperature, temperature change and total basal area. Given that all Nr deposition variables (total N deposition, NH_x, NO_y and NH_x:NO_y) were strongly co-linear (Extended Data Table 1), we selected four separate models, substituting each Nr deposition variable in successive model runs, as well as successive model variants that included either latitude and longitude, and absolute temperature or temperature change (Extended Data Tables 2 and 3).

The model results showed that CO_2 was consistently the strongest predictor of $\delta^{15}N$ values (see partial marginal coefficient of determination (R^2m) values in Extended Data Tables 1–3). This conclusion persisted among model variants that held space constant by including latitude and longitude as fixed factors (Extended Data Table 2), as well as when absolute temperature or temporal temperature change was considered (Extended Data Table 3). The relationship between $\delta^{15}N$ and CO_2 was strongly negative for both *P. sylvestris* (-0.04 ± 0.005‰ $\delta^{15}N$ ppm^{-1} CO_2) and *P. abies* (-0.028 ± 0.005‰ $\delta^{15}N$ ppm^{-1} CO_2; Fig. 2a). The emergence of CO_2 as the strongest predictor of declining $\delta^{15}N$ values for both tree species is consistent with ecosystem oligotrophication in response to increasing atmospheric CO_2 (Fig. 2). Furthermore, *P. sylvestris* showed a small but significantly more negative relationship with CO_2 than *P. abies* (Fig. 2a). It is plausible that this small difference between the two species is related to their N-use efficiencies. Specifically, *P. sylvestris* has a higher rate of needle turnover and thus lower N-use efficiency than *P. abies*[43], making *P. sylvestris* more reliant on annual soil N uptake for growth, and which may reveal stronger effects of CO_2 on $\delta^{15}N$ chronologies in this species.

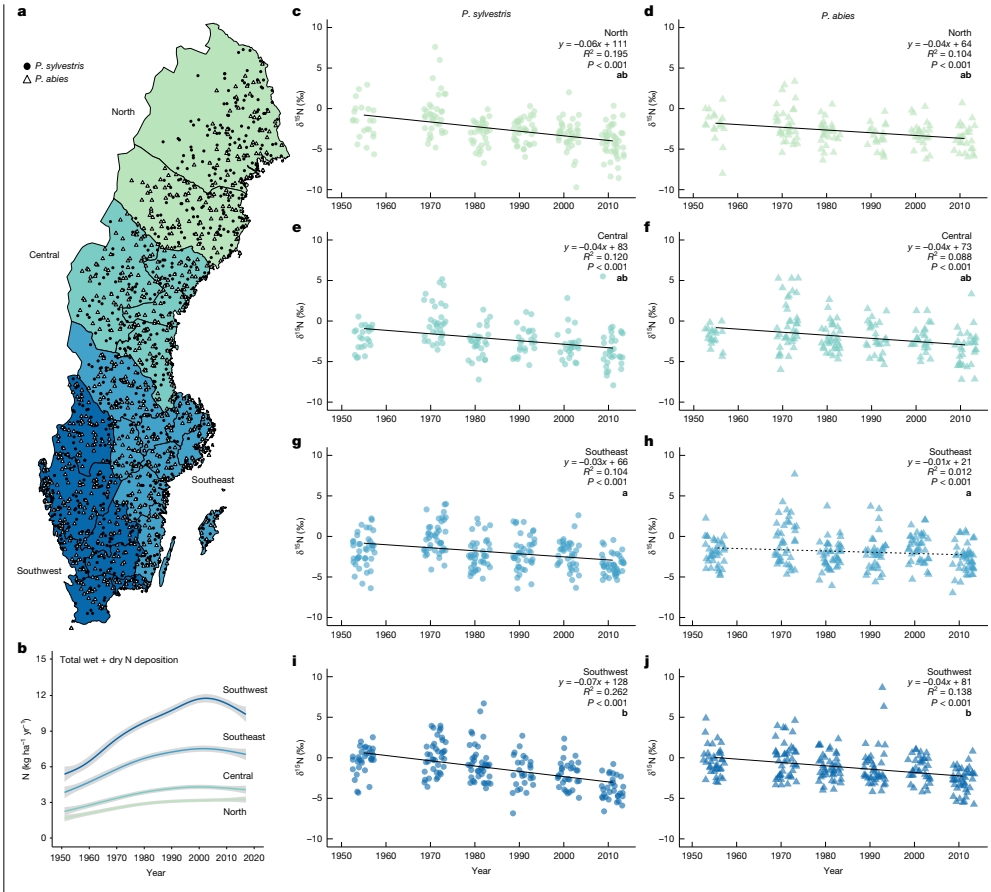

Fig. 1 | Spatial and temporal patterns of wood $\delta^{15}N$ and N deposition across Sweden. a, Spatial distribution of independent samples ($n = 1609$) across 4 Nr deposition regions spanning Sweden's north–south gradient, representing increasing deposition rates from lowest (north) to highest (southwest). **b**, Temporal change in total wet plus dry N deposition (kg ha^{-1} yr^{-1}) for samples across the regions. **c**–**j**, Temporal linear regression trends in stemwood $\delta^{15}N$ (‰) for *P. sylvestris* (**c**,**e**,**g**,**i**) and *P. abies* (**d**,**f**,**h**,**j**) from 1951 to 2017 in each of the Nr deposition regions: north (**c**,**d**), central (**e**,**f**), southeast (**g**,**h**) and southwest (**i**,**j**). All relationships are significant ($P < 0.001$) except for *P. abies* in the southeast region (**h**), where the non-significant relationship is shown as a dashed line. Lowercase bold letters in **c**–**j** denote significant differences in regression slopes among regions, within each species ($\alpha = 0.05$). Shading in **b** indicates the 95% confidence interval. A small horizontal offset was applied to time plots **c**–**j** to increase the visibility of points (see 'Statistical methods'). Data sources are cited in Methods. Sweden boundary map in **a** from Lantmäteriet under a Creative Commons licence CC0 1.0.

Regarding Nr deposition variables, the NH_x:NO_y ratio had no significant relationship with $\delta^{15}N$. However, the remaining three Nr deposition variables (total N deposition, NH_x and NO_y) showed weak positive relationships with $\delta^{15}N$, which could indicate either that higher Nr deposition increases N availability or that changing $\delta^{15}N$ values of Nr deposition directly alters the $\delta^{15}N$ values of trees. Regardless of the mechanism, the positive relationship we identified between these Nr deposition variables and $\delta^{15}N$ provides some support that declining Nr deposition can steer $\delta^{15}N$ chronologies in the negative direction, given that Nr deposition has been declining since the late 1990s in southern Sweden[6] (Fig. 1b). However, we highlight that the explanatory power of these Nr deposition variables is substantially lower than CO_2 (partial R^2m values ≤0.005 versus 0.176, respectively; Extended Data Table 1), and further, the suggested importance of NH_x:NO_y dynamics was not supported by our data.

Our analysis also showed that $\delta^{15}N$ showed a positive relationship with 10-year averages of both annual temperature and total basal area (Fig. 2f,g). The positive relationship between temperature and $\delta^{15}N$ persisted regardless of whether absolute temperature or temperature change were considered in the model. Positive relationships of $\delta^{15}N$ with temperature or temperature change[23,44] are attributed to faster N cycling and greater fractionating N loss in warmer and warming climates, which increases the $\delta^{15}N$ value of soil inorganic N for plant uptake. Basal area was the only predictor variable derived from

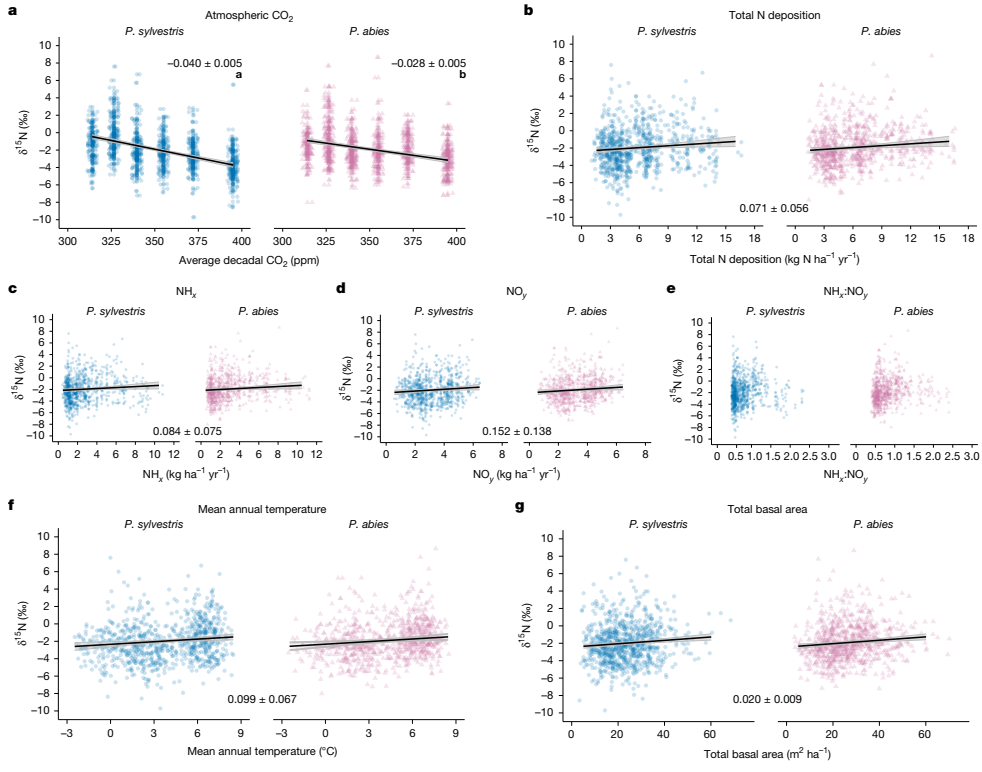

Fig. 2 | Modelled relationship between wood $\delta^{15}N$ and environmental drivers across Sweden. a–g, Wood $\delta^{15}N$ as a function of: the main predictors in the final model, atmospheric CO_2 (**a**) and total N deposition (**b**); alternative N deposition variables, NH_x (**c**), NO_y (**d**) and NH_x:NO_y (**e**) (Extended Data Table 1b–d); mean annual temperature (**f**); and total basal area (**g**). Regression lines show modelled $\delta^{15}N$ values accounting for fixed and random effects. Numbers within each panel indicate modelled slopes ± 95% confidence intervals. Shading represents 95% confidence intervals. Lowercase bold letters in **a** denote significant differences in regression slopes between species ($\alpha = 0.05$). The relationship between $\delta^{15}N$ and NH_x:NO_y in **e** was not significant; therefore, no regression line is shown. A small horizontal offset was applied to plots **a**–**e** to increase visibility of points (see 'Statistical methods'). Data sources are cited in Methods.

individual sample plots and thus accounted for plot-to-plot variation in stand productivity within grid cells, while also representing forest biomass variation with latitude and time[45,46] (Extended Data Fig. 2i,j). The weak positive relationship may reflect that higher-fertility sampling plots within a given grid cell have higher basal area, after accounting for some degree of broad spatial or temporal co-linearity with temperature and CO_2, which were environmental factors with greater explanatory power in our model[47]. Despite the additional significant effects of temperature and basal area in our models, CO_2 consistently emerged as the dominant factor explaining forest $\delta^{15}N$ variation, indicated by its much larger partial R^2m in all model variants (Extended Data Tables 1–3).

Implications

Our results have multiple implications for understanding the response of boreal forest N availability to environmental change factors, particularly rising atmospheric CO_2 and anthropogenic Nr deposition. Foremost, the highly significant effect of atmospheric CO_2 on tree-ring $\delta^{15}N$ that we observed, using a well-constrained sampling methodology that minimizes isotopic effects associated with tree ageing and N translocation across tree rings[38], provides robust evidence that negative $\delta^{15}N$ chronologies are an indicator of ecosystem oligotrophication in response to rising CO_2 (refs. 2,4,16,25), rather than a symptom of changing Nr deposition patterns[3,6]. As our sampling area spanned a large gradient in latitude, forest biomass, mean annual temperature and Nr deposition, these findings are broadly relevant for understanding the trajectory of N availability in northern forests where declining $\delta^{15}N$ chronologies have previously been identified[48,49]. Furthermore, global increases in CO_2 may indirectly influence $\delta^{15}N$ chronologies owing to the influence that rising CO_2 has on climate warming. Our analysis showed that temperature and temperature change had opposite and weaker relationships than CO_2 with $\delta^{15}N$ (positive versus negative, respectively), reinforcing that the direct influence of rising CO_2 was a more dominant driver than any potential indirect effect that rising CO_2 has on warming. These findings are further consistent with meta-analysis of elevated CO_2 (eCO_2) experiments showing a predominance of declines in foliar $\delta^{15}N$ across multiple experiments[50], and datasets indicating that CO_2 may be tightening the N cycle in many environments, including

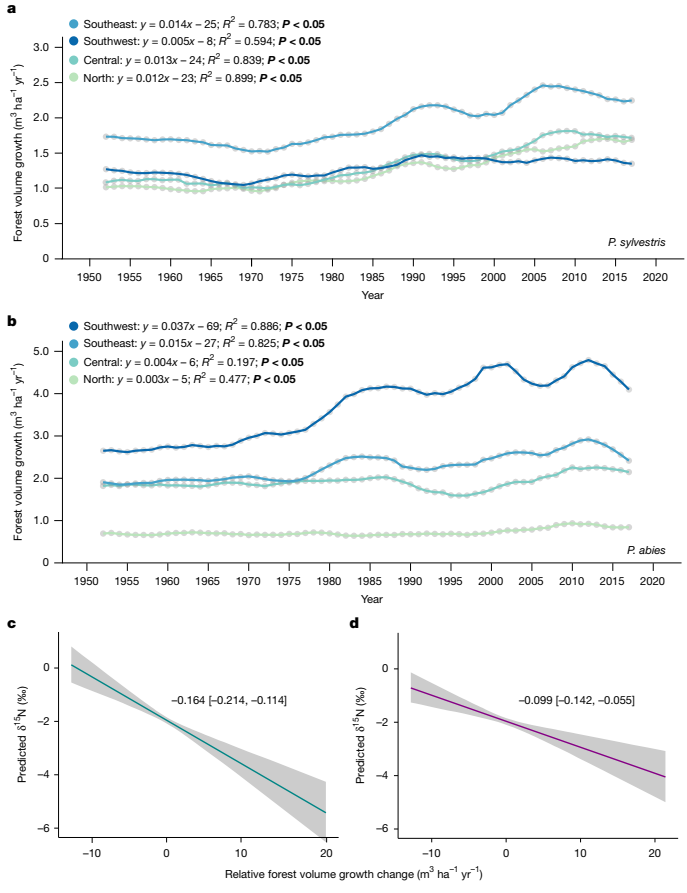

Fig. 3 | Forest growth dynamics and their relationship with $\delta^{15}N$ across Swedish regions. a,**b**, Annual forest volume growth ($m^3\ ha^{-1}\ yr^{-1}$) for *P. sylvestris* (**a**) and *P. abies* (**b**) by region—north, central, southeast and southwest Sweden—over 1950–2017. Significant linear regression slopes ($P < 0.05$) are in bold; however, piecewise linear interpolation is shown for enhanced visualization. **c**, Predicted $\delta^{15}N$ (‰) values as a function of relative forest volume growth change ($m^3\ ha^{-1}\ yr^{-1}$) accounting for random effects (grid) and fixed effect of absolute forest volume growth ($m^3\ ha^{-1}\ yr^{-1}$). **d**, Predicted $\delta^{15}N$ (‰) values as a function of relative forest volume growth change ($m^3\ ha^{-1}\ yr^{-1}$) accounting for random effects (grid) and fixed effects of total basal area ($m^2\ ha^{-1}$). Regression lines show modelled $\delta^{15}N$ values accounting for all fixed and random effects. Shading in **c** and **d** indicates 95% confidence intervals. Data sources are cited in Methods.

declining foliar N content in Europe and North American forests[2,26], declining riverine N exports in central Europe and North America[4,51], and declining stream water N exports in northernmost Sweden, where Nr deposition is very low[52–55].

Boreal forests similar to those we studied across Sweden have an important role in the global C cycle by accumulating and storing a considerable amount of terrestrial C (about 17% of the terrestrial land area, but accounting for about 32% of terrestrial C)[46,56]. Our findings have further implications for understanding how rising CO_2 may impact their future C sink strength. Two non-mutually exclusive mechanisms provide a link between rising CO_2 and declining N availability and $\delta^{15}N$ chronologies. First, rising CO_2 can increase plant photosynthesis, growth and N demand[57] in accumulating biomass, thus depleting available N from soil and reducing fractionation associated with ecosystem N losses[16,22]. At the same time, rising CO_2 can increase plant C:N ratios and the production of high C:N litter, which increases the N demand for detritus decomposition, and stimulates soil microbial N immobilization[9,58,59]. Both of these responses to rising CO_2 would be expected to reduce fractionating N loss and the $\delta^{15}N$ values of inorganic N in soil, and thus steer $\delta^{15}N$ chronologies more negative through time[4].

In support that increased forest growth may contribute to reducing N availability, data from the Swedish NFI show that growth of mesic pine and spruce forests, similar to those from which we established $\delta^{15}N$ chronologies, shows a long-term growth increase since the 1950s in all regions (Fig. 3a,b). Our analysis further indicates a strong negative relationship between the temporal change in forest growth and

wood $\delta^{15}N$ (Fig. 3c,d), which is consistent with the prediction of PNL that increasing plant N demand promotes a negative feedback on N availability (Fig. 3 and Extended Data Table 4). It has alternatively been suggested that photosynthetic downregulation of foliar N is a dominant process that reduces plant N demand in response to rising CO_2 (refs. 3,60). Although not mutually exclusive, our analysis indicates that increasing forest N demand at the stand level, owing to increasing biomass and growth, appears to outweigh any potential physiological reduction in N demand at the leaf level[60]. Furthermore, given that the photosynthetic downregulation hypothesis predicts reduced plant N demand in response to rising CO_2, this alternative hypothesis does not provide a mechanism to explain the declining $\delta^{15}N$ chronologies we observe, nor the observed patterns of declining aquatic N exports from Swedish forest landscapes[53,55]. In recent decades, forest growth has levelled off in many parts of Sweden (Fig. 3a,b), which is also consistent with predictions by some Earth-system models that PNL feedbacks eventually constrain the response of terrestrial NPP to rising CO_2 (refs. 18,61–63), possibly interacting with other factors (for example, drought and disease). Two previous experiments in northern Sweden that applied experimental CO_2 treatments, that is, eCO_2, also reached the conclusion that forest growth response to eCO_2 is constrained by N availability[64]. These findings support our interpretation that reduced N availability, as indicated by our $\delta^{15}N$ chronologies, may reduce the sensitivity of boreal forest growth to future increases in CO_2 (refs. 7,16).

In addition to increased growth and plant C:N ratios of plant biomass and detritus, mycorrhizal fungi provide the other non-mutually exclusive mechanism that links rising CO_2 to declining $\delta^{15}N$ chronologies. As forest N demand increases, trees may enhance their C investment in mycorrhizal fungi to enhance soil N acquisition, particularly as soil inorganic N availability declines[65–67]. Many tree species worldwide, and especially those in high-latitude regions such as boreal forests, associate with ectomycorrhizal fungi that mobilize N from the soil[65,68]. During N transfer from fungus to host trees, mycorrhizal fungi disproportionately retain ^{15}N in their hyphal mass, and pass ^{14}N to their tree hosts, with the degree of such ^{15}N fractionation increasing as N availability declines[20]. Thus, the declining $\delta^{15}N$ chronologies we observed may reflect that an increasing proportion of plant N is obtained via ectomycorrhizal fungi, possibly owing to an increase in fungal biomass that sequesters a larger fraction of the mobilized N pool. Furthermore, studies from boreal forest fertility gradients indicate that some specific ectomycorrhizal taxa are especially responsive to increasing N limitation intensity, including some taxa that acquire N by degrading soil organic matter (that is, 'ectomycorrhizal decomposers')[65,66,68,69]. A recent meta-analysis of 108 eCO_2 experiments showed that although eCO_2 leads to increased soil C in most ecosystem types, ecosystems dominated by ectomycorrhizal tree species showed no such increase, despite positive NPP responses[70]. This suggests that acquisition of soil organic N by ectomycorrhizal decomposers may allow sustained forest growth in response to rising CO_2 (ref. 71), but this may subsequently constrain soil C accumulation in these forest mycorrhizal types.

Resolving the dominant mechanisms of the boreal forest ecosystem response to rising CO_2 has important implications for C balances, and especially the distribution of above- versus belowground C (ref. 67). Carbon stocks of boreal soils are about fivefold greater than C stored in aboveground biomass[66] and may respond differently to eCO_2 owing to increases in tree growth versus upregulation of ectomycorrhizal fungal partners for N acquisition[70]. Both mechanisms probably operate simultaneously and contribute to our finding of declining $\delta^{15}N$. Determining the relative importance of these two mechanisms as controls on $\delta^{15}N$ values across different boreal forest contexts, and the resulting sensitivity of above- versus belowground C compartments in response to CO_2-induced PNL may be addressed through a combination of approaches, such as intercomparisons of coupled C–N Earth-system models, and deployment of eCO_2 experiments, which are poorly represented in boreal ecosystems. Although it is clear that humans have already surpassed several of Earth's planetary boundaries[10], in part owing to alterations of both the N and C cycles, our data show that these cycles are not changing independently. It further suggests that declining N availability in response to rising CO_2 will be a more dominant driver of boreal forest C exchange in the future, compared with N enrichment from atmospheric Nr deposition.

Online content

Any methods, additional references, Nature Portfolio reporting summaries, source data, extended data, supplementary information, acknowledgements, peer review information; details of author contributions and competing interests; and statements of data and code availability are available at https://doi.org/10.1038/s41586-025-10039-5.

1. Galloway, J. N. et al. Transformation of the nitrogen cycle: recent trends, questions, and potential solutions. *Science* **320**, 889–892 (2008).
2. Craine, J. M. et al. Isotopic evidence for oligotrophication of terrestrial ecosystems. *Nat. Ecol. Evol.* **2**, 1735–1744 (2018).
3. Hiltbrunner, E., Körner, C., Meier, R., Braun, S. & Kahmen, A. Data do not support large-scale oligotrophication of terrestrial ecosystems. *Nat. Ecol. Evol.* **3**, 1285–1286 (2019).
4. Mason, R. E. et al. Evidence, causes, and consequences of declining nitrogen availability in terrestrial ecosystems. *Science* **376**, eabh3767 (2022).
5. Mason, R. E. et al. Explanations for nitrogen decline: response. *Science* **376**, 1170–1170 (2022).
6. Olff, H. et al. Explanations for nitrogen decline. *Science* **376**, 1169–1170 (2022).
7. Norby, R. J. et al. Enhanced woody biomass production in a mature temperate forest under elevated CO_2. *Nat. Clim. Change* **14**, 983–988 (2024).
8. Terrer, C. et al. Nitrogen and phosphorus constrain the CO_2 fertilization of global plant biomass. *Nat. Clim. Change* **9**, 684–689 (2019).
9. Norby, R. J., Warren, J. M., Iversen, C. M., Medlyn, B. E. & McMurtrie, R. E. CO_2 enhancement of forest productivity constrained by limited nitrogen availability. *Proc. Natl Acad. Sci. USA* **107**, 19368–19373 (2010).
10. Rockström, J. et al. Planetary boundaries: exploring the safe operating space for humanity. *Ecol. Soc.* **14**, 32 (2009).
11. Galloway, J. N. et al. Nitrogen cycles: past, present, and future. *Biogeochemistry* **70**, 153–226 (2004).
12. Ackerman, D., Millet, D. B. & Chen, X. Global estimates of inorganic nitrogen deposition across four decades. *Glob. Biogeochem. Cycles* **33**, 100–107 (2019).
13. Galloway, J. N., Bleeker, A. & Erisman, J. W. The human creation and use of reactive nitrogen: a global and regional perspective. *Annu. Rev. Environ. Resour.* **46**, 255–288 (2021).
14. Lan, X. & Keeling, R. Trends in atmospheric CO_2. *Global Monitoring Laboratory* https://gml.noaa.gov/ccgg/trends (2025).
15. Yue, K. et al. Stimulation of terrestrial ecosystem carbon storage by nitrogen addition: a meta-analysis. *Sci. Rep.* **6**, 19895 (2016).
16. Luo, Y. et al. Progressive nitrogen limitation of ecosystem responses to rising atmospheric CO_2. *Bioscience* **54**, 731–739 (2004).
17. Hungate, B. A., Dukes, J. S., Shaw, M. R., Luo, Y. Q. & Field, C. B. Nitrogen and climate change. *Science* **302**, 1512–1513 (2003).
18. Canadell, J. G. in *Climate Change 2021: The Physical Science Basis* (eds Masson-Delmotte, V. et al.) 673–816 (Cambridge Univ. Press, 2021).
19. Robinson, D. $\delta^{15}N$ as an integrator of the nitrogen cycle. *Trends Ecol. Evol.* **16**, 153–162 (2001).
20. Hobbie, E. A. & Högberg, P. Nitrogen isotopes link mycorrhizal fungi and plants to nitrogen dynamics. *New Phytol.* **196**, 367–382 (2012).
21. Gerhart, L. M. & McLauchlan, K. K. Reconstructing terrestrial nutrient cycling using stable nitrogen isotopes in wood. *Biogeochemistry* **120**, 1–21 (2014).
22. Craine, J. M. et al. Ecological interpretations of nitrogen isotope ratios of terrestrial plants and soils. *Plant Soil* **396**, 1–26 (2015).
23. Craine, J. M. et al. Global patterns of foliar nitrogen isotopes and their relationships with climate, mycorrhizal fungi, foliar nutrient concentrations, and nitrogen availability. *New Phytol.* **183**, 980–992 (2009).
24. Chen, Q. et al. Global mycorrhizal status drives leaf $\delta^{15}N$ patterns. *J. Ecol.* **113**, 1150–1163 (2025).
25. McLauchlan, K. K. et al. Centennial-scale reductions in nitrogen availability in temperate forests of the United States. *Sci. Rep.* **7**, 7856 (2017).
26. Peñuelas, J. et al. Increasing atmospheric CO_2 concentrations correlate with declining nutritional status of European forests. *Commun. Biol.* **3**, 125 (2020).
27. Vitousek, P. M., Cen, X. Y. & Groffman, P. M. Has nitrogen availability decreased over much of the land surface in the past century? A model-based analysis. *Biogeochemistry* **167**, 793–806 (2024).
28. Doucet, A., Savard, M. M., Bégin, C. & Smirnoff, A. Is wood pre-treatment essential for tree-ring nitrogen concentration and isotope analysis? *Rapid Commun. Mass Spectom.* **25**, 469–475 (2011).
29. Bukata, A. R. & Kyser, T. K. Response of the nitrogen isotopic composition of tree-rings following tree-clearing and land-use change. *Environ. Sci. Technol.* **39**, 7777–7783 (2005).
30. Poulson, S. R., Chamberlain, C. P. & Friedland, A. J. Nitrogen isotope variation of tree rings as a potential indicator of environmental change. *Chem. Geol.* **125**, 307–315 (1995).

31. Thurner, M. et al. Nitrogen concentrations in boreal and temperate tree tissues vary with tree age/size, growth rate and climate. *Biogeosciences* **22**, 1475–1493 (2025).
32. United Nations Economic Commission for Europe. *1999 Protocol to Abate Acidification, Eutrophication and Ground-level Ozone to the Convention on Long-range Transboundary Air Pollution. Protocol to Abate Acidification, Eutrophication and Ground-level Ozone* (UNECE, 1999).
33. Pihl Karlsson, G., Akselsson, C., Hellsten, S. & Karlsson, P. E. Atmospheric deposition and soil water chemistry in Swedish forests since 1985—effects of reduced emissions of sulphur and nitrogen. *Sci. Total Environ.* **913**, 169734 (2024).
34. Hakkarainen, J., Ialongo, I., Maksyutov, S. & Crisp, D. Analysis of four years of global XCO_2 anomalies as seen by Orbiting Carbon Observatory-2. *Remote Sens.* **11**, 850 (2019).
35. Mead, D. J. & Preston, C. M. Distribution and retranslocation of ^{15}N lodgepole pine over eight growing seasons. *Tree Physiol.* **14**, 389–402 (1994).
36. Nõmmik, H. *The Uptake and Translocation of Fertilizer N^{15} in Young Trees of Scots Pine and Norway Spruce* (Predecessors to SLU, Royal School of Forestry, Sveriges lantbruksuniversitet, 1966).
37. Tomlinson, G. et al. The mobility of nitrogen across tree-rings of Norway spruce (*Picea abies* L.) and the effect of extraction method on tree-ring $\delta^{15}N$ and $\delta^{13}C$ values. *Rapid Commun. Mass Spectrom.* **28**, 1258–1264 (2014).
38. Bassett, K. R., Östlund, L., Gundale, M. J., Fridman, J. & Jämtgård, S. Forest inventory tree core archive reveals changes in boreal wood traits over seven decades. *Sci. Total Environ.* **900**, 165795 (2023).
39. Michaud, T. J., Cline, L. C., Hobbie, E. A., Gutknecht, J. L. M. & Kennedy, P. G. Herbarium specimens reveal that mycorrhizal type does not mediate declining temperate tree nitrogen status over a century of environmental change. *New Phytol.* **242**, 1717–1724 (2024).
40. Ferm, M. et al. Wet deposition of ammonium, nitrate and non-sea-salt sulphate in Sweden 1955 through 2017. *Atmos. Environ. X* **2**, 100015 (2019).
41. Kranabetter, J. M., Saunders, S., MacKinnon, J. A., Klassen, H. & Spittlehouse, D. L. An assessment of contemporary and historic nitrogen availability in contrasting coastal Douglas-Fir forests through $\delta^{15}N$ of tree rings. *Ecosystems* **16**, 111–122 (2013).
42. Oulehle, F. et al. Changes in forest nitrogen cycling across deposition gradient revealed by $\delta^{15}N$ in tree rings. *Environ. Pollut.* **304**, 119104 (2022).
43. Ťupek, B. et al. Foliar turnover rates in Finland—comparing estimates from needle-cohort and litterfall-biomass methods. *Boreal Environ. Res.* **20**, 283–304 (2015).
44. Hu, C. C. et al. Global distribution and drivers of relative contributions among soil nitrogen sources to terrestrial plants. *Nat. Commun.* **15**, 6407 (2024).
45. Balderas Torres, A. & Lovett, J. C. Using basal area to estimate aboveground carbon stocks in forests: La Primavera Biosphere's Reserve, Mexico. *Forestry* **86**, 267–281 (2013).
46. Gauthier, S., Bernier, P., Kuuluvainen, T., Shvidenko, A. Z. & Schepaschenko, D. G. Boreal forest health and global change. *Science* **349**, 819–822 (2015).
47. Bergh, J., Linder, S., Lundmark, T. & Elfving, B. The effect of water and nutrient availability on the productivity of Norway spruce in northern and southern Sweden. *Forest Ecol. Manag.* **119**, 51–62 (1999).
48. Elmore, A. J., Nelson, D. M. & Craine, J. M. Earlier springs are causing reduced nitrogen availability in North American eastern deciduous forests. *Nat. Plants* **2**, 16133 (2016).
49. McLauchlan, K. K., Craine, J. M., Oswald, W. W., Leavitt, P. R. & Likens, G. E. Changes in nitrogen cycling during the past century in a northern hardwood forest. *Proc. Natl Acad. Sci. USA* **104**, 7466–7470 (2007).
50. BassiriRad, H. et al. Widespread foliage $\delta^{15}N$ depletion under elevated CO_2: inferences for the nitrogen cycle. *Glob. Change Biol.* **9**, 1582–1590 (2003).
51. Sabo, R. D. et al. Positive correlation between wood $\delta^{15}N$ and stream nitrate concentrations in two temperate deciduous forests. *Environ. Res. Commun.* **2**, 025003 (2020).
52. Isles, P. D. F., Creed, I. F. & Bergström, A. K. Recent synchronous declines in DIN:TP in Swedish lakes. *Glob. Biogeochem. Cycles* **32**, 208–225 (2018).
53. Lucas, R. W. et al. Long-term declines in stream and river inorganic nitrogen (N) export correspond to forest change. *Ecol. Appl.* **26**, 545–556 (2016).
54. Goedkoop, W., Adler, S., Huser, B., Gardfjell, H. & Lau, D. C. P. Climate change-induced landscape alterations increase nutrient sequestration and cause severe oligotrophication of subarctic lakes. *Glob. Change Biol.* **31**, e70314 (2025).
55. Nilsson, J. L., Camiolo, S., Huser, B., Agstam-Norlin, O. & Futter, M. Widespread and persistent oligotrophication of northern rivers. *Sci. Total Environ.* **955**, 177261 (2024).
56. Pan, Y. et al. A large and persistent carbon sink in the world's forests. *Science* **333**, 988–993 (2011).
57. Stocker, B. D. et al. Empirical evidence and theoretical understanding of ecosystem carbon and nitrogen cycle interactions. *New Phytol.* **245**, 49–68 (2025).
58. Norby, R. J. & Zak, D. R. Ecological lessons from Free-Air CO_2 Enrichment (FACE) experiments. *Annu. Rev. Ecol. Evol. Syst.* **42**, 181–203 (2011).
59. Reich, P. B. & Hobbie, S. E. Decade-long soil nitrogen constraint on the CO_2 fertilization of plant biomass. *Nat. Clim. Change* **3**, 278–282 (2013).
60. Bassiouni, M., Smith, N. G., Reu, J. C., Peñuelas, J. & Keenan, T. F. Observed declines in leaf nitrogen explained by photosynthetic acclimation to CO_2. *Proc. Natl Acad. Sci. USA* **122**, e2501958122 (2025).
61. Thomas, R. Q., Brookshire, E. N. J. & Gerber, S. Nitrogen limitation on land: how can it occur in Earth system models? *Glob. Change Biol.* **21**, 1777–1793 (2015).
62. Davies-Barnard, T. et al. Nitrogen cycling in CMIP6 land surface models: progress and limitations. *Biogeosciences* **17**, 5129–5148 (2020).
63. Gerber, S., Hedin, L. O., Oppenheimer, M., Pacala, S. W. & Shevliakova, E. Nitrogen cycling and feedbacks in a global dynamic land model. *Glob. Biogeochem. Cycles* **24**, GB1001 (2010).
64. Sigurdsson, B. D., Medhurst, J. L., Wallin, G., Eggertsson, O. & Linder, S. Growth of mature boreal Norway spruce was not affected by elevated $[CO_2]$ and/or air temperature unless nutrient availability was improved. *Tree Physiol.* **33**, 1192–1205 (2013).
65. Read, D. J. Mycorrhizas in ecosystems. *Experientia* **47**, 376–391 (1991).
66. Gundale, M. J. et al. The biological controls of soil carbon accumulation following wildfire and harvest in boreal forests: a review. *Glob. Change Biol.* **30**, e17276 (2024).
67. Cambron, T. W. et al. Plant nutrient acquisition under elevated CO_2 and implications for the land carbon sink. *Nat. Clim. Change* **15**, 935–946 (2025).
68. Bunn, R. A. et al. What determines transfer of carbon from plants to mycorrhizal fungi? *New Phytol.* **244**, 1199–1215 (2024).
69. Lindahl, B. D. et al. A group of ectomycorrhizal fungi restricts organic matter accumulation in boreal forest. *Ecol. Lett.* **24**, 1341–1351 (2021).
70. Terrer, C. et al. A trade-off between plant and soil carbon storage under elevated CO_2. *Nature* **591**, 599–603 (2021).
71. Palmroth, S. et al. Increased leaf area index and efficiency drive enhanced production under elevated atmospheric CO_2 in a pine-dominated stand showing no progressive nitrogen limitation. *Glob. Change Biol.* **30**, e17190 (2024).

Methods

Sample collection and preparation

We used tree cores archived by the Swedish NFI between 1961 and 2018 (ref. 72). The Swedish NFI samples approximately 10,000 plots per year on productive, evergreen-dominated forestlands (range 55–69° N, 11–24° E), from which tree cores are collected and archived. To systematically sample independent tree cores from the archive, we applied a grid of 250 square cells (50 × 50 km) over Sweden. We then identified samples in the archive by filtering their associated database, for cores originating from dominant or co-dominant Norway spruce (*P. abies* (L.) H. Karst) and Scots pine (*P. sylvestris* L.) samples from inventory plots categorized as mesic site types, with slopes of 20% slope or less, and from trees in the 41–60-year-old age class. This age class was selected to minimize the likelihood of N fertilization application; forest fertilization treatment in Sweden is applied to a relatively small area and late in stand rotation[73]. Samples were then randomly selected for each tree species from each grid cell, and for each of 6 sampling decades (1960s–2010s). Specific sampling years were chosen for each decade based on the available number of archived samples: 1961, 1977, 1986–1988, 1996–1998, 2006–2008 and 2016–2018. Three-year periods were sampled for the 1980s, 1990s, 2000s and 2010s because the NFI's sampling intensity was reduced from this period onwards, requiring an expanded selection period to ensure a comparable number of samples to those available in 1961 and 1977. Some grid cells did not contain trees, and occasionally samples were not available for a given species, grid cell and decade combination, resulting in a total of $n = 1{,}609$ samples collected from the archive for analysis. Data for two counties in Sweden (Jämtland and Västernorrland) were previously reported[38] and were combined with new data for all other counties in Sweden. For each sample, collected at breast height (1.3 m), we removed the outer bark and cambial layers, and the most recent annual ring to exclude incomplete ring growth during the collection year. Then, to obtain sufficient material for chemical analysis, the subsequent 10-year annual growth segment was separated from the remainder of the core[38]. Dissections were performed using a No. 11 stainless steel surgical blade under a stereo microscope with ×20 magnification, with an accuracy of 0.01 mm. As the samples represent a 10-year growth segment, we designated each sample by its corresponding intermediate 10-year growth increment year (for example, samples collected in 1961 were representative of the period 1951 to 1960 and were consequently referred to as 1955).

Measurement and analysis of N isotopes

Nitrogen isotope ratios ($\delta^{15}N$) were analysed at the Central Appalachians Stable Isotope Facility (CASIF), University of Maryland Center for Environmental Science (UMCES) Appalachian Laboratory (Frostburg, MD, USA) with a Carlo Erba NC2500 elemental analyser (CE Instruments) interfaced with a Thermo Finnigan Delta V+ isotope-ratio mass spectrometer (IRMS). The Carlo Erba NC2500 Elemental Analyser with Costech zero-blank autosampler modifications permits for analysis of N isotopes in solid organic samples with content less than 0.5% N, such as wood[47]. From each tree core, a radial slice was precisely sectioned to represent each 10-year segment and chopped with a steel razor. Approximately 10 mg of wood from the radial core slice was then weighed, placed in a tin and analysed for the $\delta^{15}N$ value. Samples were analysed with a Carbosorb trap to remove CO_2 in advance of removing water vapour with magnesium perchlorate ($MgClO_4$). The $\delta^{15}N$ data were normalized to the Ambient Inhalable Reservoir (AIR) scale using a two-point normalization curve with internal standards, including ground corn, cocoa and caffeine powder calibrated against international standards, USGS40 and USGS41. Analytical precision (1σ) of an internal wood standard (ground pine powder) analysed alongside samples was 0.3‰ for $\delta^{15}N$; atropine powder was used for determining N-content values.

The ratio of heavy (^{15}N) to light (^{14}N) isotopes of samples is expressed in standard delta (δ) notation with reference to a standard of known isotopic ratio.

$$\delta^{15}N = (R_{sample}/R_{standard} - 1) \times 1{,}000$$

where R_{sample} and $R_{standard}$ are the ratios of the heavy to light isotopes in the sample and standard, respectively, and are expressed in units of parts per thousand or per mil (‰). The chosen standard for N is AIR. Corresponding wood %N data are reported in Extended Data Fig. 3.

Climate, Nr deposition and forest data

We leveraged external databases for use in the linear mixed-effects model, including the climate parameters mean annual temperature (°C) and atmospheric CO_2 concentrations (ppm); the N deposition parameters NH_x and NO_y (g m^{-2}); and the forest stand parameters total basal area and stand age. Monthly temperature data were extracted from CRU TS v4.07 (ref. 74) (resolution 0.5°) from which we calculated a 10-year mean annual temperature specific to each wood core sample, using its unique geographic coordinates. In addition to absolute temperature, we also calculated a relative temperature change variable, using 1961 as the reference temperature value for each grid cell, to minimize the large latitudinal gradient in temperature across our study area. We acquired CO_2 data from previously compiled measurements for the period 1951–2004 (ref. 75) and atmospheric CO_2 dry air mole fraction data for the period 2005–2017 from the National Oceanic and Atmospheric Administration (NOAA) Global Monitoring Laboratory recorded at PAL: Pallas-Sammaltunturi, GAW Station, Finland (67.9733° N, 24.1157° E; 565 m above sea level)[76]. We obtained monthly wet plus dry deposition as NH_x and NO_y between 1951 and 2017 from the global gridded Inter-Sectoral Impact Model Intercomparison Project (ISIMIP3a; resolution 0.5 × 0.5°)[77] dataset to compile 4 variables describing spatially explicit atmospheric Nr deposition: NH_x, NO_y, NH_x:NO_y and the 10-year average total N deposition for each sample based on specific geographic location. The forest stand parameter total basal area was used as a proxy for forest biomass variation, collected at the time of each tree-core collection in the field and archived in the Swedish NFI database. The observed increase in total basal area over time can be attributed to the combined influence of forest management and environmental change factors[78]. Notably, commercial forestry in the north is relatively recent compared with southern Sweden, which has undergone multiple forest rotations[79].

Swedish NFI growth data

Data from the NFI are acquired through annual systematic sampling of plots covering Swedish forests. The NFI sampling protocol is based on probability sampling, using a stratified systematic cluster design with a combination of permanent and temporary circular plots. Temporary plots, from where cores are extracted from sample trees, have a 7-m radius, whereas permanent plots have a 10-m radius. Permanent plots are resampled every 5 years and temporary plots are measured once[80]. The survey includes over 100,000 individual tree measurements each year (that is, obtained from about 10,000 survey plots). The growth rate is estimated using different approaches for both permanent and temporary plots. For permanent plots, growth is estimated as the difference in volume estimates (using tree species, diameter at breast height, tree height and crown height) between two consecutive inventories. Growth from temporary plots is estimated via the collection of tree cores, from which radial increment is measured on a microscope, upon which regression models are used to estimate volume growth. The estimated growth rate for permanent and temporary plots is then combined into a weighted mean, with the uncertainty of the estimate ≤1% (ref. 72). For the current study, the total volume growth (that is, the total growth for all of Sweden) for mesic *P. sylvestris*- and *P. abies*-dominated forests, respectively, was acquired from the NFI database.

Within each year and each species, we converted total volume growth to stand-level growth data by dividing the total volume growth by the forest area of the respective species.

Statistical methods

We analysed data using R Statistical Software[81]. First, we conducted linear regressions of the response variable, $\delta^{15}N$, as a function of time (predictor variable) for each of the two tree species across the geographical regions: north, central, southeast and southwest (Fig. 1c–j); a modified delineation (Fig. 1a) based on regions commonly used to evaluate Swedish environmental quality in relation to acidification and eutrophication[32]. This resulted in sample counts ranging from 18 to 45 samples per region and decade combination by species. In addition, we performed separate follow-up two-way analysis of variance with Tukey's post hoc pairwise comparisons ($\alpha = 0.05$) to identify differences in regression slopes between the four regions for each species (Fig. 1c–j). We checked for normal distribution and homoscedasticity of all model residuals. Next, we constructed a linear mixed-effects model (lme function; nlme package in R[82,83]) using stepwise forwards and backwards selection combined with Akaike information criteria using maximum likelihood to choose the model with the best combination of predictors to explain the observed patterns on the response variable, $\delta^{15}N$. The initial model included fixed effects: atmospheric CO_2, mean annual temperature, total Nr deposition, total basal area, stand age and tree species, and the interactions of tree species with CO_2 and total Nr deposition with CO_2. Numerical fixed effects were centred and scaled using the scale function in R. Grid cell was included as a random effect (intercept) to account for spatial autocorrelation among plots within the same grid. The variance inflation factor (VIF), a check for multi-collinearity of continuous numerical main predictors in the model, was calculated and a VIF limit of five was used to indicate an acceptable level of collinearity (Extended Data Table 1). The final model with the lowest Akaike information criterion retained all variables with the exception of stand age and the interaction of CO_2 with total Nr deposition. Finally, we repeated the linear mixed-effects model and replaced total Nr deposition with each of the remaining N deposition variables: NH_x, NO_y and NH_x:NO_y. The final model was run using restricted maximum likelihood (REML). We calculated the marginal (fixed effects), conditional (fixed and random effects) and partial R^2m values for each model (Extended Data Table 1) using the MuMIn[84] package (MuMIn::r.squaredGLMM function) in R. We also ran the final model with two variations: (1) all fixed and random effects of the final model with the addition of latitude and longitude (Extended Data Table 2); and (2) all fixed and random effects from the final model with mean annual temperature replaced by temperature change (Extended Data Table 3). We modelled $\delta^{15}N$ as a function of the significant and non-significant scaled variables (emmeans function) and estimated the slopes of significant model variables (emtrends function) using the emmeans package[85]. Finally, scaled explanatory variables were backtransformed for plotting significant and non-significant main effects (Fig. 2).

To investigate the potential role of forest volume growth change on wood $\delta^{15}N$ values, we calculated an additional forest growth variable describing 'relative forest volume growth change' in each grid cell. This was done by calculating a mean forest volume growth value for all sampling times for each species in each grid cell for which we had $\delta^{15}N$ values and then subtracting this mean value from each of the absolute forest volume growth values for each individual sample plot. We note that forest volume growth change and $\delta^{15}N$ values were based on 5-year and 10-year increments before the sampling date, respectively. We then constructed two linear mixed-effects models where relative forest volume growth change and either absolute forest volume growth or basal area were included as an additional fixed factor, and grid cell was included as a random factor (Extended Data Table 4). Both models were run using REML. We calculated the marginal (fixed effects) and conditional (fixed and random effects) R^2 values for each model using the MuMIn[84] package (MuMIn::r.squaredGLMM function) in R (Extended Data Table 4).

We modelled $\delta^{15}N$ as a function of relative forest volume growth change, including either absolute forest volume growth (Fig. 3c) or absolute basal area (Fig. 3d) as additional fixed effects, while also accounting for the random effect of grid. Slopes of the significant fixed effects were estimated from the models. We conducted a principal component analysis with normalized climate, N, and forest stand parameters that were significant in the final model, as well as the remaining three Nr deposition parameters to provide a visual representation of the impact of the specific parameters (Extended Data Fig. 1). All variables were scaled using the scale function in R. We conducted linear regression of all predictor variables in the final model: atmospheric CO_2, mean annual temperature, total N deposition and total basal area, and temperature difference as a function of predictor variables time (average year; Extended Data Fig. 2a,c,e,g,i) and space (latitude; Extended Data Fig. 2b,d,f,h,j). Finally, we conducted linear regressions of response variables: annual volume growth ($m^3\ ha^{-1}\ yr^{-1}$) and %N as a function of time (predictor variable) to determine whether a change through time occurred for each of the two species (*P. sylvestris* and *P. abies*) across the geographical regions: north, central, southeast and southwest (Fig. 3a,b and Extended Data Fig. 3, respectively). To enhance the visual differentiation of overlapping data points, the geom jitter function (ggplot2; ref. 86) was applied in the horizontal plane to Fig. 1c–j, Extended Data Fig. 2a,c,e,g,i, and Extended Data Fig. 3. Graphical representations were made using ggplot2 and FactoMineR[87] in R.

Data availability

The data supporting the findings of this study are accessible in the figshare repository, available at https://doi.org/10.6084/m9.figshare.30675002 (ref. 88). Atmospheric reactive nitrogen (Nr) deposition data from the Inter-Sectoral Impact Model Intercomparison Project phase 3a (ISIMIP3a) datasets are available at https://www.isimip.org. Temperature data from the CRU TS v4.07 dataset are available at https://crudata.uea.ac.uk/cru/data/hrg/, and atmospheric CO_2 data are available from the National Oceanic and Atmospheric Administration (NOAA) Global Monitoring Laboratory.

Code availability

All R scripts used for data processing and analysis are available in the figshare repository, available at https://doi.org/10.6084/m9.figshare.30675002 (ref. 88).

72. Fridman, J. et al. Adapting National Forest Inventories to changing requirements—the case of the Swedish National Forest Inventory at the turn of the 20th century. *Silva Fenn* **48**, 1095 (2014).
73. Hedwall, P.-O., Gong, P., Ingerslev, M. & Bergh, J. Fertilization in northern forests—biological, economic and environmental constraints and possibilities. *Scand. J. For. Res.* **29**, 301–311 (2014).
74. Harris, I., Osborn, T. J., Jones, P. & Lister, D. Version 4 of the CRU TS monthly high-resolution gridded multivariate climate dataset. *Sci. Data* **7**, 1–18 (2020).
75. McCarroll, D. & Loader, N. J. Stable isotopes in tree rings. *Q. Sci. Rev.* **23**, 771–801 (2004).
76. Lan, X., Tans, P. & Thonin, K. W. Atmospheric carbon dioxide dry air mole fractions from the NOAA GML Carbon Cycle Cooperative Global Air Sampling Network, 1968–2023, version: 2024-07-30. *Global Monitoring Laboratory* https://doi.org/10.15138/wkgj-f215 (2024).
77. Yang, J. & Tian, H. ISIMIP3a N-deposition input data (v1.3). *ISIMIP* https://doi.org/10.48364/ISIMIP.759077.3 (2023).
78. Elfving, B. & Tegnhammar, L. Trends of tree growth in Swedish forests 1953–1992: an analysis based on sample trees from the National Forest Inventory. *Scand. J. For. Res.* **11**, 26–37 (1996).
79. Östlund, L., Zackrisson, O. & Axelsson, A. L. The history and transformation of a Scandinavian boreal forest landscape since the 19th century. *Can. J. For. Res.* **27**, 1198–1206 (1997).
80. Fridman, J. & Westerlund, B. in *National Forest Inventories: Assessment of Wood Availability and Use* (ed. Vidal, C.) 769–782 (Springer, 2016).

81. R Core Team. *R: A Language and Environment for Statistical Computing* (R Foundation for Statistical Computing, 2023).
82. Pinheiro, J. C. & Bates, D. M. *Mixed-Effects Models in S and S-PLUS* (Springer, 2000).
83. Pinheiro, J. et al. nlme: linear and nonlinear mixed effects models. R package v.3.1-166 (CRAN, 2024).
84. Bartoń, K. MuMIn: multi-model inference. R package v.1.47.5 (2023).
85. Lenth, R. V. emmeans: estimated marginal means, aka least-squares means. R package v.1.9.0 (CRAN, 2023).
86. Wickham, H. *ggplot2: Elegant Graphics for Data Analysis* (Springer, 2009).
87. Lê, S., Josse, J. & Husson, F. FactoMineR: a package for multivariate analysis. *J. Stat. Softw.* **25**, 1–8 (2008).
88. Bassett, K. Reduces nitrogen availability in boreal forests (dataset). *figshare* https://doi.org/10.6084/m9.figshare.30675002 (2026).

Acknowledgements We thank the Swedish NFI field crews (1961–2018) for sample and data collection; and F. Johansson, M. Karlsson, T. Sundvall, P. Edlund and K. Spies for archive assistance. We thank the Central Appalachians Stable Isotope Facility, Maryland Center for Environmental Science Appalachian Laboratory, for laboratory analysis. We also thank F. Maillard for manuscript review. The research was funded by Stiftelsen Gunnar och Birgitta Nordins fond (KSLA) to K.R.B.; Brattås Stiftelsen, Troëdssons Stiftelsen, VR (2020-09308) to M.J.G.; T4F, and the Wallenberg Foundation (2018.0259). Any use of trade, firm, or product names is for descriptive purposes only and does not imply endorsement by the US Government.

Author contributions M.J.G. formulated the original concept presented in the paper. K.R.B., M.J.G., S.S.P., S.J., J.F. and L.Ö. contributed to discussions regarding the study design. K.R.B. managed all archival procedures and prepared samples for analysis. K.R.B. conducted all statistical analyses with assistance from S.F.H. in data management and R programming. K.R.B., S.F.H., M.J.G., S.J., L.Ö. and S.S.P. analysed and interpreted the results. K.R.B. authored the initial draft of the paper. All authors engaged in the discussion and revision processes of the paper.

Funding Open access funding provided by Swedish University of Agricultural Sciences.

Competing interests The authors declare no competing interests.

Additional information

Supplementary information The online version contains supplementary material available at https://doi.org/10.1038/s41586-025-10039-5.

Correspondence and requests for materials should be addressed to Kelley R. Bassett.

Peer review information *Nature* thanks the anonymous reviewers for their contribution to the peer review of this work. Peer reviewer reports are available.

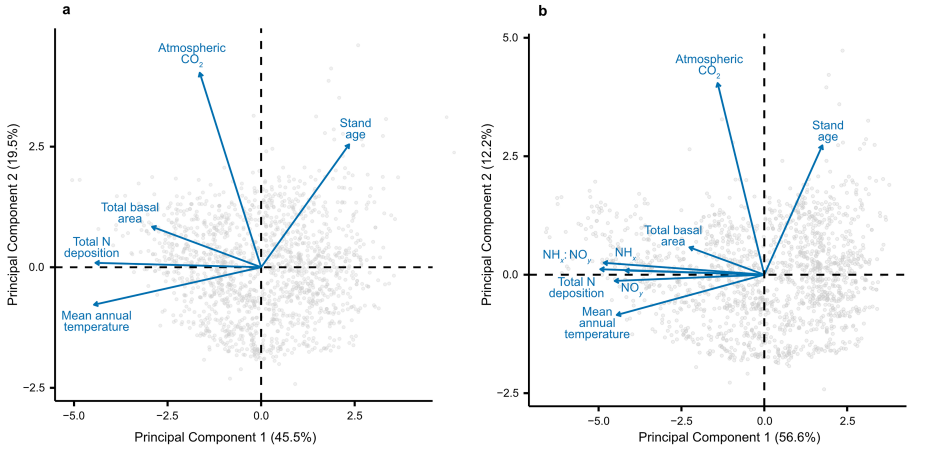

Extended Data Fig. 1 | Principal Component Analysis (PCA) biplot of scaled variables. a, Scaled variables: atmospheric carbon dioxide (CO_2), mean annual temperature, total basal area, stand age, and total nitrogen (N) deposition; and **b**, all aforementioned variables plus the addition of NH_x, NO_y, and NH_x:NO_y. Individual observations in grey ($n = 1609$) are plotted based on their scores along the first two principal components, which explain 45.5% and 19.5% of the variance, respectively (**a**); and 56.6% and 12.2% of the variance, respectively (**b**). Data sources are cited in the Methods.

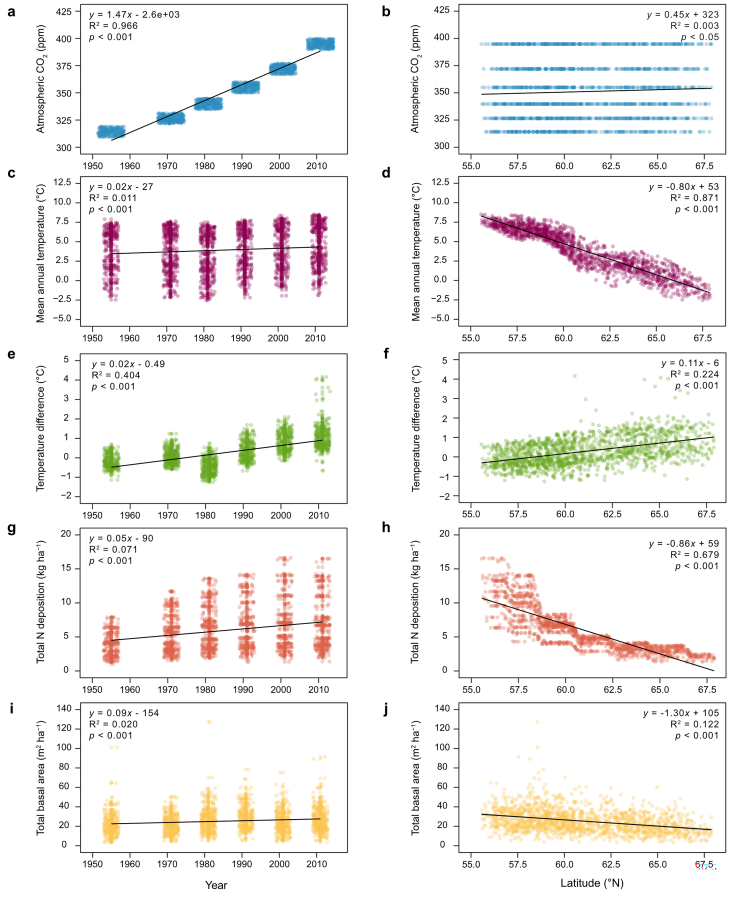

Extended Data Fig. 2 | Temporal and spatial trends in significant model variables. Linear regression of atmospheric carbon dioxide (CO_2, ppm; **a**,**b**); mean annual temperature (°C; **c**,**d**); temperature change (°C; **e**,**f**); total nitrogen (N) deposition (kg ha^{-1}; **g**, **h**); and total basal area (m^2 ha^{-1}; **i**,**j**) plotted over time (average year) and space (latitude), respectively. All relationships are significant ($P < 0.05$). A small horizontal offset was applied to the time plots (**a**,**c**,**e**,**g**,**i**) to increase the visibility of the data points (see Statistical methods). Data sources are cited in the Methods.

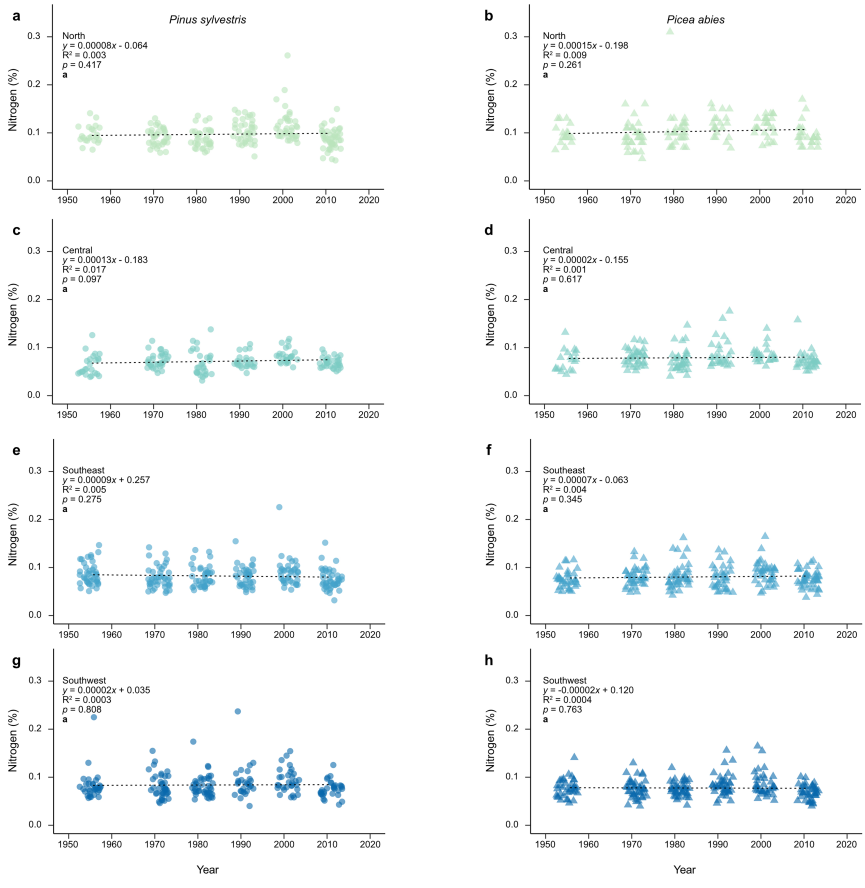

Extended Data Fig. 3 | Regional and temporal variation in wood nitrogen concentration across Sweden. Linear regressions of nitrogen (N) % for *P. sylvestris* and *P. abies* by region: north (**a**,**b**); central (**c**,**d**); southeast (**e**,**f**); and southwest (**g**,**h**) Sweden over the study period, 1950-2017. Slopes indicated with dashed lines were not significant ($P < 0.05$). Data sources are cited in the Methods.

Extended Data Table 1 | Summarised results of linear mixed-effects models

a

Variable	SE	df	t-value	*p*-value	VIF	Partial R^2m
Atmospheric CO_2	0.070	1403	-15.828	**0.0000**	2.04	0.176
Mean annual temperature	0.093	1403	2.923	**0.0035**	2.86	0.006
Total N deposition	0.094	1403	2.484	**0.0131**	2.99	0.004
Total basal area	0.054	1403	4.228	**0.0000**	1.17	0.009
Species	0.099	1403	0.130	0.8964	1.02	0.005
CO_2:Species	0.098	1403	3.456	**0.0006**	1.96	0.006

R^2m = 0.214; R^2c = 0.241

b

Variable	SE	df	t-value	*p*-value	VIF	Partial R^2m
Atmospheric CO_2	0.070	1403	-15.760	**0.0000**	2.04	0.174
Mean annual temperature	0.084	1403	3.819	**0.0001**	2.34	0.009
NH_x	0.084	1403	2.156	**0.0312**	2.38	0.004
Total basal area	0.054	1403	4.389	**0.0000**	1.17	0.010
Species	0.099	1403	0.119	0.9052	1.03	0.005
CO_2:Species	0.098	1403	3.442	**0.0006**	1.86	0.005

R^2m = 0.213; R^2c = 0.240

c

Variable	SE	df	t-value	*p*-value	VIF	Partial R^2m
Atmospheric CO_2	0.069	1403	-15.806	**0.0000**	2.00	0.174
Mean annual temperature	0.090	1403	3.385	**0.0007**	2.60	0.009
NO_y	0.089	1403	2.164	**0.0307**	2.71	0.003
Total basal area	0.055	1403	4.043	**0.0001**	1.19	0.007
Species	0.098	1403	0.165	0.8687	1.02	0.005
CO_2:Species	0.097	1403	3.518	**0.0004**	1.96	0.005

R^2m = 0.212; R^2c = 0.245

d

Variable	SE	df	t-value	*p*-value	VIF	Partial R^2m
Atmospheric CO_2	0.069	1403	-15.592	**0.0000**	2.00	0.171
Mean annual temperature	0.075	1403	5.760	**0.0000**	1.80	0.023
NH_x: NO_y ratio	0.071	1403	0.380	0.7038	1.69	0.001
Total basal area	0.054	1403	4.436	**0.0000**	1.17	0.010
Species	0.099	1403	0.143	0.8859	1.02	0.006
CO_2:Species	0.098	1403	3.497	**0.0005**	1.96	0.006

R^2m = 0.210; R^2c = 0.242

Summarised results of linear mixed-effects models with response variable, $\delta^{15}N$, as a function of scaled, fixed main effects of atmospheric carbon dioxide (CO_2); mean annual temperature; four nitrogen (N) deposition variables: **a**, Total N deposition; **b**, NH_x; **c**, NO_y; and **d**, NH_x:NO_y total basal area; species; the interaction of atmospheric CO_2 and species; and the random effect of grid cell using restricted maximum likelihood (REML). Significant values ($P < 0.05$) in bold. The variance inflation factor (VIF) limit of 5 was used to indicate an acceptable level of collinearity. R^2marginal (R^2m, fixed effects only) and R^2conditional (R^2c, fixed and random effects) are reported for each model. The partial R^2m values indicate the proportion of variance in the response variable uniquely explained by each respective fixed effect, after accounting for the effects of other variables in the model. Data sources are cited in the Methods.

Extended Data Table 2 | Summarised results of alternative (2) linear mixed-effects models

a

Variable	SE	df	t-value	*p*-value	VIF	Partial R^2m
Atmospheric CO_2	0.082	1401	-13.941	**0.0000**	2.88	0.096
Mean annual temperature	0.201	1401	2.496	**0.0127**	13.23	0.004
Total N deposition	0.109	1401	2.532	**0.0114**	3.96	0.004
Total basal area	0.054	1401	4.145	**0.0000**	1.17	0.008
Latitude	0.261	1401	1.356	0.1755	21.90	0.001
Longitude	0.091	1401	-1.466	0.1428	2.72	0.001
Species	0.099	1401	0.043	0.9657	1.03	0.005
CO_2:Species	0.097	1401	3.456	**0.0005**	1.96	0.005
R^2m = 0.215; R^2c = 0.245						

b

Variable	SE	df	t-value	*p*-value	VIF	Partial R^2m
Atmospheric CO_2	0.082	1401	-13.850	**0.0000**	2.82	0.093
Mean annual temperature	0.201	1401	2.505	**0.0124**	13.35	0.004
NH_x	0.096	1401	2.127	**0.0336**	3.04	0.003
Total basal area	0.054	1401	4.324	**0.0000**	1.17	0.009
Latitude	0.256	1401	1.103	0.2702	21.24	0.001
Longitude	0.091	1401	-1.400	0.1617	2.72	0.001
Species	0.099	1401	0.026	0.9792	1.03	0.005
CO_2:Species	0.098	1401	3.453	**0.0006**	1.96	0.004
R^2m = 0.214; R^2c = 0.242						

c

Variable	SE	df	t-value	*p*-value	VIF	Partial R^2m
Atmospheric CO_2	0.079	1401	-14.137	**0.0000**	2.65	0.106
Mean annual temperature	0.203	1401	2.308	**0.0212**	13.01	0.003
NO_y	0.097	1401	2.146	**0.0321**	3.13	0.002
Total basal area	0.055	1401	3.959	**0.0001**	1.19	0.007
Latitude	0.252	1401	1.019	0.3085	19.64	0.000
Longitude	0.093	1401	-1.378	0.1685	2.70	0.001
Species	0.099	1401	0.075	0.9400	1.03	0.004
CO_2:Species	0.097	1401	3.539	**0.0004**	1.96	0.005
R^2m = 0.213; R^2c = 0.248						

d

Variable	SE	df	t-value	*p*-value	VIF	Partial R^2m
Atmospheric CO_2	0.079	1401	-13.653	**0.0000**	2.61	0.097
Mean annual temperature	0.204	1401	2.288	**0.0223**	13.16	0.003
NH_x: NO_y ratio	0.077	1401	0.171	0.8642	1.95	0.000
Total basal area	0.055	1401	4.330	**0.0000**	1.17	0.010
Latitude	0.250	1401	0.358	0.7204	19.35	0.000
Longitude	0.093	1401	-1.213	0.2255	2.69	0.001
Species	0.099	1401	0.044	0.9649	1.02	0.006
CO_2:Species	0.098	1401	3.524	**0.0004**	1.96	0.006
R^2m = 0.211; R^2c = 0.245						

Summarised results of alternative (2) linear mixed-effects models with response variable, $\delta^{15}N$, as a function of scaled, fixed main effects of atmospheric carbon dioxide (CO_2), mean annual temperature, total basal area, four nitrogen (N) deposition variables: **a**, Total N deposition; **b**, NH_x; **c**, NO_y; and **d**, NH_x:NO_y; latitude, longitude, species, and random effect of grid cell using restricted maximum likelihood (REML). Significant values (P < 0.05) in bold. We permitted our variance inflation factor (VIF) to surpass the limit of 5, as we intended this variable to capture spatial variation in the other model factors. R^2marginal (R^2m, fixed effects only) and R^2conditional (R^2c, fixed and random effects) are reported for each model. The partial R^2m values indicate the proportion of variance in the response variable uniquely explained by each respective fixed effect, after accounting for the effects of other variables in the model. Data sources are cited in the Methods.

Extended Data Table 3 | Summarised results of alternative (1) linear mixed-effects models

a

Variable	SE	df	t-value	*p*-value	VIF	Partial R^2m
Atmospheric CO_2	0.093	1403	-14.055	**0.0000**	3.67	0.108
Temperature change	0.081	1403	3.010	**0.0027**	2.61	0.005
Total N deposition	0.068	1403	8.093	**0.0000**	1.58	0.047
Total basal area	0.054	1403	4.943	**0.0000**	1.16	0.012
Species	0.099	1403	0.120	0.9041	1.02	0.006
CO_2:Species	0.098	1403	3.513	**0.0005**	1.96	0.006

R^2m = 0.213; R^2c = 0.237

b

Variable	SE	df	t-value	*p*-value	VIF	Partial R^2m
Atmospheric CO_2	0.092	1403	-13.590	**0.0000**	3.54	0.101
Temperature change	0.078	1403	2.127	**0.0336**	2.43	0.002
NH_x	0.065	1403	7.292	**0.0000**	1.43	0.040
Total basal area	0.053	1403	5.560	**0.0000**	1.13	0.016
Species	0.099	1403	0.099	0.9215	1.02	0.005
CO_2:Species	0.098	1403	3.504	**0.0005**	1.96	0.006

R^2m = 0.206; R^2c = 0.230

c

Variable	SE	df	t-value	*p*-value	VIF	Partial R^2m
Atmospheric CO_2	0.093	1403	-13.952	**0.0000**	3.66	0.102
Temperature change	0.082	1403	3.150	**0.0017**	2.69	0.004
NO_y	0.069	1403	7.668	**0.0000**	1.61	0.041
Total basal area	0.055	1403	4.523	**0.0000**	1.18	0.010
Species	0.098	1403	0.211	0.8328	1.02	0.006
CO_2:Species	0.097	1403	3.669	**0.0003**	1.96	0.006

R^2m = 0.207; R^2c = 0.240

d

Variable	SE	df	t-value	*p*-value	VIF	Partial R^2m
Atmospheric CO_2	0.089	1403	-12.518	**0.0000**	3.24	0.082
Temperature change	0.075	1403	0.472	0.6372	2.17	0.000
NH_x:NO_y ratio	0.059	1403	4.804	**0.0000**	1.17	0.021
Total basal area	0.053	1403	6.392	**0.0000**	1.10	0.024
Species	0.100	1403	0.119	0.9051	1.02	0.005
CO_2:Species	0.099	1403	3.595	**0.0003**	1.96	0.006

R^2m = 0.187; R^2c = 0.218

Summarised results of alternative (1) linear mixed-effects models with response variable, $\delta^{15}N$, as a response to scaled, fixed main effects of atmospheric CO_2, temperature change, total basal area, four nitrogen (N) deposition variables: **a**, Total N deposition; **b**, NH_x; **c**, NO_y; and **d**, NH_x:NO_y; species, and random effect of grid cell using restricted maximum likelihood (REML). Significant values (P <0.05) in bold. The variance inflation factor (VIF) threshold of 5 was employed to denote an acceptable level of collinearity. R^2marginal (R^2m, fixed effects only) and R^2conditional (R^2c, fixed and random effects) are reported for each model. The partial R^2m values indicate the proportion of variance in the response variable uniquely explained by each respective fixed effect, after accounting for the effects of other variables in the model. Data sources are cited in the Methods.

Extended Data Table 4 | Summarised results of linear mixed-effects models

a

Variable	Coefficient	SE	df	t-value	*p*-value	VIF
Absolute forest volume growth	0.154	0.0195	1407	7.904	**0.0000**	2.36
Relative forest volume growth change	-0.163	0.0256	1407	-6.351	**0.0000**	2.36
$R^2m = 0.044$; $R^2c = 0.075$						

b

Variable	Coefficient	SE	df	t-value	*p*-value	VIF
Total basal area	0.039	0.039	1407	6.294	**0.0000**	1.73
Relative forest volume growth change	-0.010	-0.098	1407	-4.497	**0.0000**	1.73
$R^2m = 0.027$; $R^2c = 0.080$						

Summarised results of linear mixed-effects models with response variable, $\delta^{15}N$, as a response to fixed main effects: **a**, absolute volume growth ($m^3\ ha^{-1}\ yr^{-1}$), relative forest volume growth change ($m^3\ ha^{-1}$), and random effect of grid cell; and **b**, total basal area ($m^2\ ha^{-1}$), relative forest volume growth change ($m^3\ ha^{-1}$), and random effect of grid cell in relation to response variable, $\delta^{15}N$. Restricted maximum likelihood (REML) was applied to both models. Significant values ($P < 0.05$) in bold, italics. A variance inflation factor (VIF) limit of 5 was used to indicate an acceptable level of collinearity. R^2marginal (R^2m, fixed effects only) and R^2conditional (R^2c, fixed and random effects) are reported for each model. Data sources are cited in the Methods.